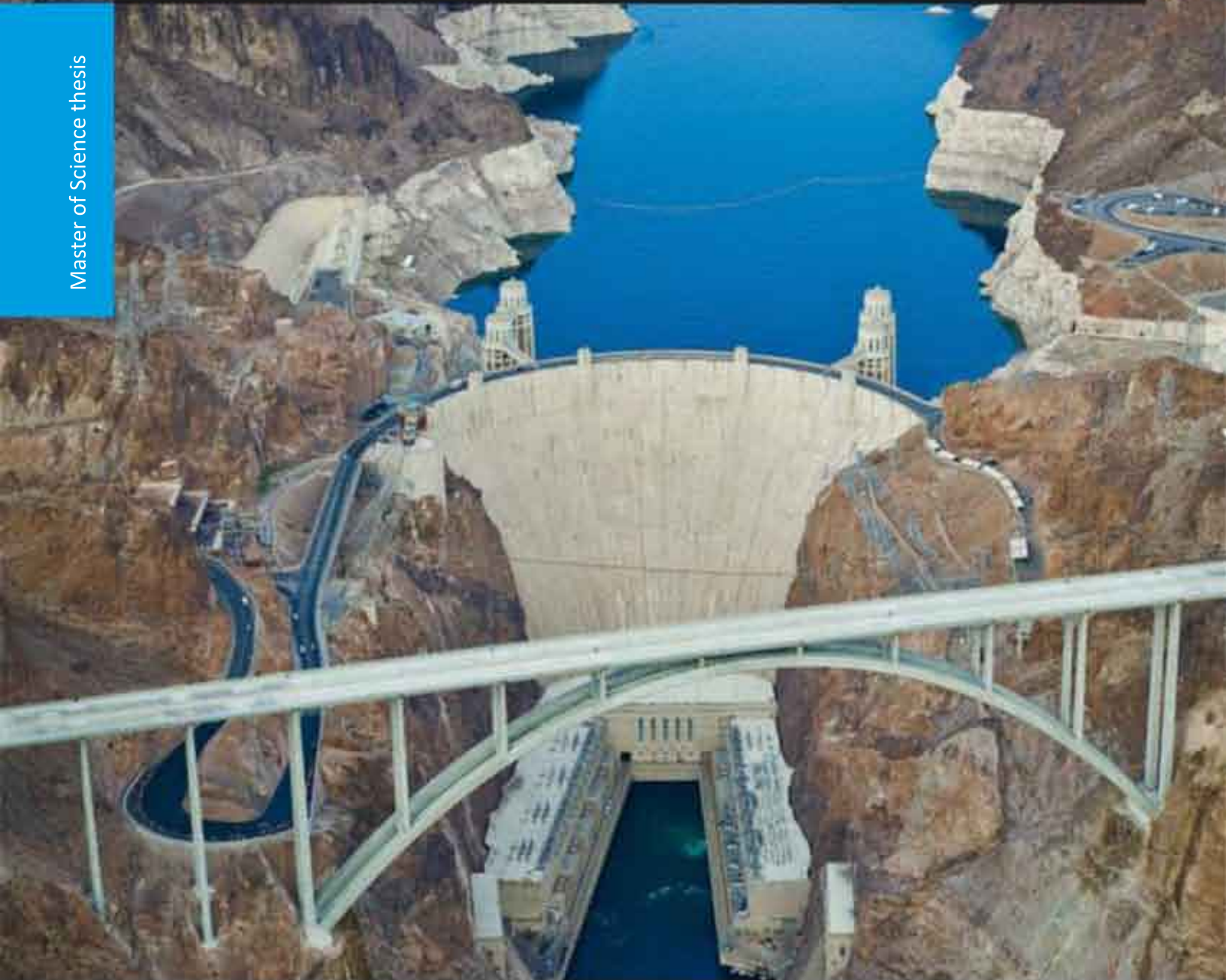
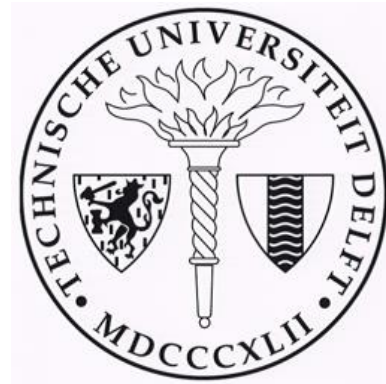
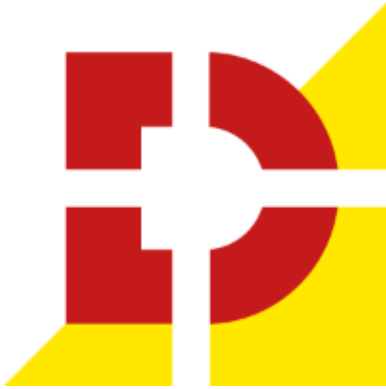


DESIGN OF DOUBLE-CURVATURE ARCH DAMS IN TERMS OF GEOMETRIC AND STRESS CONSTRAINTS BY USING SCRIPT-BASED FINITE ELEMENT MODELLING

E. Goulas

Master of Science thesis





Master Project:

DESIGN OF DOUBLE-CURVATURE ARCH DAMS IN TERMS
OF GEOMETRIC AND STRESS CONSTRAINTS BY USING
SCRIPT-BASED FINITE ELEMENT MODELLING

Student:

Evangelos Goulas (4421442)

Assessment Committee:

prof. Dr. ir. J.G. Rots, CEG Structural Mechanics section, TU Delft

prof. Dr. ir. M.A.N. Hendriks, CEG Structural Mechanics section, TU Delft

Dr. ir. G. Schreppers, TNO DIANA BV

Dr. R.M. Gunn, Swiss Federal Office of Energy

ir. A. van der Toorn, CEG Hydraulic Structures and Flood Risk section, TU Delft

Copyright © 2016 TNO DIANA BV

Copyright © 2016 Delft University of Technology

This document is property of TNO DIANA and Evangelos Goulas and contains confidential information. It may not be used for any other purpose than for which is supplied. This document may not be wholly or partly disclosed, copied, duplicated or in any way made use of without prior written approval of TNO DIANA or Evangelos Goulas. All rights are reserved.

Acknowledgements

The following report is not the outcome of an individual person but of many people who cooperated and struggled together to find the best solution for each problem.

For this reason, I would first like to thank Dr. ir. G. Schreppers for giving me the unique opportunity to do my internship and my master project at TNO DIANA BV. He was always willing to help me when I ran into a problem, no matter how busy he was.

I would also like to thank prof. Dr. ir. M.A.N. Hendriks who believed in me from the beginning, his help was more than vital. Furthermore, I want to thank prof. Dr. ir. J.G. Rots and and ir. A van der Toorn for being critical during our meetings, their remarks and recommendations were very useful.

Moreover, I would like to thank Dr. R.M. Gunn, an excellent dam specialist, who shared his experience and devoted time and effort in reviewing my work. Without his help I could not develop such a realistic code.

I want to express my very profound gratitude to all my colleagues at TNO DIANA BV and especially to Jonna Manie, Wijtze Pieter Kikstra and Anne van de Graaf for their valuable help and their comments on my problems.

Finally, I would like to thank my parents deeply for providing me with unfailing and continuous encouragement throughout my years of study.

Author,

Evangelos V. Goulas

Abstract

An arch dam is a curved surface structure that is designed to resist water pressure at the convex side. An arch dam is usually constructed in a narrow V-shape valley with strong rock foundations. Through the arched shape the water pressure is distributed from the upstream face of the dam to the abutment edges of the dam which are embedded in the rock-foundation. An arch dam is designed to be under compressive stresses when it is submitted to the dominant dead-weight and hydrostatic loadings. In comparison with other dam-types, such as an embankment dam, an arch dam is considerably thinner and requires less construction material, which can make this type of dam the most economical. Due to the thin shell structure, an arch dam cannot resist concentrated loadings resulting from strong variations of strength of the foundations or impact from e.g. falling rocks. Hence, a proper assessment of design conditions is essential and this also applies for other dam-types.

To design an arch dam an initial dam layout is used, usually obtained from empirical methods, and it is reshaped until the essential constraints are satisfied within the design objectives. The application of finite element analysis during this iterative process is elaborative and therefore often postponed to the stage of design when the basic design parameters such as location, height and orientation of the dam have been defined.

The aim of this master project is to develop a procedure that allows to define in an automatic way the generation of a finite element model of double-curved arch dams. In this way, the model can be efficiently used from the beginning of the design process taking into account the dam and excavation volume, the stresses and deformations in the dam body and the foundation for a variation of loading conditions for different basic design parameters of the dam.

In this thesis guidelines applied in practice are the reference for the design of the shape of the dam. The general workflow consists of a preliminary and a final design stage. Through the first stage the best location of the dam and height must be defined such that geometric constraints as defined in the guidelines are satisfied. For this purpose, different potential locations for the dam are chosen by the designer. For each location an assessment must be made, considering many factors, such as state of the foundation, environmental and social conditions and also costs, which are predominantly defined by the volume of rock excavation and volume of the dam-body. When this information is collected for the chosen locations the best alternative can be defined. In the second stage, the dam of the best alternative is reshaped by modifying the entire geometry of the dam until stress constraints are satisfied. An important condition is to check and minimize the effect of design-changes on the costs under the condition that the shape of the dam remains smooth.

This master project was done at TNO DIANA BV, this company develops the DIANA Finite Element software that is used by dam-engineering consultants and dam-owners to design new and assess existing dams. Based on Python scripting a procedure is defined for automatic generation of a finite element model of double-curved arch dam with rock foundation. The script starts with a topological surface. From the basic design parameters (location, orientation, height) a preliminary shape of the dam with abutments is defined following the US Army corps guidelines. With this model, the design engineer can perform efficiently different analyses, such as calculation of volume of dam-body and excavated

rock, but also predict deformations and stresses and eigen-modes more accurately in the preliminary design stage. In the subsequent final design phase the same model can be optimized by including joints between different columns in the dam and define thickening at the edges of the dam to reduce stresses in the abutments. In the final design phase all kind of loadings and analysis types can be considered, such as thermal loadings during young-hardening phase of concrete or damage development during earthquake loadings.

In this thesis first general information regarding double-curvature arch dams is given and their geometry is divided into four main parts from which the dam geometry is derived. Then the general workflow is introduced which describes the entire design process and is based on empirical methods used in practice. Each step in the geometry definition leads to mathematical expressions, which can be translated into Python commands. The entire process is inserted into the Finite Element software DIANA as a script and the dam is analyzed. The developed script is applied on a topographic surface which is based on real data. Three different locations are used and the most economical one is assessed. This design was reshaped based on the designer's judgement. Finally, the analysis results are used to investigate the dependency of the theoretical with numerical volume and how basic design parameters influence the stresses and deformations of the structure.

The conclusion of the thesis is that the developed procedure can sufficiently describe the design of double-curvature arch dams using any location, whereas the modelling effort is drastically reduced. It is recommended that further research is needed to further improve the code towards needs from dam-engineers in practice. When the developed procedure will be more integrated in the DIANA software it can be a very efficient tool to help dam-engineers around the world to make use of advanced finite element analysis already in the early preliminary design stage of curved arched dams.

Glossary

The following definitions are organized based on the order found in the following sections and not on alphabetical order.

Arch dam: An arch dam is a concrete or masonry dam that is curved in plan view so as to transmit the major part of the water load to the abutments [4].

Single-curvature arch dam: A single curvature arch dam is an arch dam that is curved in plan (horizontally) only.

Double-curvature arch dam: A double curvature arch dam is an arch dam that is curved in plan (horizontally) and in elevation (vertically), with undercutting of the heel and has a downstream overhang near the crest [4].

Upstream face: The curved surface of the dam which is in connection with the water.

Downstream face: The curved surface of the dam which is not in connection with the water.

Topographical data: Both the surface area surrounding the dam and the interval of contour lines (10 m, 15 m, 20 m etc.).

Crown cantilever section: The crown cantilever section is a vertical upstream to downstream section through an arch dam at the maximum height. This is generally also along the reference plane [4].

Upstream contact line: The line that passes through the base crown cantilever point, the start point and the end point of the upstream crest elevation parabola.

Main parabolas: The sets of parabolic functions that describe the geometry of the main faces of the dam.

Side parabolas: The sets of parabolic functions that describe the abutment thickening to the downstream face of the dam for each side.

Foundation area: The dam-rock interface geometry which consists of the endpoints of the upstream and downstream face.

Abutment: An abutment is that part of the valley wall against which the dam is constructed and the part of a dam that contacts the riverbank [4].

Reference cylinder: The reference cylinder is the upstream crest elevation parabola and it is very important as it controls the general shape of the dam [2].

Reference plane: The reference plane is an imaginary upstream to downstream vertical section through the crown cantilever of a concrete dam and line of centers. The orientation of the dam can be defined by positioning the top of the line of centers by State Plane coordinates and the bearing of the reference plane from this point. The geometry of the upstream face, downstream face, and lines of centers are along the reference plane [4].

Dam axis: The axis of the dam is a vertical cylindrical reference plane along the upstream side of the dam crest [4].

Crest: The crest is the top surface of the main body of the dam (excluding parapet walls) or the high point of a spillway. A roadway may be constructed across the crest to permit vehicular traffic or facilitate operation, maintenance, and examination of the dam [4].

Line of (main) centers: The line of centers defines the geometry of the centers of radii of the upstream and downstream faces of an arch dam along the reference plane [4].

Tailwater: Refers to waters located immediately downstream from a hydraulic structure [9].

Developed cylinder: A cylinder used to create the developed profile view. The dimensions of the developed cylinder must be close to the largest parabola of the dam, which is the upstream crest elevation parabola (reference cylinder). For this reason, the developed cylinder is calculated using the focus point and the symmetry point of the reference cylinder.

Developed profile view: The view of the upstream/downstream face of the dam (looking downstream) with the foundation topography shown, which uses a cylindrical coordinate system projecting the end points of the face and the respective topographic points. Note that a developed view is not the projection of the upstream face onto a flat plane.

Contraction joints: The joints between the dam cantilevers are referred to contraction joints and must be grouted to form the monolith structure. Contraction joints are not planar, but rather warped or helical in shape. Their definition is critical in the design and analysis process [2].

Bezier: A special case of NURB, in which the knot set takes a predefined form. In this case the B-spline basis functions are the Bernstein polynomials of the given order. [8]

Bezier surface: A surface $P(u, v)$ where u and v vary orthogonally from 0 to 1, from one edge of the surface to the other, is defined by a set of $(n+1)*(m+1)$ "control points" $(X(i, j), Y(i, j), Z(i, j))$ for $i = 0$ to n , $j = 0$ to m [9].

Transition (Tangent) points: The contact points of the main downstream parabolas and the side parabolas. The tangent of both parabolas in this point must be equal, so a smooth transition from the one geometry to the other is achieved. In this way a dam profile is generated which is smooth and free of geometric points of stress singularities [2]. Each transition point must be between the boundaries of the respective main downstream parabola, or else it cannot be accepted as a valid point.

Line of side centers: The line of side centers defines the geometry of the centers of radii of side parabolas. Each side center must be on the line that connects the transition point with the respective main downstream center point.

Interface elements: Elements that facilitate discontinuities of a model in the displacement field.

Structural plane interface elements: The structural interface elements describe the interface behavior in terms of a relation between the normal and shear tractions and the normal and shear relative displacements across the interface. Plane interface elements are placed between faces of three-dimensional elements. With these elements the interface surface and directions are also evaluated automatically from the geometry of the element itself [7].

Contents

Acknowledgements.....	iv
Abstract.....	vi
Glossary.....	viii
1. Introduction.....	5
1.1. Problem definition.....	5
1.2. Research objectives.....	5
1.3. Research approach.....	5
1.4. Basic assumptions.....	6
1.5. Chapter description.....	7
2. Background on arch dams.....	9
2.1. General information.....	9
2.2. Parabolic equation.....	12
2.3. Main parts of a double-curvature arch dam geometry.....	14
2.3.1. Crown cantilever section.....	14
2.3.2. Main parabolas.....	15
2.3.3. Side parabolas.....	16
2.3.4. Foundation area.....	18
3. General workflow of design stages.....	19
4. Preliminary design stage.....	23
4.1. Potential dam sites.....	23
4.2. Original topography.....	24
4.3. Excavated topography.....	25
4.4. Basic variables.....	26
4.5. Dam axis and reference cylinder.....	28
4.6. Crown cantilever section.....	31
4.7. Layout of the arches.....	33
4.8. Smooth dam shape method.....	37
4.9. Review of the arches.....	43
4.10. Developed profile view.....	46
4.11. Contraction joints.....	50

4.12. Diana Interactive Environment (DianaE) Model	56
4.12.1. Preliminary upstream cloud of points.....	56
4.12.2. Preliminary downstream cloud of points	57
4.12.3. Preliminary foundation clouds of points.....	57
4.12.4. Preliminary solid shape of the dam	58
4.12.5. Preliminary solid shape of the topography.....	61
4.12.6. Preliminary contraction joints.....	62
4.12.7. Preliminary boundary conditions	63
4.12.8. Preliminary mesh guidelines	65
4.13. Selection of the best alternative	66
5. Final design stage	67
5.1. Design improvement.....	67
5.1.1. Definition of side parabolas.....	68
5.1.2. Redefinition of crown cantilever section	71
5.1.3. Redefinition of line of main centers	72
5.2. Interface elements.....	74
5.2.1. Concrete-concrete connection	75
5.2.2. Concrete-rock connection	75
5.3. Final stress analysis.....	76
5.4. Evaluation of results	77
6. Application of the code.....	81
6.1. Selection of the topographic surface.....	81
6.2. Selection of the potential dam sites.....	82
6.3. Selection of the basic variables.....	83
6.3.1. Location A-Selection of the best fitting dam.....	83
6.3.2. Location B-Selection of the best fitting dam	85
6.3.3. Location C-Selection of the best fitting dam	87
6.4. Preliminary model properties.....	89
6.5. Preliminary results.....	89
6.5.1. Location A-Dam mesh size 10.....	90
6.5.2. Location B-Dam mesh size 10.....	91

6.5.3. Location C-Dam mesh size 10	92
6.6. Selection of the best alternative	93
6.7. Final results.....	94
6.7.1. Iteration 0.....	97
6.7.2. Iteration 1.....	100
6.7.3. Iteration 2.....	103
6.7.4. Iteration 3.....	106
7. Discussion of research questions.....	109
7.1. Comparison of the theoretical with the numerical volume	109
7.2. The influence of the excavation length.....	111
7.3. The influence of the shape of the foundation area.....	114
8. Conclusions.....	115
9. Recommendations.....	117
References	119
List of symbols.....	121
List of figures.....	127
List of Tables.....	131
Appendix 1: Preliminary results	133
Appendix 2: Part of the code	Error! Bookmark not defined.
Appendix 3: The cloud of points of Location B	Error! Bookmark not defined.

1. Introduction

1.1. Problem definition

Double-curvature arch dams are concrete structures that are curved in plan (horizontally) and in elevation (vertically) [Figure 1]. They are very important structures due to their high cost, purpose and catastrophic impact in case of failure.

Their design is a very complex and sensitive process, as it aims to find the most efficient solution in terms of cost and stress level, taking into account many constraints at the same time. As a result there is no software that can provide a fully automated process.

1.2. Research objectives

The main research question is formed in combination with the company, the assessment committee and the author:

“Investigate the potential to develop a fully automated process that can design a double-curvature arch dam based on a given topography.”

Having this process developed and fully functional, special attention is given in the following aspects:

“How accurate is the empirical formula which computes the concrete volume of the dam compared to the numerical volume.”

“How the orientation of the dam axis influences the dam volume.”

“How the initial excavation length influences the dam volume.”

“How the shape of the foundation area influences the dam volume and the stress level.”

1.3. Research approach

First, a literature study is essential to expand the knowledge on arch dam design, analyzing in depth the main research question. A validated method must be followed which can provide all the essential design rules.

As a result, the Engineer Manual 1110-2-2201 of the U.S Army of Engineers [1] is used as a guideline which provides general information for the construction and design of double-curvature arch dams. However, there are many assumptions that have been made and differences between this method and the author’s method and they are shown in the following section.

Afterwards, a script is developed using the programming language Python as it is compatible with the Finite Element Software “Diana Interactive Environment” (DianaIE) so all the essential design rules can be translated into automatic processes.

Finally, the script is tested to generate the best-fitting double-curvature arch dam for a topography obtained from real data.

1.4. Basic assumptions

The majority of the assumptions were discussed with the full assessment committee and they were tested during the development of the code.

In the Engineer Manual [1] sets of circular equations are used to describe the dam geometry. However, in the context of this master project sets of parabolic equations are used, as industry is familiar with parabolic and elliptical definitions. Furthermore, using parabolic equations the abutment thickening is described much more efficiently than using circular arches.

The Engineer Manual [1] mentions that, the designer must consider a reasonable amount of overburden, based on core borings or sound judgment, but there are no specific guidelines. A variable is proposed, which describes the initial excavation length in the lateral direction and it is uniform along the height. In this way, a realistic user-defined excavated foundation can be generated.

The Engineer Manual [1] does not take into account the excavation volume that is essential to create a good-shaped foundation area, while the proposed method takes this parameter into account.

A realistic arch dam must have a base length which is very important for the stress constraints as well. This parameter is not taken into account in the Engineer Manual [1], while the proposed process defines the best fitting base length based on the surrounding topography.

There are no guidelines to define the dam base elevation in the Engineer Manual [1] and as a result the dam base is always placed 8 meters below the lowest contour in riverbed, based on the document [5].

The contraction joints are very important for the dam design in the pre and post-processing as they divide the dam into cantilevers and they simulate the construction stage in practice. In the Engineer Manual [1] there is no relevant information and the document [2] is used to define their geometry.

For simplification purposes, the hydrostatic pressure is applied only on the dam and more specifically on the upstream face, while it is neglected from the upstream topography.

The density of the rock is assumed to be zero. Stresses due to the rock self-weight are not of high importance.

The temperature load on the arch dam is neglected.

Tailwater conditions are not taken into account, as their contribution is negligible [3].

Interface elements are taken into account between the dam cantilevers and between the dam cantilevers and rock. There is no relevant information in the Engineer Manual [1] and the whole method is proposed in one of the Section 5.2

1.5. Chapter description

This report is set as follows. Chapter 2 gives general information for dams and introduces the main parts of a double-curvature arch dam. Then in Chapter 3, the general workflow of the process to design the best fitting dam based on the given topography is shown. Chapter 4 presents the preliminary design stage where the best alternative in terms of geometric constraints is chosen. Chapter 5 shows how the best alternative can be reshaped so the stress constraints can be satisfied as well.

Chapter 6 contains the application of the entire process generating a dam based on real topographical data. In Chapter 7 the research questions are discussed using the results from the example. Chapters 8 and 9 present the conclusions and the recommendations.

2. Background on arch dams

In this chapter the main function, the different categories, the constraints and the objectives of dams are explained. Afterwards, the main geometric parts of double-curvature arch dams are described.

2.1. General information

Dams are solid barriers that are usually constructed across a stream channel to store water which can be used for several reasons like water supply, irrigation or energy generation. There are many categories of dams and they can be classified as follows.

The following construction materials can be used to build a dam.

- Masonry, mainly consists of stone and brick.
- Concrete, the most commonly used material.
- Steel, rarely used as it is uneconomical.
- Timber, rarely used due to its relatively short lifespan.
- Earth, like gravel, sand, silt, clay etc.
- Tailings, waste or refuse obtained from mines

There are five main categories based on the structural behavior.

- Gravity dam, is constructed from concrete or stone masonry and designed to hold back water by primarily utilizing the weight of the material alone to resist the horizontal pressure of water pushing against it. Gravity dams are designed so that each section of the dam is stable, independent of any other dam section [9].
- Arch dam, is a solid dam made of concrete that is curved in plan (single-curvature) or in plan and elevation (double-curvature). An arch dam takes advantage of the surrounding topographic area using its shape for stability. So the force of the water, the hydrostatic pressure, is redirected into the canyon walls by compressing and strengthening the entire structure. An arch dam is most suitable for narrow gorges or canyons with steep walls of stable rock to support the structure and stresses. Since they are thinner than any other dam type, they require much less construction material, making them economical and practical in remote areas [9].
- Arch-gravity dam, is a dam with both the characteristics of an arch dam and a gravity dam. It bends upstream in a narrowing curve that directs most of the water against the canyon rock walls, providing the force to compress the dam [9].
- Buttress dam, is a dam with a solid water-tight upstream side that is supported at intervals on the downstream side by a series of buttresses or supports. The dam wall may be straight or curved. Most buttress dams are made of reinforced concrete and are heavy, pushing the dam into the ground. Water pushes against the dam, but the buttresses are inflexible and prevent the dam from falling over [9].
- Embankment dam, is typically created by the placement and compaction of a complex semi-plastic mound of various compositions of soil, sand, clay and/or rock. It has a semi-pervious waterproof natural covering for its surface and a dense, impervious core. This makes such a dam impervious to surface or seepage erosion. Such a dam is composed of fragmented independent material particles.

The friction and interaction of particles binds the particles together into a stable mass rather than by the use of a cementing substance [9].

In the context of this master project, only arch dams are investigated because they are the most economical as long as the canyon characteristics are appropriate. Arch dams are classified with respect to the shape of the arches and the highest cross-section which is commonly located in the riverbed. Single-curvature arch dams are only curved in plan (horizontally), while double-curvature arch dams are curved in plan (horizontally) and in elevation (vertically) [Figure 1].

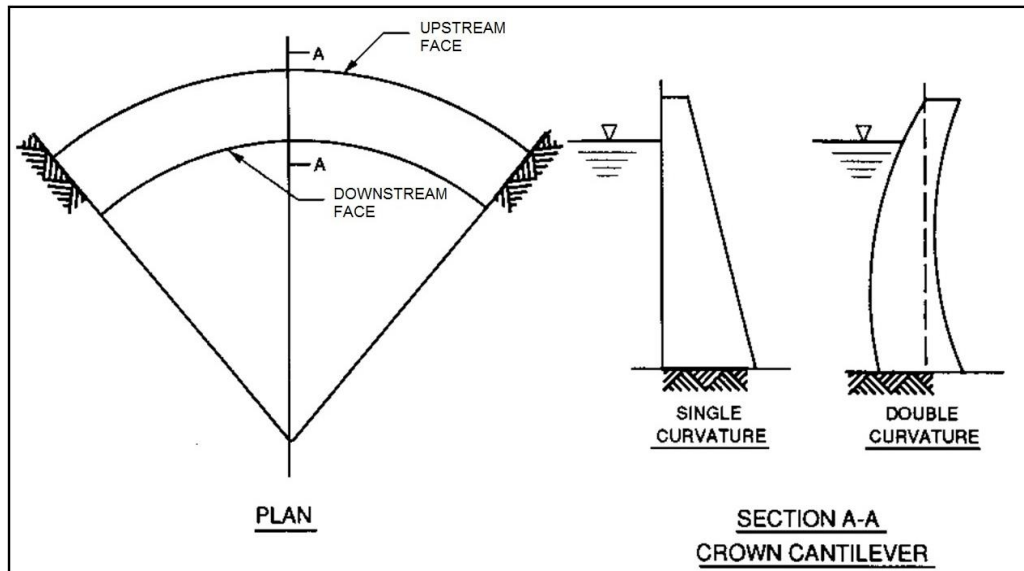


Figure 1: Single- and double-curvature arch dam [1].

The main goal is to design an arch dam that carries static and dynamic loads into the abutments and foundation as efficiently and effectively as possible, while at the same time the least essential concrete volume is used to optimize the concrete strength [4]. This can result in a much more economical dam in terms of concrete and excavation volume but at the same time the modelling effort is significantly increased.

Hence, the design of arch dams is a very complex and sensitive process. It starts with an initial dam layout, usually obtained from empirical methods, and it is reshaped until the geometric and stress constraints are satisfied within the design objectives.

Note that, possible concrete cracks are only avoided by reshaping the affected areas of the dam and reducing the respective tensile stresses. Reinforcement in arch dams is usually avoided due to the high cost.

The geometric constraints are guidelines which should be followed so a valid dam shape can be obtained [3]. They are thoroughly described in Chapter 4 and the most important ones are.

- The base thickness must be greater than the crest thickness.

- The radius at the crest must be greater than the radius at the base.
- At every elevation, the angle between the arches and the rock contour lines must be greater than 30° to avoid shear stress concentrations around the rock surface.
- The shape of the dam must be as smooth as possible. No sharp corner points are allowed which may result in local anomalies and consequently to stress concentration areas.
- No gaps are allowed between the arch dam and the surrounding topography.

The stress constraints indicate the allowable stress level in tension and compression for a combination of static loads, like gravity, shrinkage or water, and dynamic loads, like seismic [3].

- The principal tensile stresses should be avoided, but this is almost impossible. It is generally accepted that they are smaller than 1 MPa.
- The principal compressive stresses must be smaller than the chosen concrete strength class divided by a factor of safety.

The design objectives refer to the economic point of view of the structure. As a result, the least possible concrete and excavation volumes must be chosen while at the same time the design constraints are satisfied. This combination is mostly based on the designer's judgement and experience.

In the context of this master project, only double-curvature arch dams are investigated. The reason is that, their shape is much more flexible compared to single-curvature arch dams resulting in an even more economical design. However, the complexity of the design is significantly increased as more constraints must be taken into account.

2.2. Parabolic equation

In this section, the modified equation of a parabola (2.1) is introduced which is the basis to describe the entire geometry of a double-curvature arch dam. This equation is obtained from the document [2] where a real double-curvature arch dam is analyzed.

The geometry of double-curvature arch dams is described by several sets of equations which are most commonly based on circular or parabolic formulas. The main difference between the two formulas is that, circular formulas cannot describe the abutment thickening as efficiently as parabolic formulas. As a result, more concrete volume is used when circular formulas are applied resulting in a more expensive structure.

Furthermore, industry regarding dam design is familiar with parabolic and elliptical definitions. Therefore, the modified parabolic formula (2.1) will be used to describe the different sets of equations as it is necessary to combine engineering with theoretical considerations. Further research is essential for this part and it is out of the context of this report.

Higher order formulas may be used as well, but there are several issues that have to be taken into account. The computational effort and the complexity of the geometry are significantly increased. The symmetry, around a reference line, is not always preserved and this is one of the essential characteristics of arch dams for uniform shape. Local anomalies in the dam geometry, like dimples or wiggles, are more possible to occur resulting in stress concentration areas. More constraints have to be taken into account making the entire design process even more sensitive.

In Figure 2 a representative parabola is given showing the respective equation, the symmetry line, the focus point, the symmetry point and the radius. It is mentioned that, the focus point is called also the center of the parabola and this term will be used in the following chapters.

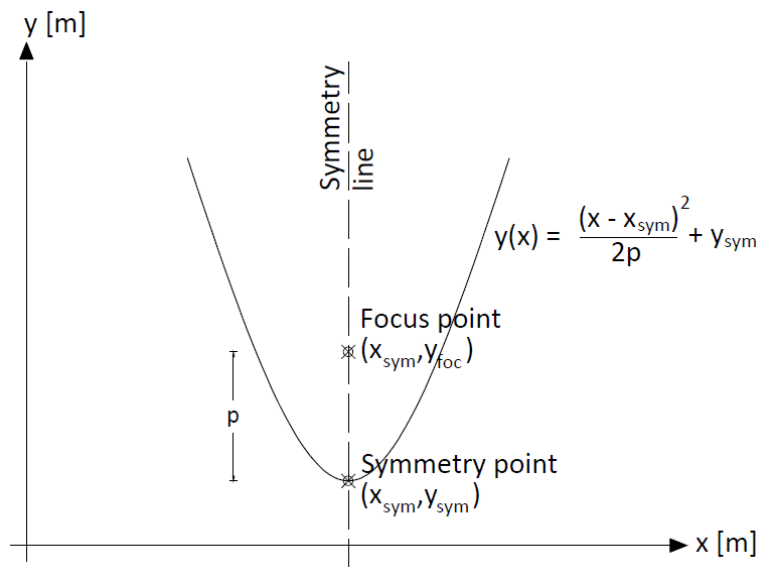


Figure 2: The equation of the parabola, the focus point and the symmetry point (plan view).

$$f(x) = \frac{(x - x_{sym})^2}{2p} + y_{sym} = \frac{1}{2p}x^2 - \frac{x_{sym}}{p}x + \left(\frac{x_{sym}^2}{2p} + y_{sym}\right) = ax^2 + bx + c \quad (2.1)$$

Where, $a = \frac{1}{2p}$, $b = -\frac{x_{sym}}{p}$, $c = \frac{x_{sym}^2}{2p} + y_{sym}$ are the constants of the parabola.

(x_{sym}, y_{sym}) is the symmetry point of the parabola [Figure 2].

(x_{sym}, y_{foc}) is the focus point of the parabola [Figure 2].

p is the distance between the symmetry and the focus point [Figure 2].

The main advantage of the latter equation is that a parabola can be described only by two control points, the focus and the symmetry point, and this is very convenient during the dam design as it uses the minimum number of control points.

2.3. Main parts of a double-curvature arch dam geometry

A double-curvature arch dam consists of four main parts which describe the geometry of the two faces, the abutment thickening and the dam-rock interface geometry. Knowing these parts a dam can be fully defined and reshaped.

2.3.1. Crown cantilever section

The crown cantilever is defined as the maximum height vertical cross-section of the dam and it is usually located in the streambed. It is the center of the dam controlling its entire shape. For this reason, it significantly influences the distribution and the magnitude of stresses within the body [1].

The upstream and the downstream line of the crown cantilever section contain the symmetry points of the parabolas which describe the main upstream and downstream dam face respectively. Knowing the equations that describe these two lines the symmetry points at every elevation can be computed [Figure 3].

The equations can be obtained from empirical methods which are thoroughly described in Section 4.6.

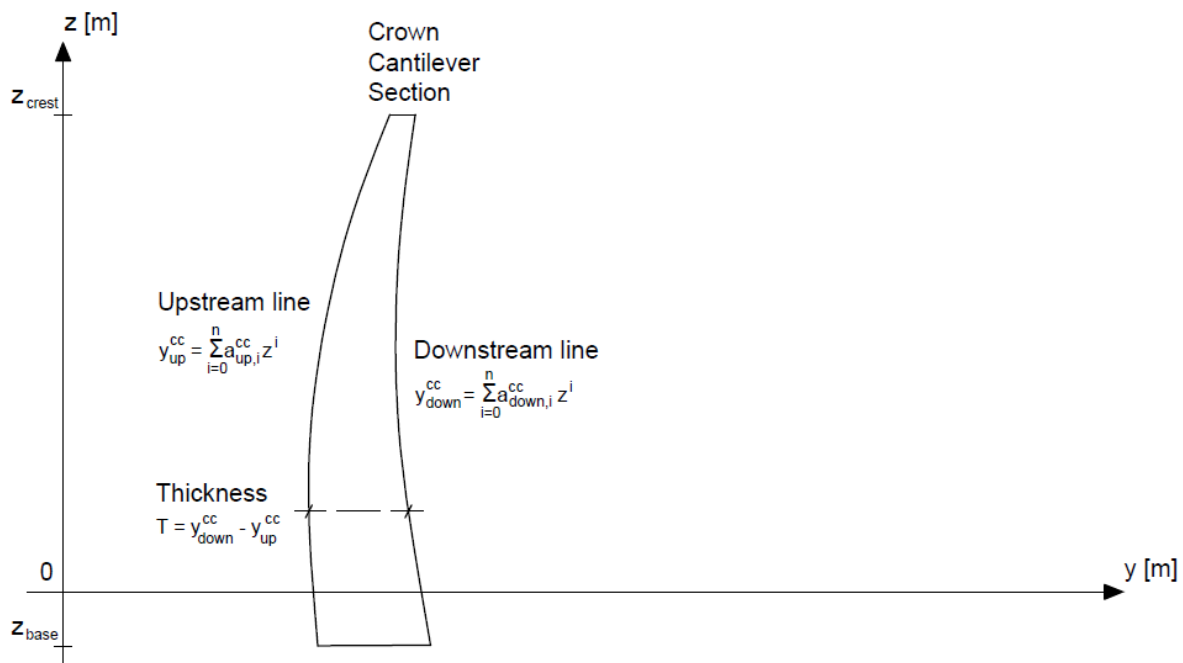


Figure 3: Crown cantilever section (side view) [2].

2.3.2. Main parabolas

There are two sets of main parabolas which define the upstream and downstream face of the dam. The two faces are fully described when the equations of the crown cantilever section and the line of centers are known [Figure 4]. The latter equations are thoroughly described in Sections 4.6 and 4.7 respectively.

Note that, both faces use the same line of centers. In this way, the thickness changes for the y-z (side) section, following the shape of the crown cantilever, while at every elevation in the x-y (plan) section it remains constant.

This is more apparent in the following two figures. Figure 4 shows the y-z (side) section of the crown cantilever, where the thickness changes along the dam height. Figure 5 shows the x-y (plan) section and the respective main parabolas at a random elevation i . Both parabolas use the same center point i , so the thickness remains constant for the entire section. This would not be the case if different centers were used.

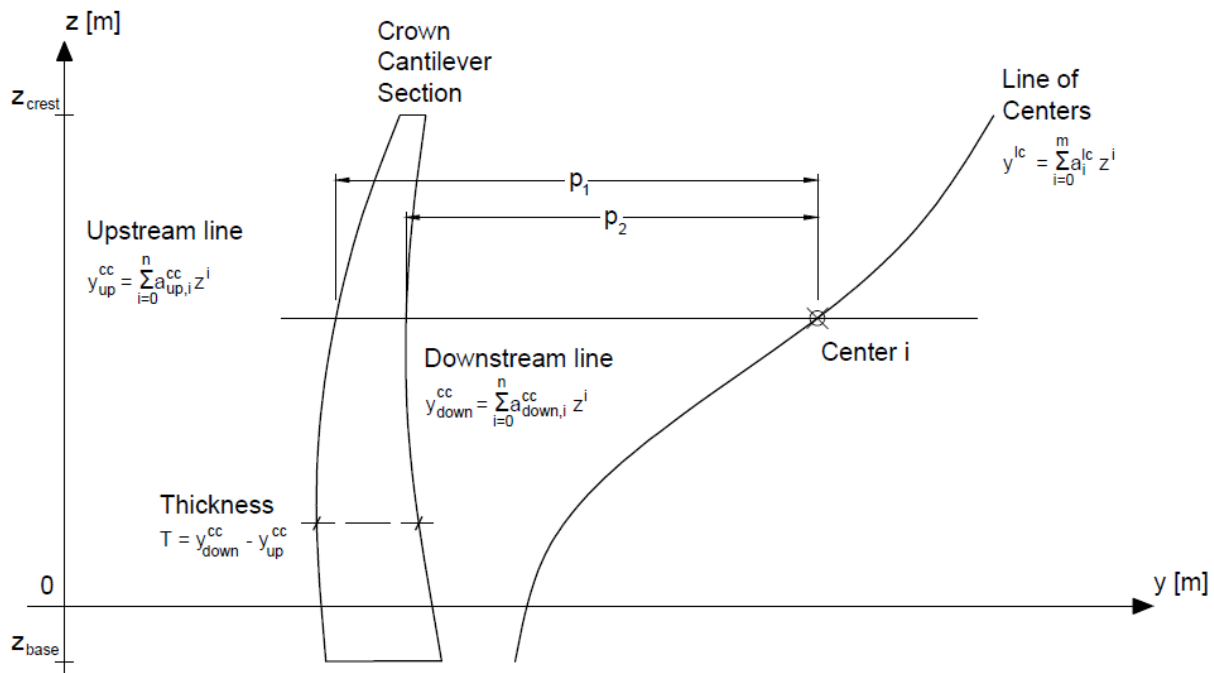


Figure 4: Upstream and downstream symmetry lines and the line of centers (side view) [2].

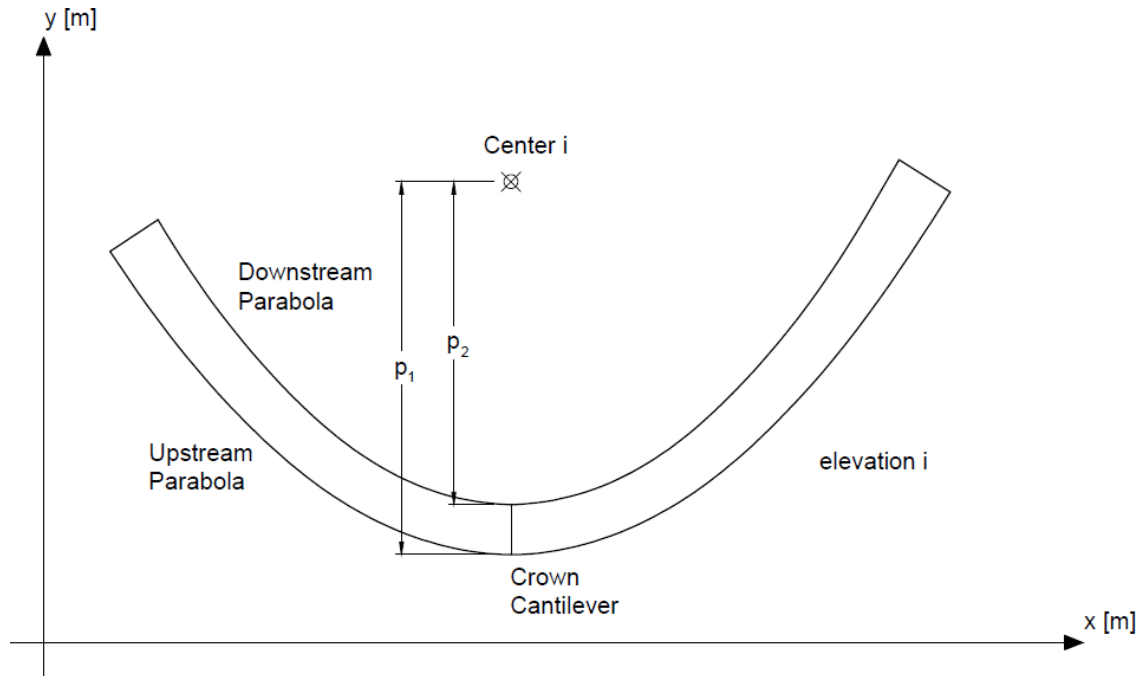


Figure 5: Upstream and the downstream main parabolas at elevation i (plan view) [2].

2.3.3. Side parabolas

In case where abutment thickening is required, two more sets of parabolas, one for each side, are used in the downstream face named side parabolas. Side parabolas are dependent on the main downstream parabolas and they define the needed abutment thickening.

The main objective is to define a side parabola which is tangent to the respective main downstream parabola at every elevation. So a uniform increase in abutment thickening over the entire dam is achieved. Figure 6 shows the basic concept of the side parabolas, where T_L and T_R are the tangent points and C_L and C_R are the side center points for the left and right bank.

A tangent point is the common point of the side parabola with the downstream main parabola. For this point the tangents of the latter parabolas must be equal so a smooth transition is achieved. In this way, geometric anomalies, like dimples, are avoided which may result in stress singularities.

In Figure 7 the line of side centers and the line of tangent points are shown. These lines must remain smooth along the dam height so the main objective is satisfied. If there are wiggles in these lines, geometric anomalies may occur as well.

This part is thoroughly explained in Section 5.1.1 where all the essential tools are described and visualized.

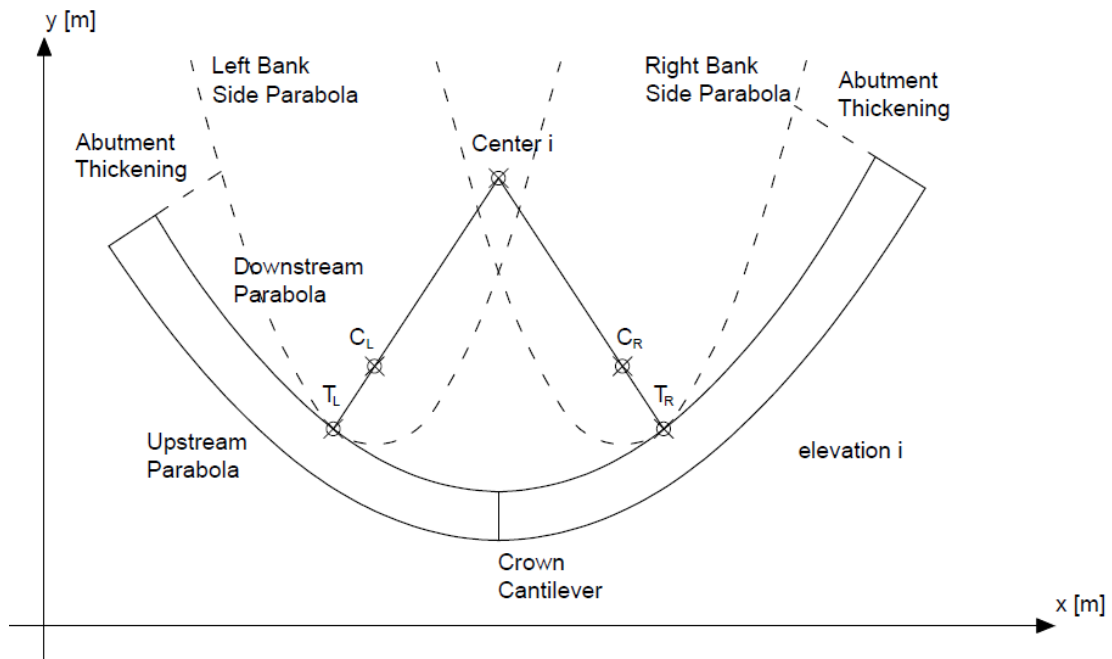


Figure 6: Left and right bank side parabolas at elevation i (plan view) [2].

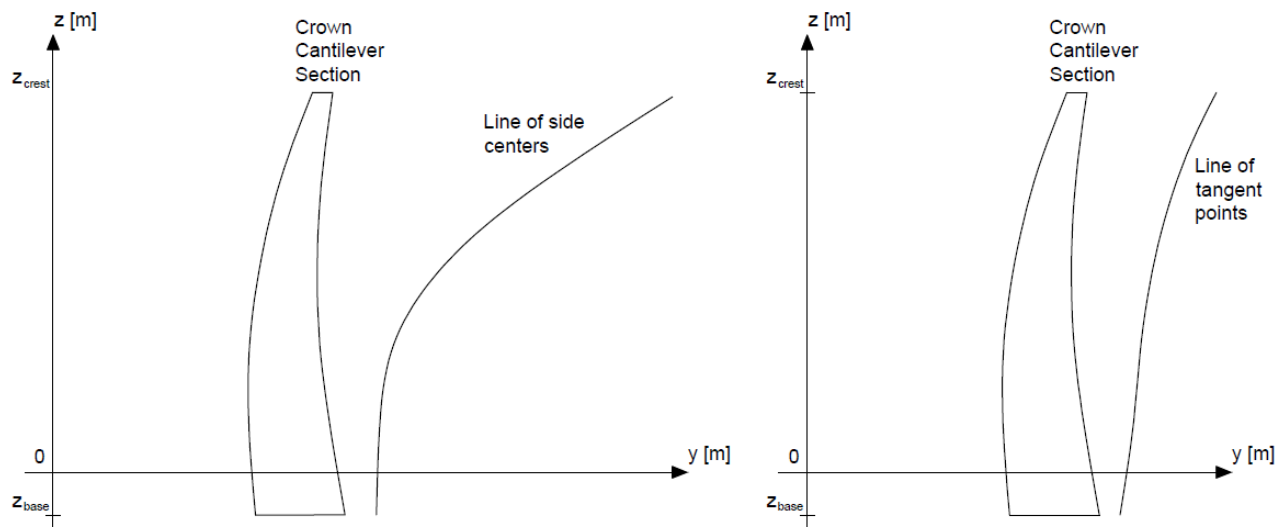


Figure 7: Left figure, line of side centers. Right figure, line of tangent points [Side view] [2].

2.3.4. Foundation area

The foundation area is the dam-rock interface geometry and it is defined by the end points of the parabolas of the upstream and downstream face. This part is very important for the geometry of the dam as it shows if there are gaps between the dam and the respective topography.

The geometry of the foundation area is very complex and special attention must be given to generate a valid and smooth shape. This part is explained in Sections 4.8 and 4.9.

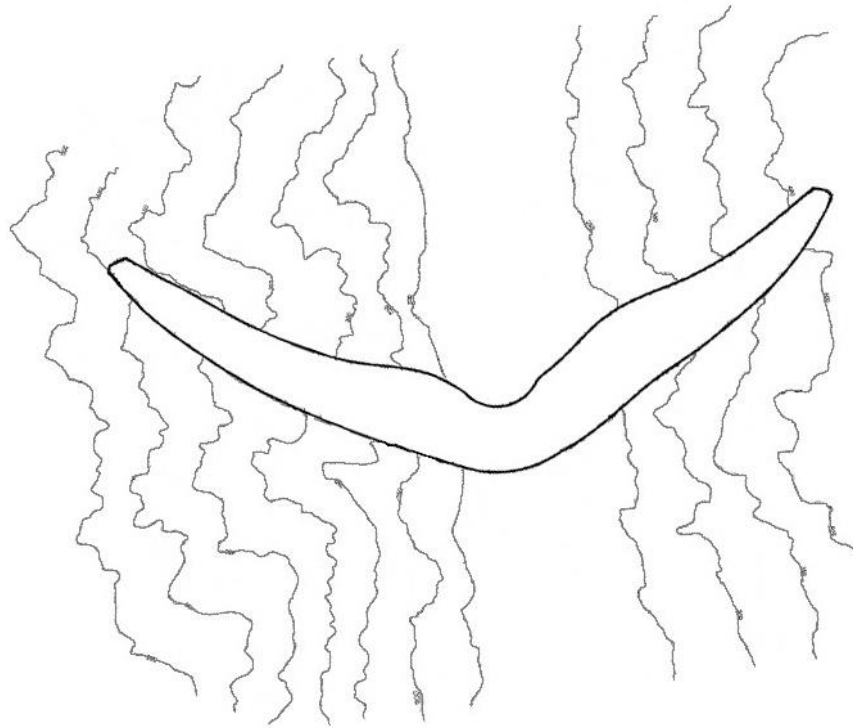


Figure 8: Foundation area (plan view) [2].

3. General workflow of design stages

In this chapter the general workflow of the process to design a double-curvature arch dam is shown. Every step is described in detail separately, pointing out all the essential assumptions. It will be explained how each step can be translated into workflows and consequently into automated processes.

The following method is based on the Engineer Manual [1] as it describes a very realistic and efficient way, which is used in practice. However, the described steps are done by hand using outdated implements, like transparent papers, rulers or French curves, and for this reason they are translated into mathematical processes so they can be described by automated processes in Python.

During the preliminary design stage the best fitting dam is determined based on the least concrete and excavation volume, which are the predominant factors. While, during the final design stage the best alternative from the previous stage is reshaped till the desirable stress levels are reached.

The preliminary and final design stages are thoroughly described in Chapters 4 and 5 respectively.

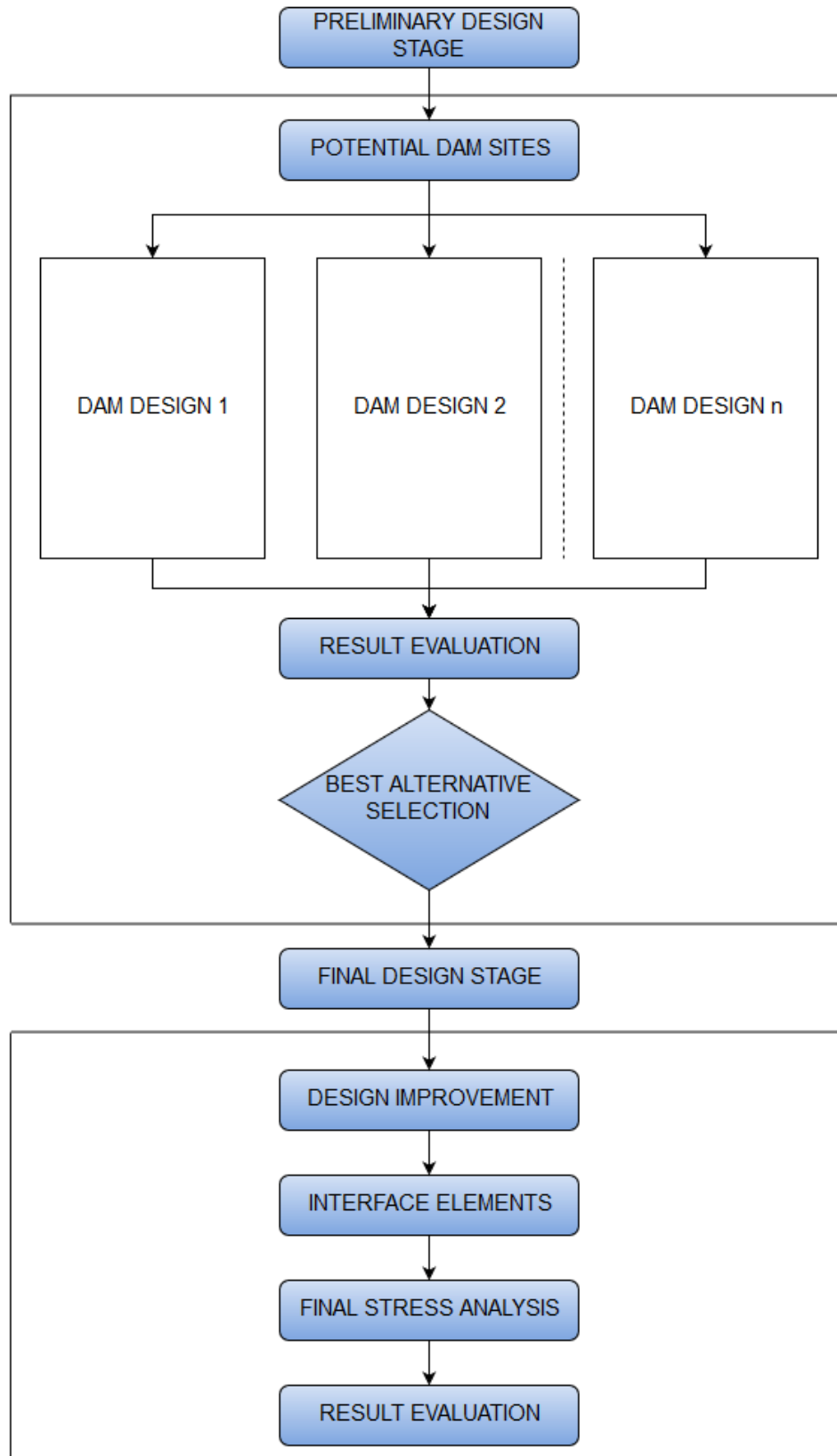


Figure 9: The general workflow.

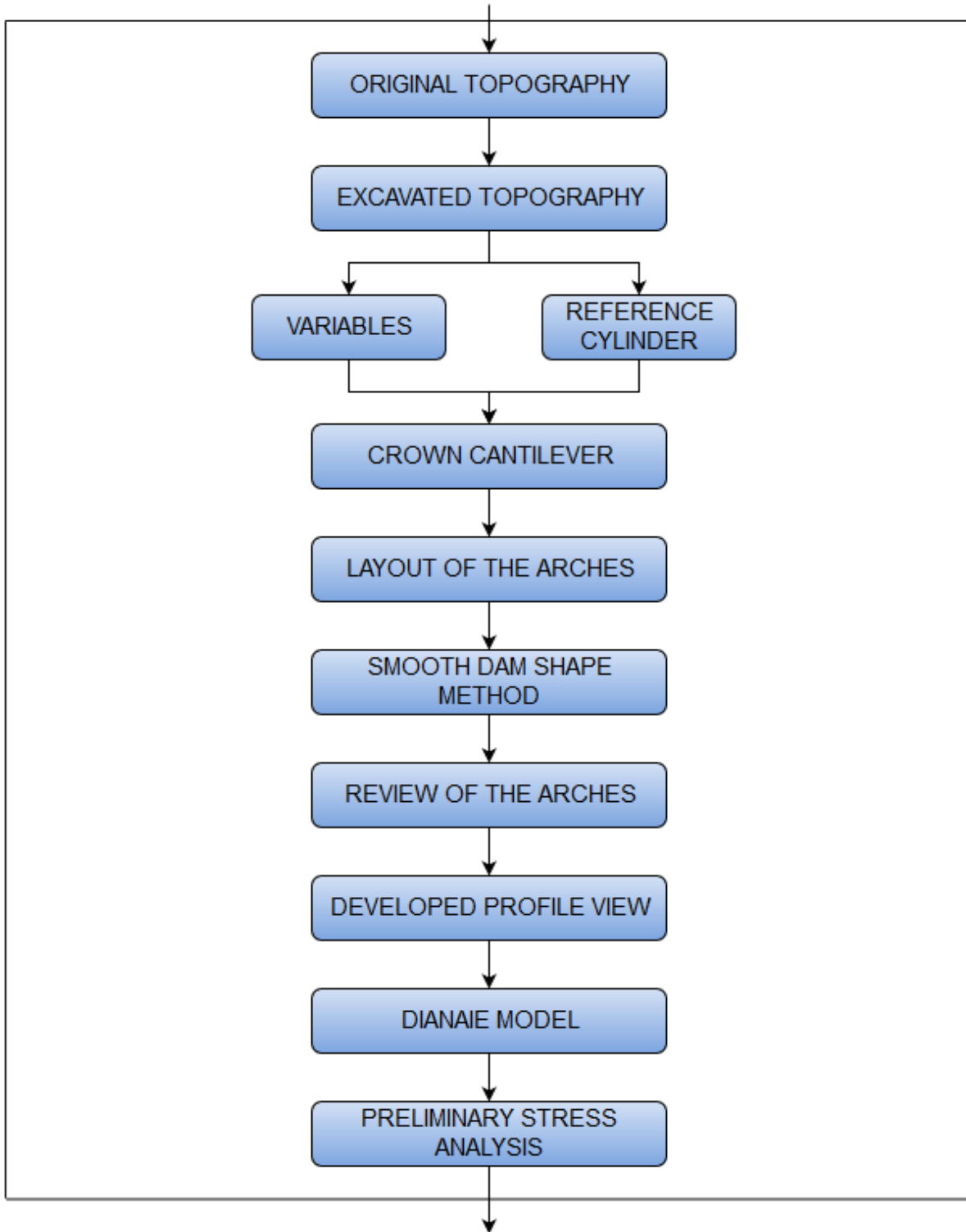


Figure 10: The workflow of the dam design.

4. Preliminary design stage

First the best fitting dam along the valley must be found. For this reason, different dam sites must be chosen, where the number of the dam sites is defined by the designer. For each site the best fitting dam must be generated based on two predominant factors; the dam concrete volume and the excavation volume. Afterwards, the different dam sites are compared so that the best alternative can be found, which will be used for the next stage, the final design.

It is also mentioned that the stress peaks for each location are not that important for the preliminary design stage as stress singularities occur around the common surfaces of the dam with the rock. During this stage, the side parabolas are not taken into account as they are used to modify the stress peaks during the next stage.

4.1. Potential dam sites

Firstly, the potential dam sites must be selected and the corresponding topographic maps must be examined in conjunction with site visits. Emphasis should be placed on the site suitability, taking into account the canyon profile and the foundation characteristics amongst other factors.

The height of the dam, geological features (rock types, faults, etc.) and the extent of the reservoir (compressible or incompressible) in the upstream direction from the dam body (tailwater conditions are normally neglected) will define the extent of the topographical data needed in the design and analysis process. By “extent” of topographical data, this means both the surface area surrounding the dam and the interval of contour lines (10 m, 15 m, 20 m etc.).

Allowing for some shifting on the dam axis along the reservoir axis, it is recommended to have topographical maps extending three (3) to five (5) times the height of the dam in the upstream and downstream directions of the dam and between two (2) and four (4) times the height of the dam perpendicular to the dam axis measured from the left and right bank crest arch points [Figure 11].

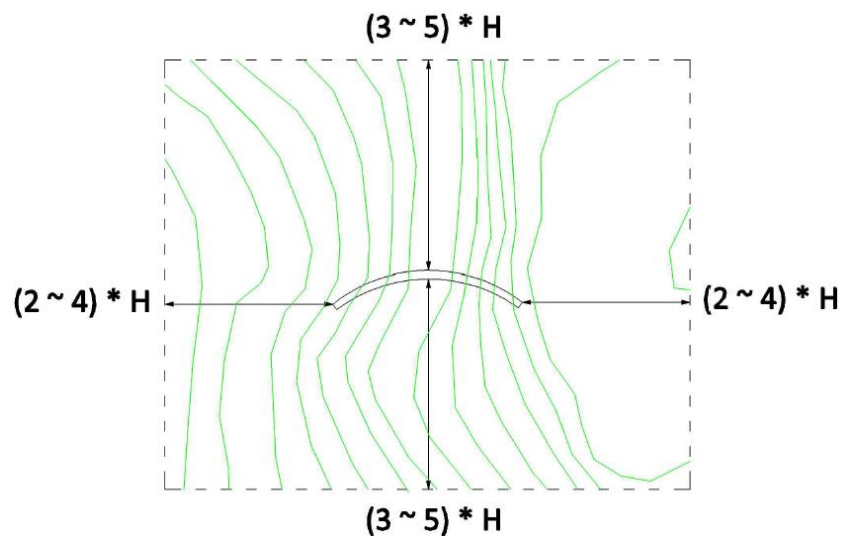


Figure 11: Recommended size of the topographical map (plan view).

4.2. Original topography

The original topography (natural ground profile) is the first input and consists of a set of polylines which represent the unexcavated topographic map contour lines. The computational effort decreases significantly using two-dimensional polylines instead of a three-dimensional surface defined as a cloud of points.

To generate a realistic topographic data the following process is proposed. The topography of Deriner Dam, a real dam constructed in Turkey, is used as an example to illustrate the process.

Through SketchUp 2015, <http://www.sketchup.com/>, a dxf file is extracted containing all the essential information for the topography of the surface area. The process to obtain the dxf file is the following [10].

- Launch SketchUp 2015
- Add location → Find the desired location → Select region → Grab
- Toggle terrain [from 2D to 3D surface, Figure 12]
- File → Export → 3D Model → Export as dxf/dwg file

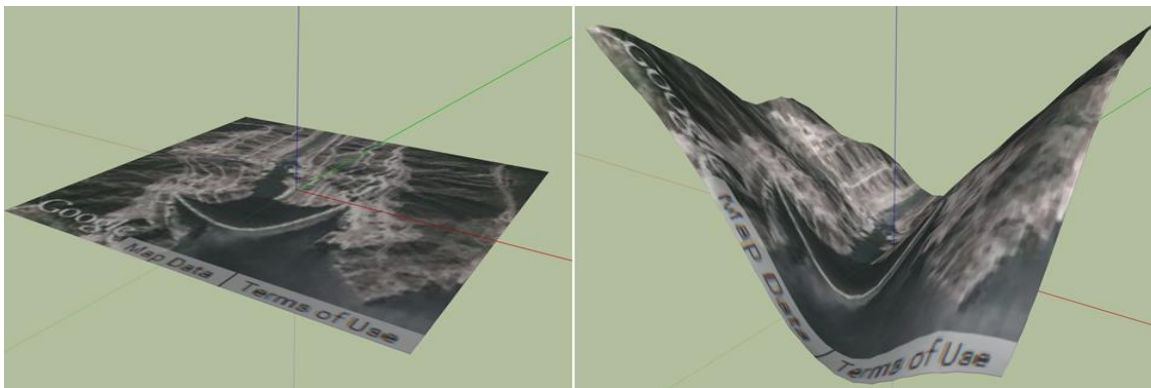


Figure 12: SketchUp 2015 – Deriner Dam – From 2D to 3D.

The dxf/dwg file exported from SketchUp 2015 is compatible with AutoCAD software.

Using AutoCAD, open the dxf/dwg file and put manually all the points that are essential for the topography. The topographic points must be created in a different layer. After drawing all the essential points all the layers except for the points' layer must be turned off. The drawing must be saved as "Autocad R14/LT98/LT97 Drawing (*.dwg)" because Dxf2xyz, the next program which is used, is compatible with AutoCAD versions up to 2002 [Figure 13].

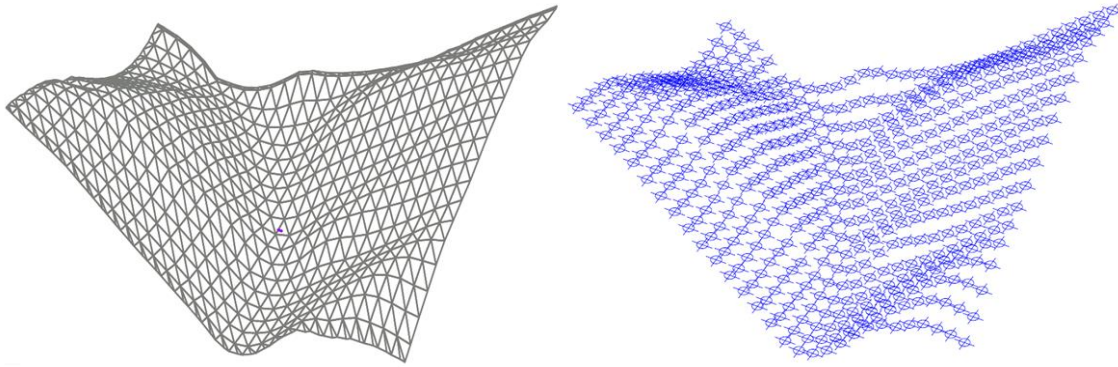


Figure 13: The dwg file obtained from SketchUp and the respective topographic points (3D view).

Using the freeware program Dxf2xyz 2.0, <http://www.guthcad.com.au/freestuff.htm>, select the AutoCAD drawing and save it as topo_points.xyz. As a result, a text file is created containing all the coordinates for the surface area. The first, second and third column contain the X, Y, Z coordinates respectively [11].

4.3. Excavated topography

The excavated topography is the second set of topographic contour lines that is required and describes the topography of the sound rock foundation on which the dam structure shall be founded. At this stage of the design only the surface topography is available and for this reason the designer must assume a reasonable amount of overburden based on core borings or sound judgement.

For this reason, an initial uniform excavation length at every elevation must be given by the designer. A reasonable value for the excavation can be from 10 to 30 meters (good rock conditions with minor weathering and a canyon profile ideally suited to an arch dam) in the lateral direction [Figure 14].

Using the Left Hand Side (LHS) crest elevation excavation polyline [Figure 14], the start and symmetry point of the reference cylinder are chosen. At this stage the end point is not used as it is calculated and checked in Section 4.5 [Figure 16]. The reference cylinder represents the upstream crest elevation parabola.

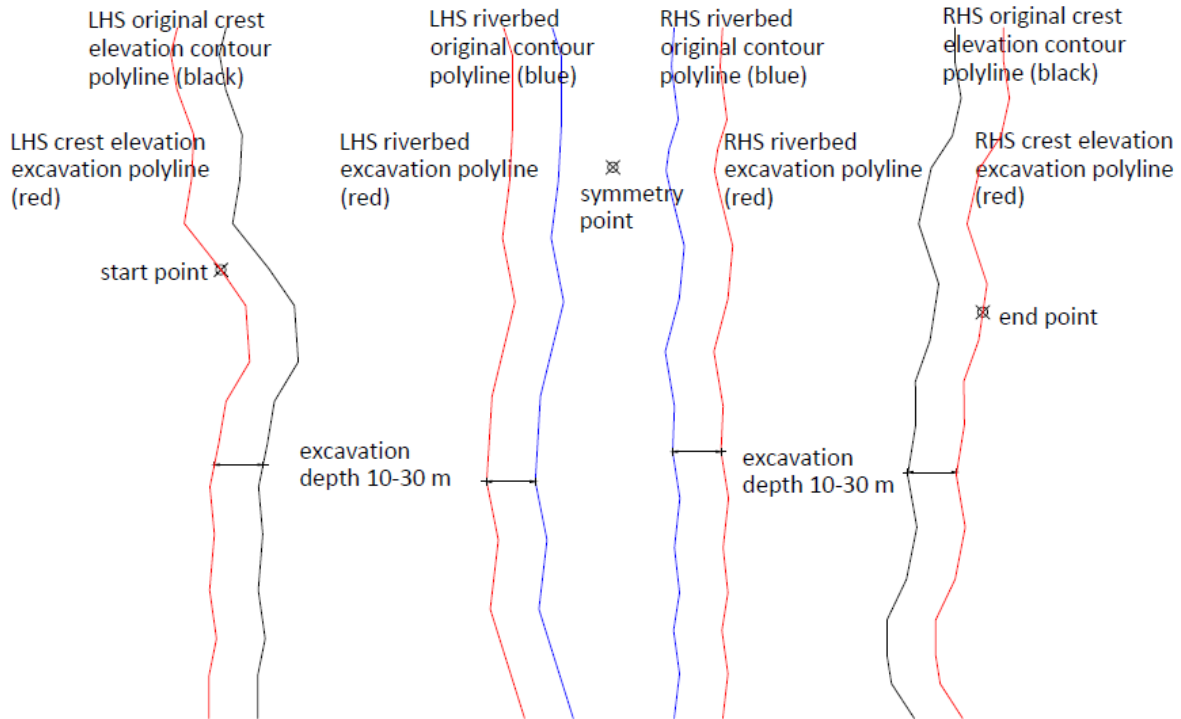


Figure 14: Excavation polylines (plan view, river profile in blue based on non-flood or conditions).

4.4. Basic variables

Having the excavated topography described by two-dimensional polylines the next step is to define the basic variables of the arch dam geometry. The present method is based on the Engineer Manual [1] and therefore implicitly defines the dam shape type in plan and in section. Plan view dam geometries vary in accordance with the canyon profile, geological conditions etc. and may be elliptical, circular, parabolic, log-spiral or some other cylindrical form.

It should be mentioned that the U.S. Bureau of Reclamation (USBR) method does not strictly allow for thickening of the arches unless the main parabola is translated downstream and defines the downstream parabola. To overcome this problem, another method is proposed in the chapters that follow.

Six basic variables are defined to describe the entire dam geometry and they must be defined by the designer.

1. y_{start} [meters] is the Left Hand Side (LHS) y-coordinate of the upstream crest elevation parabola and it controls the location of the dam, its value must be inside the borders of the topographic surface.
2. H [meters] is the height of the dam (from the lower point of the riverbed to the crest elevation), defined from the hydrologic data [Figure 20].
3. z_{base} [meters] is the elevation of the dam base. If there is no information for the base elevation, it should be about 8 meters below the riverbed [5].

4. θ_{axis} [degrees] is the angle of the dam axis and represents the orientation of the dam. Using this variable the entire dam is rotated respective to the riverbed [Figure 19].
5. $L_{excavation}$ [meters] is the assumed initial uniform excavation length and it is defined from before, a positive value is required [Section 4.3].
6. $L_{excavation}^{min}$ [meters] is the minimum excavation length that is allowed for the dam, a positive values is required [Section 4.9].

Having defined the latter variables the following variables can be computed automatically through the code.

- L_1 [meters] is the straight line distance measured between abutments excavated to assumed foundation rock at crest elevation [Figure 15]. This parameter is generated automatically.
- L_2 [meters] is the straight line distance measured between abutments excavated to assumed foundation rock at 0.15H above the base of the dam [Figure 15]. This parameter is generated automatically.
- V_{theor} [cubic meters] is the theoretical concrete volume and it is arrived at empirically by the following equation obtained from the Engineer Manual [1]. This parameter is generated automatically.

$$V_{theor} = 0.0001772H^2L_2 \frac{(H + 0.8L_1)^2}{L_1 - L_2} + 0.0108HL_1(H + 1.1L_1) \quad (4.1)$$

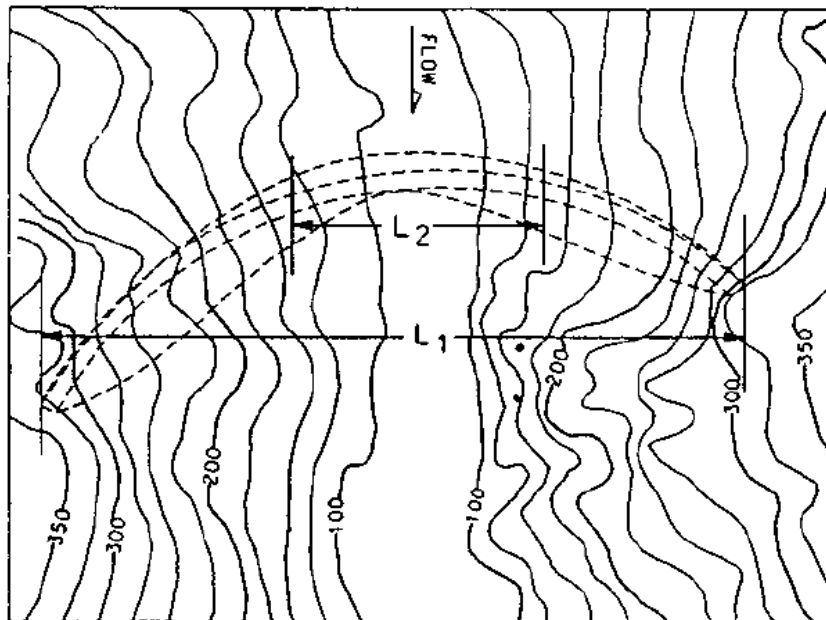


Figure 15: Definition of the values L_1 and L_2 (plan view) [1].

4.5. Dam axis and reference cylinder

For design and build reasons, the geometric definition of the dam body is defined with reference to both the dam axis and reference cylinder. The former defines the orientation of the dam body in plan with respect to the river axis and the latter, is a simple single curvature geometric shape that encompasses the dam body in plan and elevation.

The reference cylinder then becomes the projection plane for dam body developed views which are not only inherent within the modelling and post-processing concepts of DIANA, but also represent a fundamental design “element” for dam engineers allowing the coherent evaluation of computed results and the design layout, for example, of dam instrumentation.

Herein, the reference cylinder is the upstream crest elevation parabola and it is very important as it controls the general shape of the dam. The equation of a parabola can efficiently describe the geometry of the dam and is favored because it readily allows the excavation depth to be increased due to geological uncertainties (weak/weathered rock), without necessarily modifying the entire geometric shape of the dam (as might be the case for an elliptically shaped structure).

For this reason, two points must be given. The first one is already known from before and it is the start point of the reference cylinder. The second one is the crown cantilever point of the reference cylinder and it is generated automatically using the lowest contour line which represent the riverbed. This point is the symmetry point of the parabola and it must be located above the streambed [Figure 16].

The optimal location for the dam crest must be defined by the following conditions [1].

- The angle of incidence β , which is the angle between the tangent of the reference cylinder and the average contour line of the abutment rock, at the crest elevation should be approximately equal for both sides [Figure 17]. A tolerance is chosen to judge if the angles are equal and their deviation is set to 10 degrees or less.
- R_{AXIS} , which is the radius of the reference cylinder, may require lengthening if the parabola fails to make contact with the abutments and it is computed using the empirical formula $R_{AXIS} = 0.6 * L_1$ [Figure 15].
- The largest practicable central angle must be between 100 and 120 degrees. If the central angle is larger than the recommended values the radius R_{AXIS} must be increased [Figure 15].

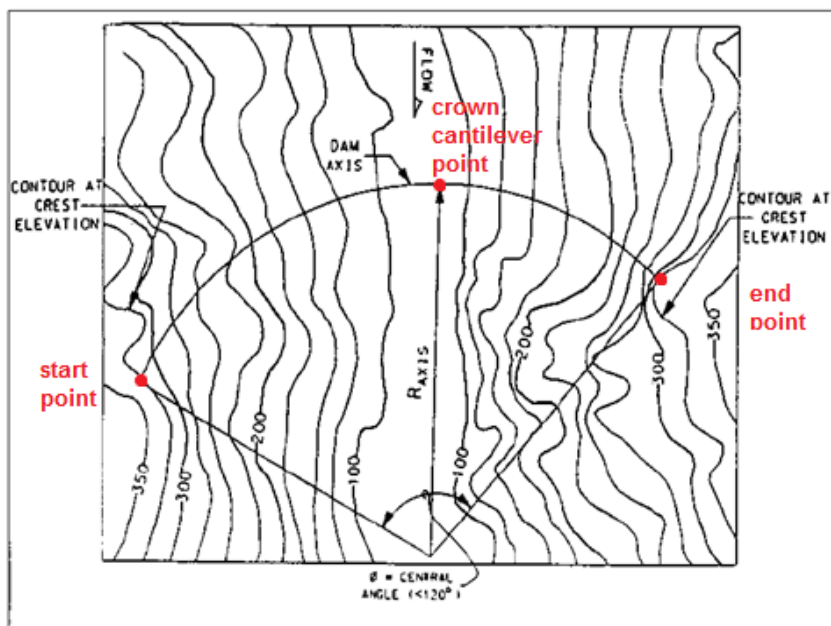


Figure 16: Layout of the dam axis, the reference cylinder and the central angle (plan view) [1].

The angle of incidence β is very important to determine the abutment rock contour lines. It is used as a guideline during the preparation of the layout and the parabolas are arranged so that β is larger than 30 degrees in the upper half [Figure 17] [1].

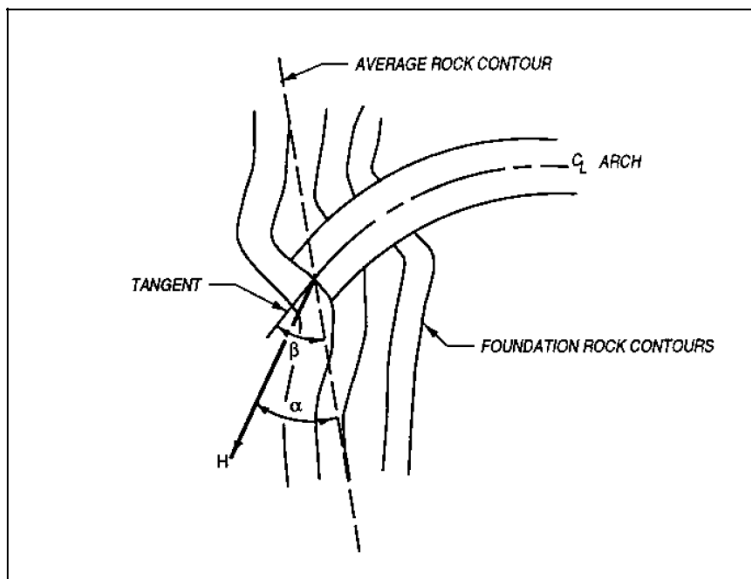


Figure 17: Angle β between thrust and rock contours (plan view) [1].

The average rock contour is computed using the method of least squares taking into account the topographic points in a range of 75-100 meters around the abutment. This method is used to compute the best fitting line for the chosen points [Figure 17].

The following workflow shows how the reference cylinder can be found following an iterative process.

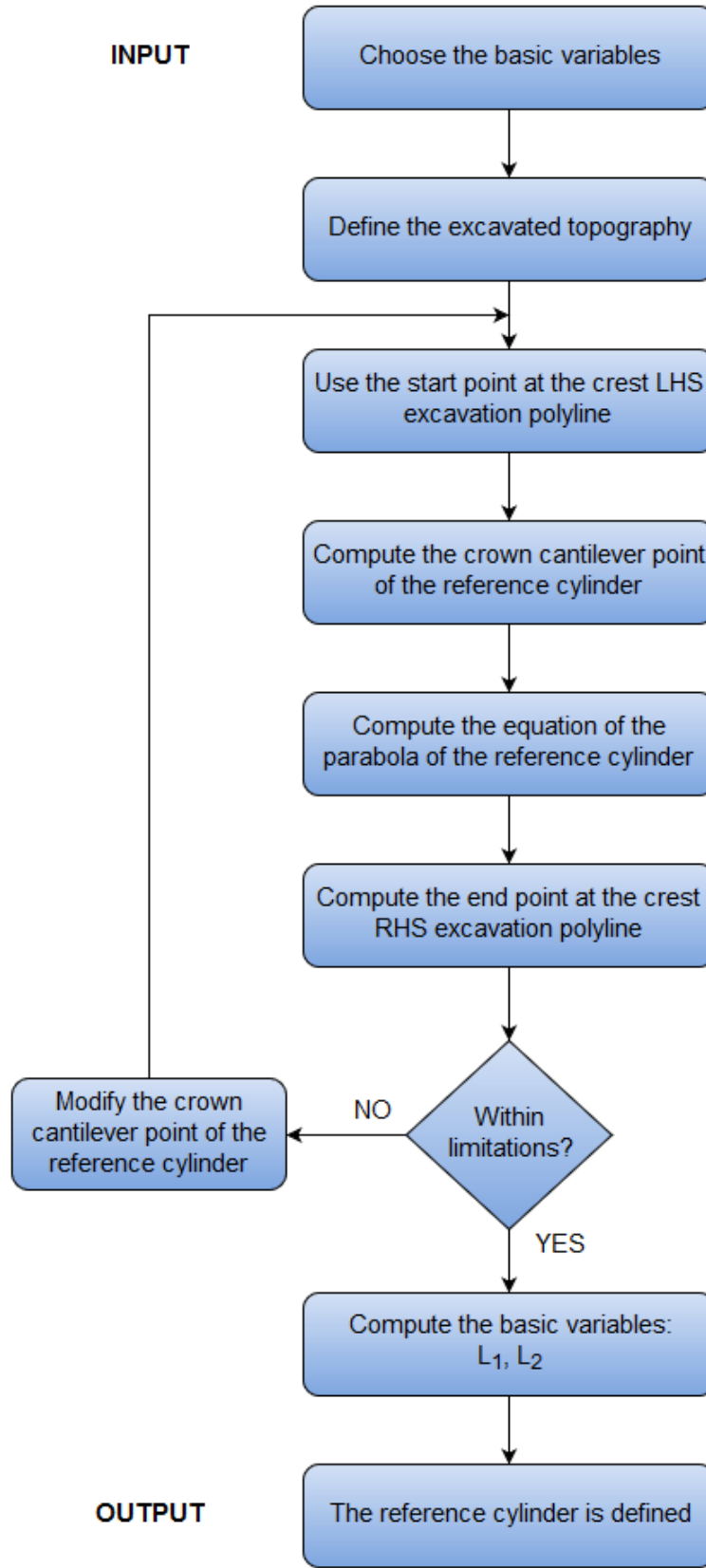


Figure 18: The workflow of the reference cylinder.

4.6. Crown cantilever section

As previously mentioned, the crown cantilever section is defined as the maximum height vertical cantilever and it is usually located in the streambed. At this stage the reference plane is detected drawing a vertical line that passes through the crown cantilever point. The reference plane contains the crown cantilever and the loci of the parabolic centers [Figure 19].

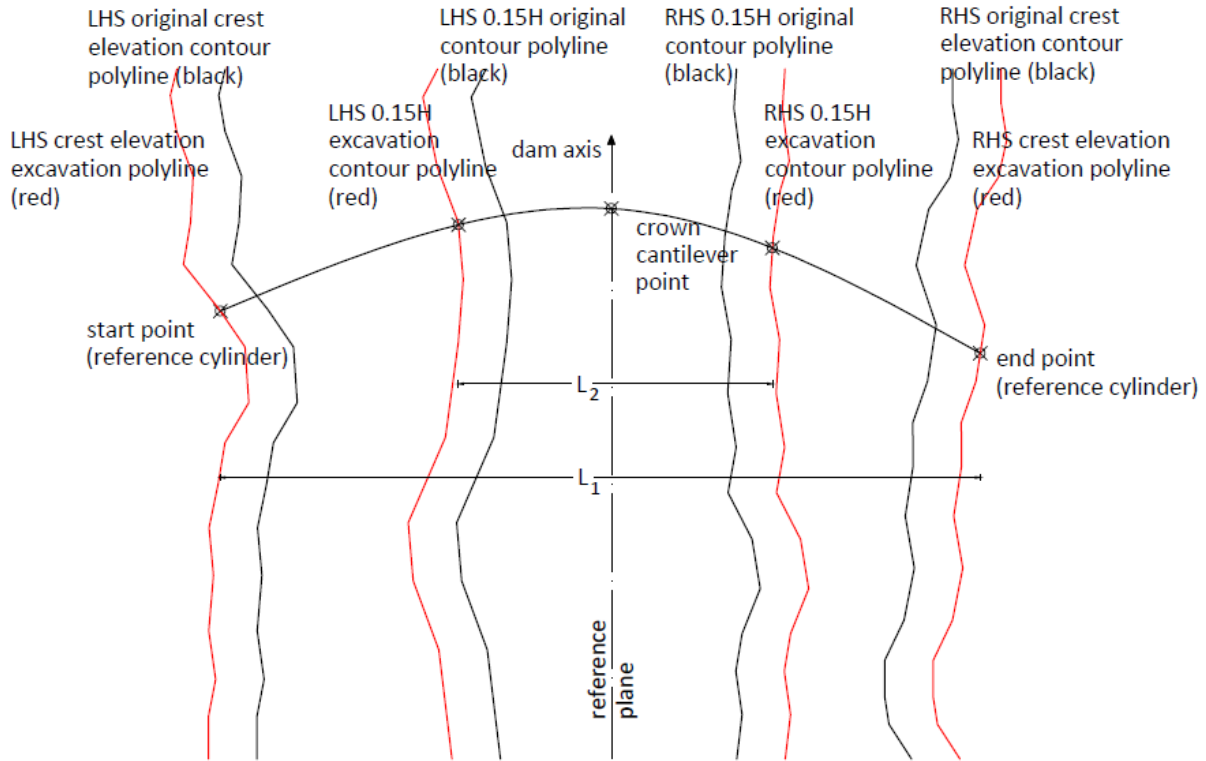


Figure 19: Reference plane of the arch dam (plan view).

According to the Engineer Manual [1], the geometry of the crown cantilever is computed using the empirical equations:

$$T_C = 0.01(H + 1.2L_1) \text{ [feet]} \quad (4.2)$$

Where, T_C is the thickness at the crest elevation.

$$T_B = \sqrt[3]{0.012HL_1L_2 \left(\frac{H}{400}\right)^{\frac{H}{400}}} \text{ [feet]} \quad (4.3)$$

Where, T_B is the thickness at the base elevation.

$$T_{0.45H} = 0.95T_B \text{ [feet]} \quad (4.4)$$

Where, $T_{0.45H}$ is the thickness at $0.45H$ above the base.

The variables of the upper formulas are based on the imperial system and therefore they are modified to the metric system.

$$T_C = 0.01(H + 1.2L_1) [meters] \quad (4.5)$$

Where, T_C is the thickness at the crest elevation.

$$T_B = \sqrt[3]{0.0012HL_1L_2 \left(\frac{H}{121.92}\right)^{\frac{H}{121.92}}} [meters] \quad (4.6)$$

Where, T_B is the thickness at the base elevation.

$$T_{0.45H} = 0.95T_B [meters] \quad (4.7)$$

Where, $T_{0.45H}$ is the thickness at $0.45H$ above the base.

In addition, the upstream and downstream projections of the crown cantilever faces at these elevations can also be arrived at empirically. Three points are known for each face and a circle can be drawn which passes through them [Figure 20].

$$USP_{CREST} = 0.0 \quad (4.8)$$

$$USP_{0.45H} = 0.67T_B \quad (4.9)$$

$$USP_{BASE} = 0.95T_B \quad (4.10)$$

$$DSP_{CREST} = T_C \quad (4.11)$$

$$DSP_{0.45H} = 0.0T_B \quad (4.12)$$

$$DSP_{BASE} = 0.33T_B \quad (4.13)$$

Where, USP_{CREST} is the upstream projection point at the crest elevation.

$USP_{0.45H}$ is the upstream projection point at $0.45H$ above the base.

USP_{BASE} is the upstream projection point at the base elevation.

DSP_{CREST} is the downstream projection point at the crest elevation.

$DSP_{0.45H}$ is the downstream projection point at $0.45H$ above the base.

DSP_{BASE} is the downstream projection point at the base elevation.

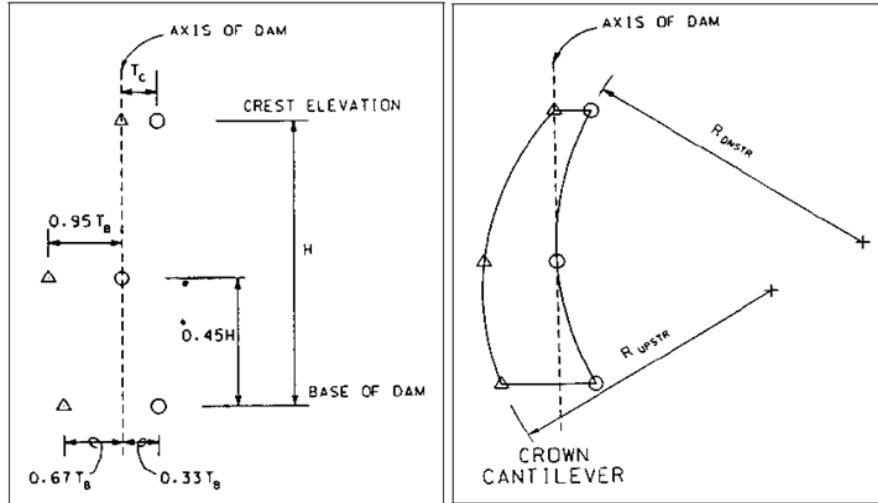


Figure 20: Projection points (left) and crown cantilever section (right) (side view) [2].

Parabolic equations are used to describe the lines of the crown cantilever section as it is assumed that they are more efficient. Knowing these equations the upstream and downstream projections can be computed at every elevation and this is very useful for the next steps.

$$y_{up}^{CC}(x) = a_{up}^{CC} z^2 + b_{up}^{CC} z + c_{up}^{CC} \quad (4.14)$$

Where, $y_{up}^{CC}(x)$ is the equation for the upstream line of the crown cantilever.

$$y_{down}^{CC}(x) = a_{down}^{CC} z^2 + b_{down}^{CC} z + c_{down}^{CC} \quad (4.15)$$

Where, $y_{down}^{CC}(x)$ is the equation for the downstream line of the crown cantilever.

4.7. Layout of the arches

The horizontal upstream and downstream parabolas must be defined. Starting from the upstream face the contact line at the dam-foundation interface is computed.

The points A, B and C are used to compute the equation of the contact line for the upstream face. The first two points are the corner points of the upstream crest elevation parabola, while the last one is the respective projection of the crown cantilever at the base. The contact line is required to compute the corner points of the lower parabolas [Figure 21].

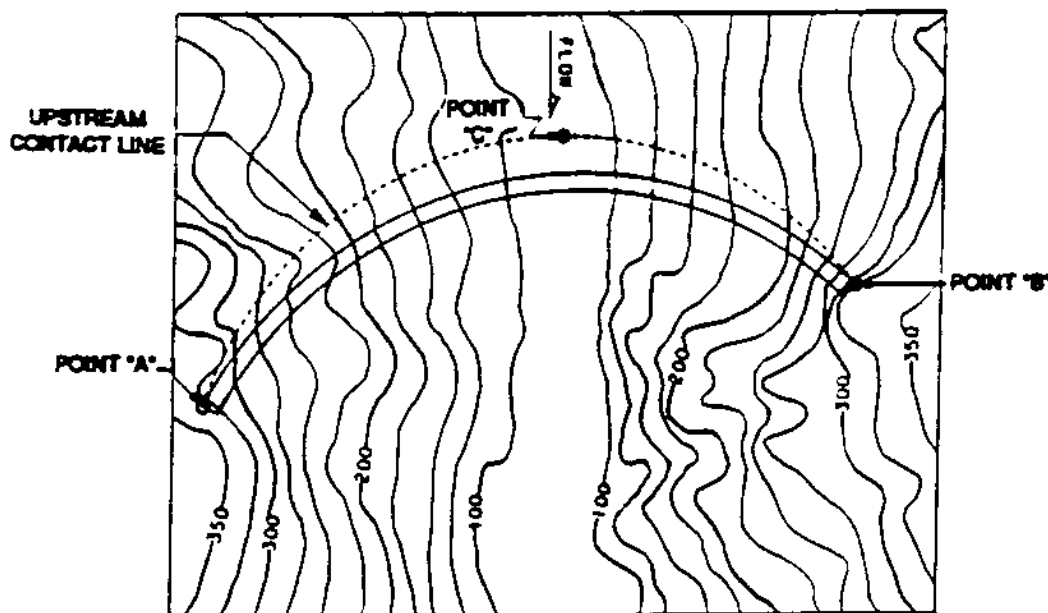


Figure 21: Upstream contact line (plan view) [1].

According to the Engineer Manual [1], the dam is divided into 5 to 10 evenly spaced horizontal arches and their respective parabolas are computed. They should be spaced not less than 3.048 meters (10 feet) nor more than 30.48 meters (100 feet) apart. The lowest parabola should be 0.15H to 0.20H above the base.

Having defined the equations of the upstream parabolas their center points are known as well. The center points can be used to calculate the equation of the line of centers. The order of the equation is dependent on the number of the divisions of the dam, for example if 5 evenly spaced arches are used then the order of the line of centers is 4. So, the set of the main upstream parabolas is defined.

Afterwards, using the respective downstream projections and the line of centers, the set of the main downstream parabolas can be found.

To compute the parabolas at the lower arches the following process is used.

First, the upstream projection in the crown cantilever section is calculated, using the equations obtained from the crown cantilever section, which is a point of the lower parabola. Then, the intersections between the respective topographic polylines and the contact line are found which give the end points of the parabola. It is mentioned that, the end points can terminate slightly deeper than the arch elevation, but there are no specific guidelines. [Figure 22]

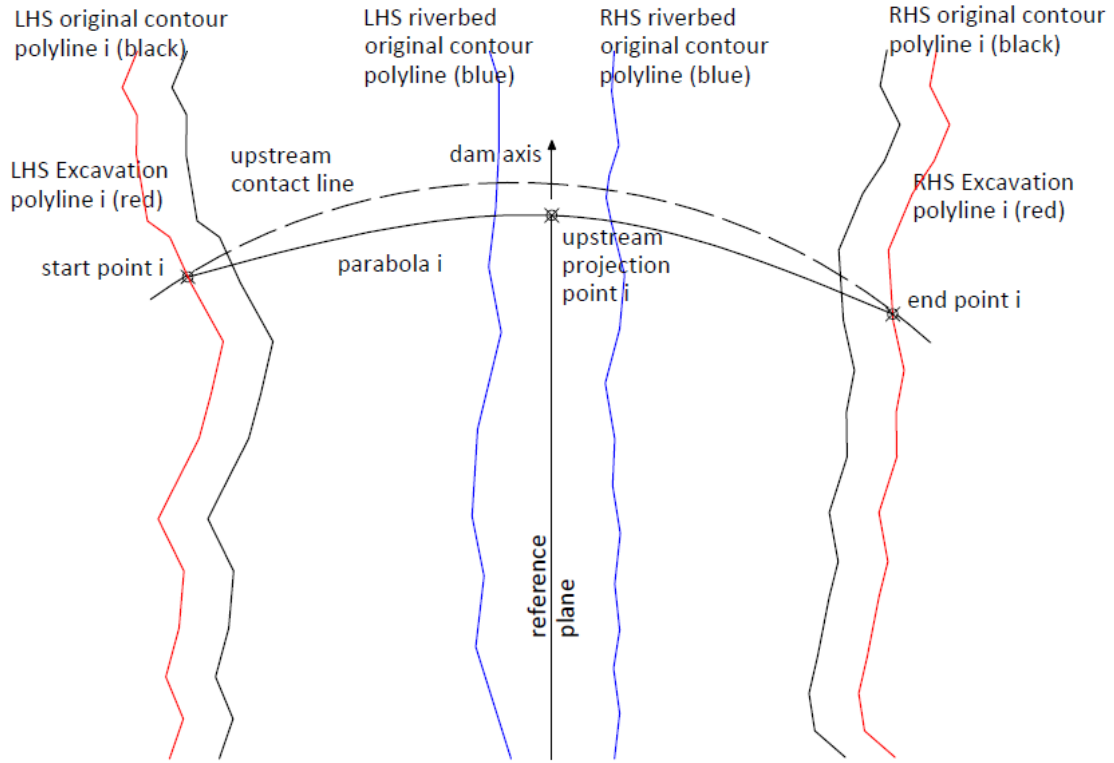


Figure 22: Start, end and upstream projection point of the parabola i (plan view).

The workflow in Figure 23 shows how the optimal parabola at each elevation can be computed using an iterative process in Python

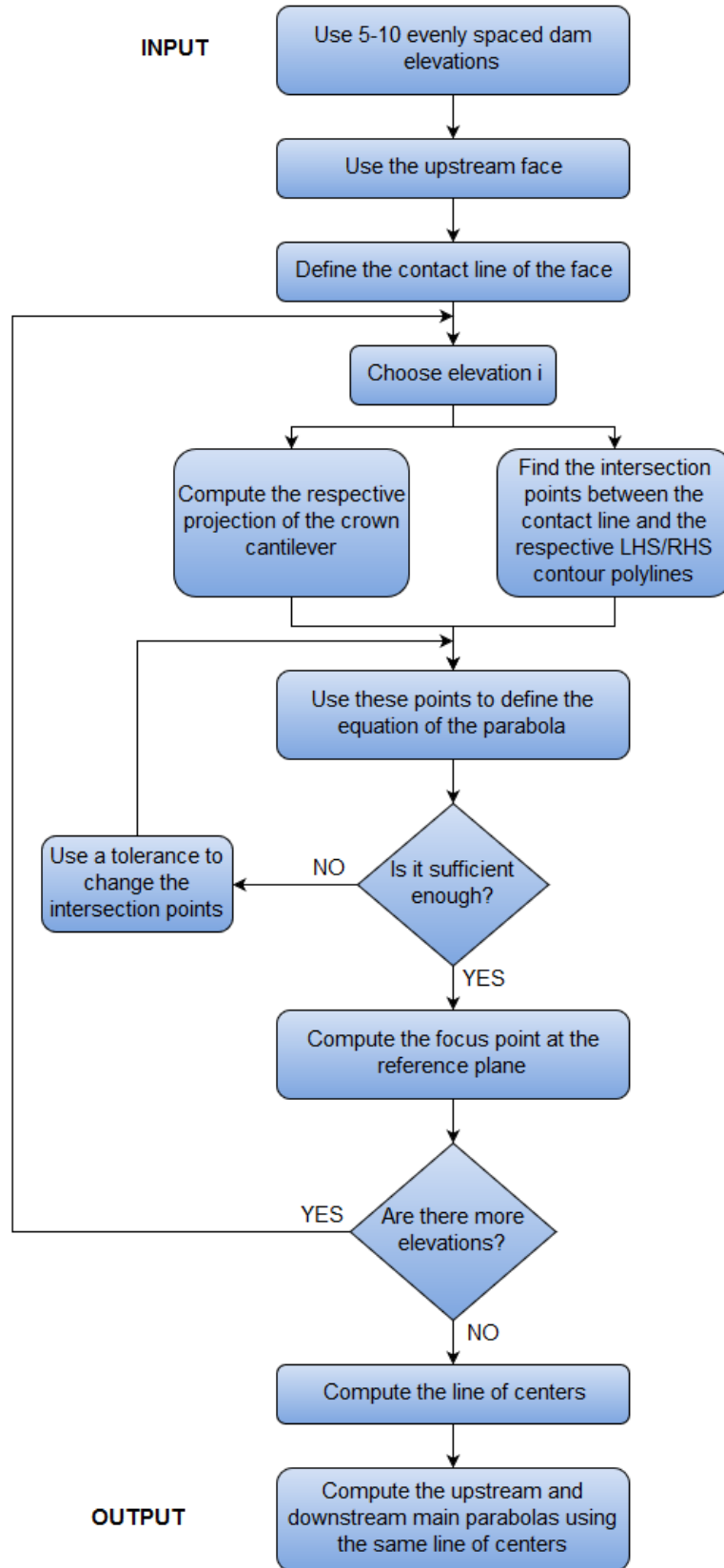


Figure 23: The workflow of the layout of the arches.

4.8. Smooth dam shape method

The geometry for an arch dam must have smooth transitions to not introduce stress concentrations. Therefore, the shape of the foundation area must be as smooth as possible. To achieve a smooth dam profile sharp corners must be avoided and from the crest to the base elevation no “wiggles” must be observed on the foundation [4].

Due to the initial assumption of the uniform excavation length the dam profile can't be smooth enough, as the end points of the parabolas follow the profile of the neighboring topography. For this reason, the following method is proposed which guarantees the smoothness of the foundation area of the dam.

First, the upstream end points are defined. For each side, two angles must be computed using three points at the crest and at base elevation. The first angle uses the end point, the center point and the symmetry point of the reference cylinder, while the other one uses the end point of the upstream base elevation parabola, the center point and the symmetry point of the reference cylinder [Figure 24].

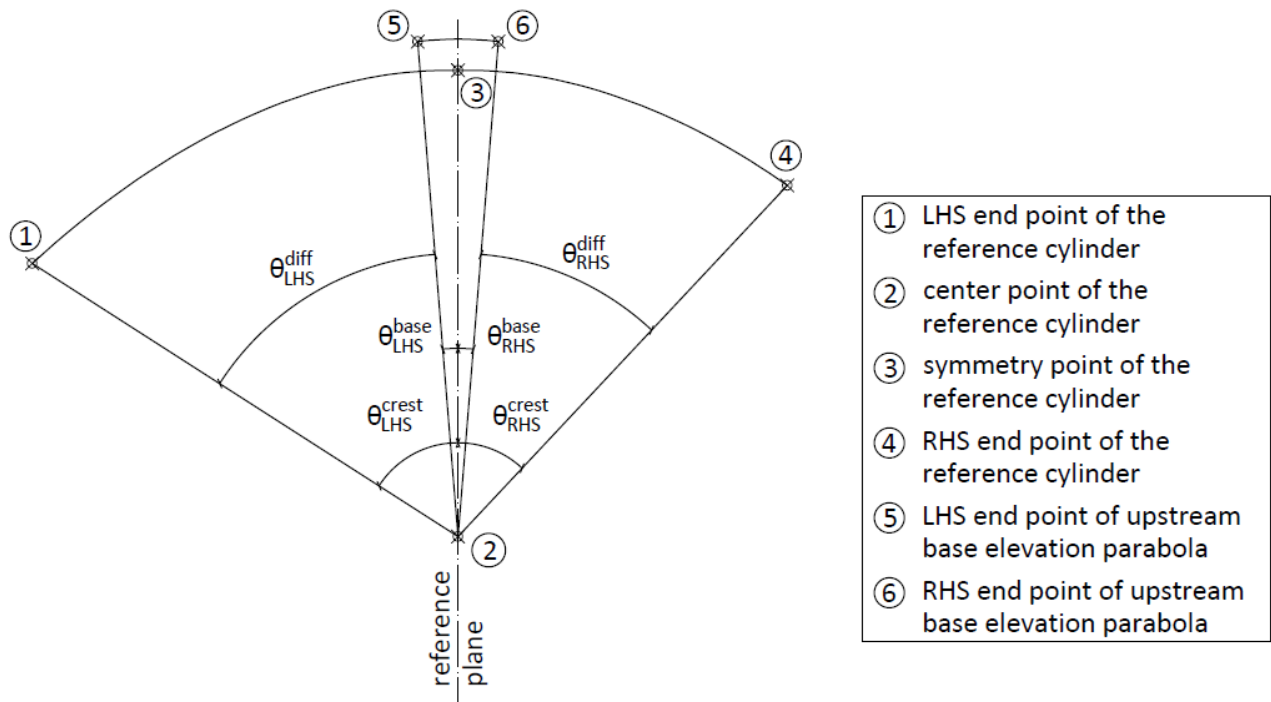


Figure 24: Angles of the reference cylinder and the upstream base elevation parabola (plan view).

$$\theta_{LHS}^{diff} = \theta_{LHS}^{crest} - \theta_{LHS}^{base} \quad (4.16)$$

$$\theta_{LHS}^{inc} = \frac{\theta_{LHS}^{diff}}{k-1} \quad (4.17)$$

$$\theta_{RHS}^{diff} = \theta_{RHS}^{crest} - \theta_{RHS}^{base} \quad (4.18)$$

$$\theta_{RHS}^{inc} = \frac{\theta_{LHS}^{diff}}{k-1} \quad (4.19)$$

Where, k is the number of the used parabolas.

The difference between the angles is computed and divided with the number of the arches which are between the two extreme elevations, so the increment of the angle is found. The number of the arches (k) is defined by the designer and there is no need to follow the previous limitation, between 5 to 10 evenly spaced arches, as the sets of the equations that describe the main parabolas are known.

The use of the angle increment is very important as it helps to pass from one elevation to another providing the essential smoothness to the end points of the parabolas. Hence, at every elevation the respective smooth angle is computed based on the angle increment. Using this angle a line is computed which passes through the center point of the reference cylinder. Afterwards, the intersection point between this line and the respective upstream parabola is found. This process must be done for both of the sides at every elevation.

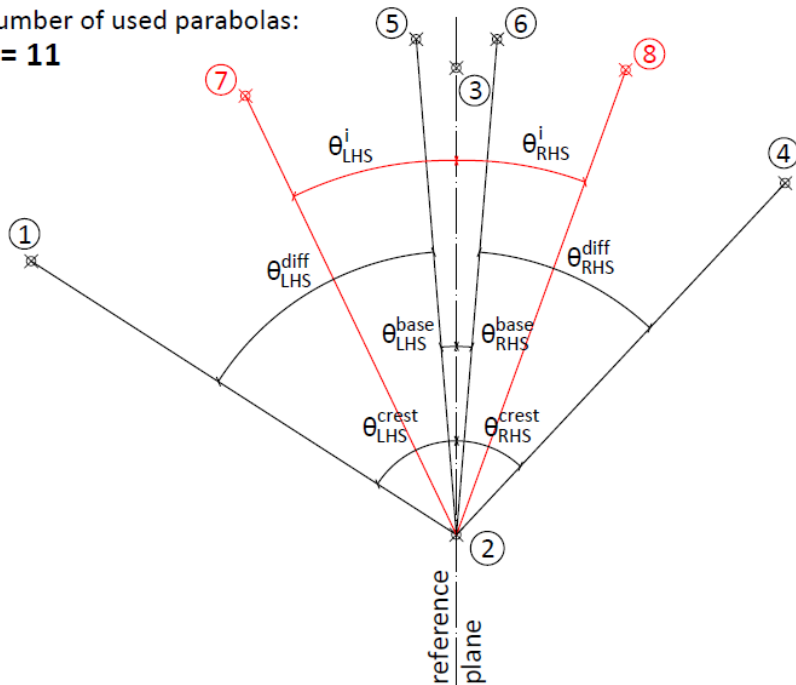
As an example the random elevation z_i is used to calculate the angle for each side [Figure 25].

$$\theta_{LHS}^i = \theta_{LHS}^{crest} - \frac{(z_{crest} - z_i)(k-1)}{H} \theta_{LHS}^{inc} \quad (4.20)$$

$$\theta_{RHS}^i = \theta_{RHS}^{crest} - \frac{(z_{crest} - z_i)(k-1)}{H} \theta_{RHS}^{inc} \quad (4.21)$$

Where, k is the number of the used parabolas.

Number of used parabolas:
k = 11

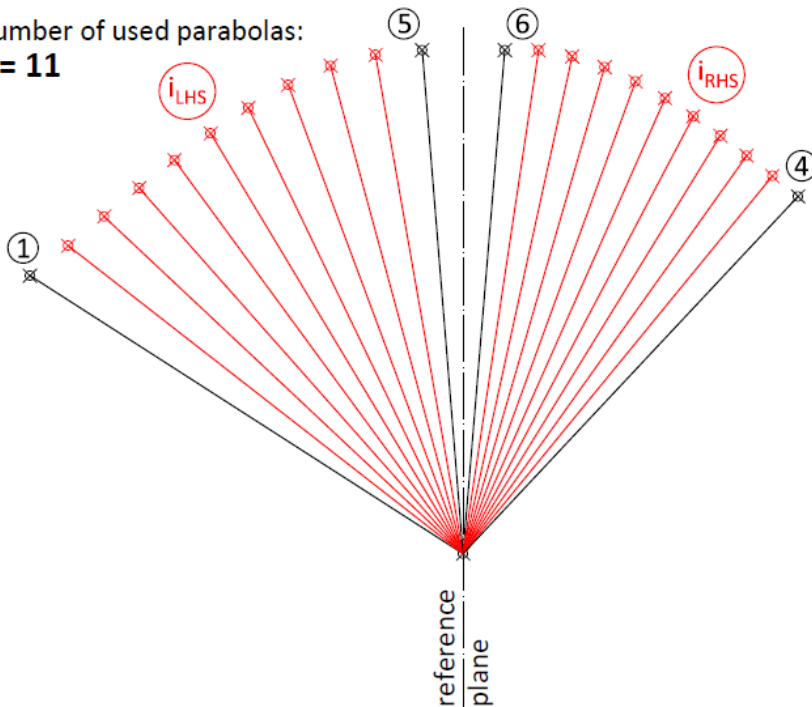


- ① LHS end point of the reference cylinder
- ② center point of the reference cylinder
- ③ symmetry point of the reference cylinder
- ④ RHS end point of the reference cylinder
- ⑤ LHS end point of upstream base elevation parabola
- ⑥ RHS end point of upstream base elevation parabola
- ⑦ LHS end point of upstream parabola i
- ⑧ RHS end point of upstream parabola i

Figure 25: Smooth end points of the upstream parabola i (plan view).

Following the same process for all the chosen elevations the smooth upstream foundation area can be obtained where no sharp corners or “wiggles” can be observed [Figure 26].

Number of used parabolas:
k = 11



Smoothed foundation area

- ① ⑤ i_{LHS}^{up} LHS end points of upstream parabolas
- ④ ⑥ i_{RHS}^{up} RHS end points of upstream parabolas

Figure 26: Points of the smooth upstream foundation area (plan view).

To compute the smooth end points for the downstream face a line that is perpendicular to each upstream parabola at the end point is computed. The intersection point with the respective downstream parabola is the desirable point. To visualize this method the same random elevation z_i is used and the respective downstream points are computed [Figure 27].

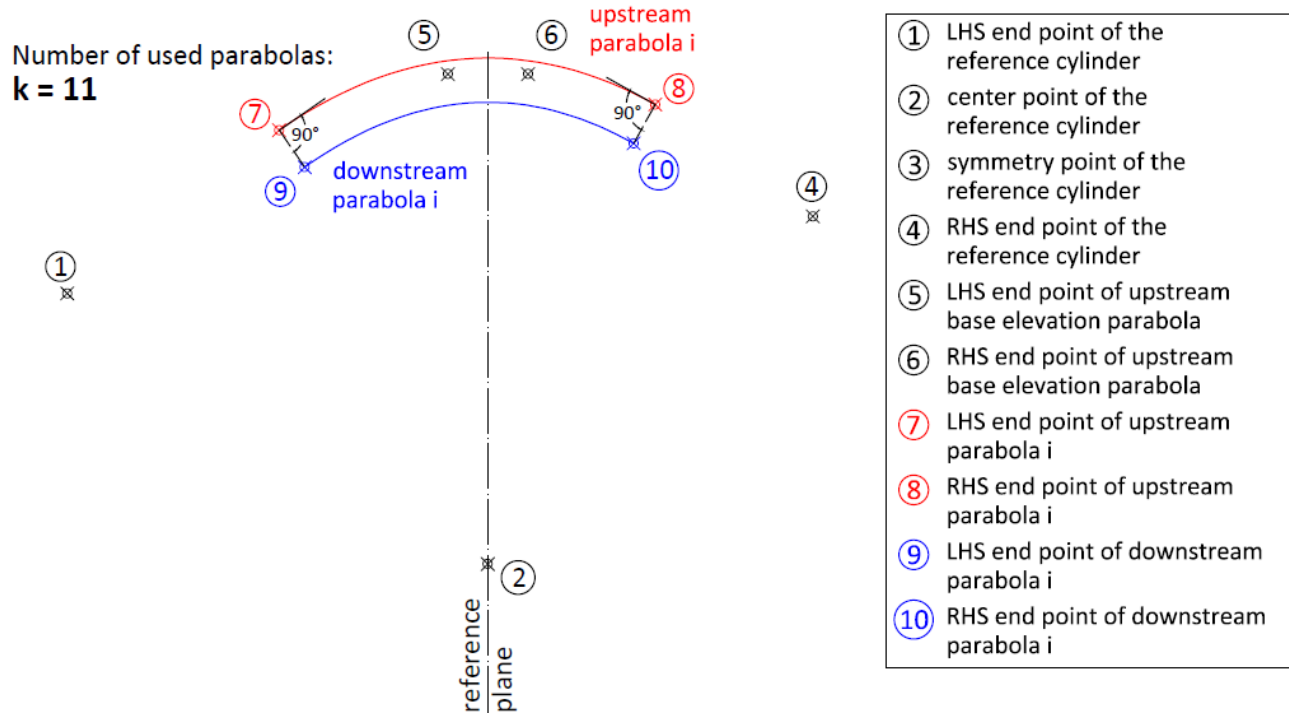


Figure 27: End points of the downstream parabola i (plan view).

Following the same process for all the chosen elevations Figure 28 is obtained which shows the entire foundation area consisting of the upstream and downstream end points.

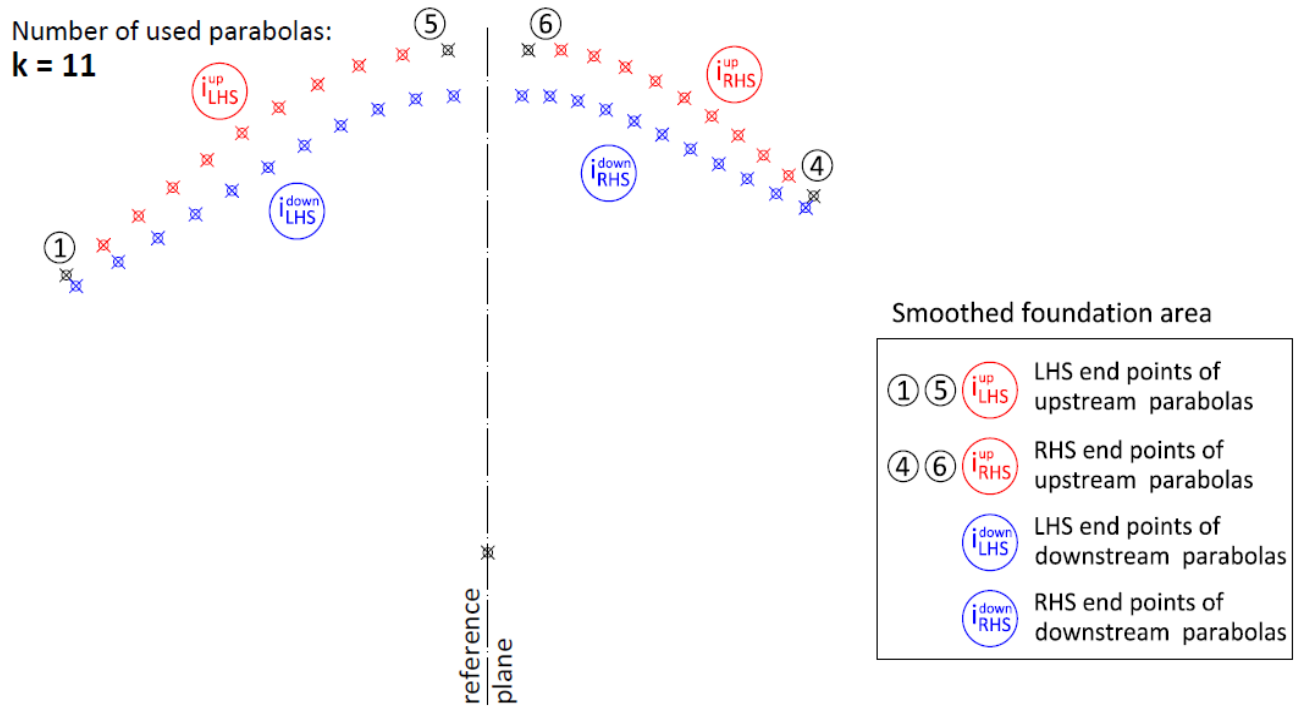


Figure 28: Upstream and downstream points of the smooth foundation area (plan view).

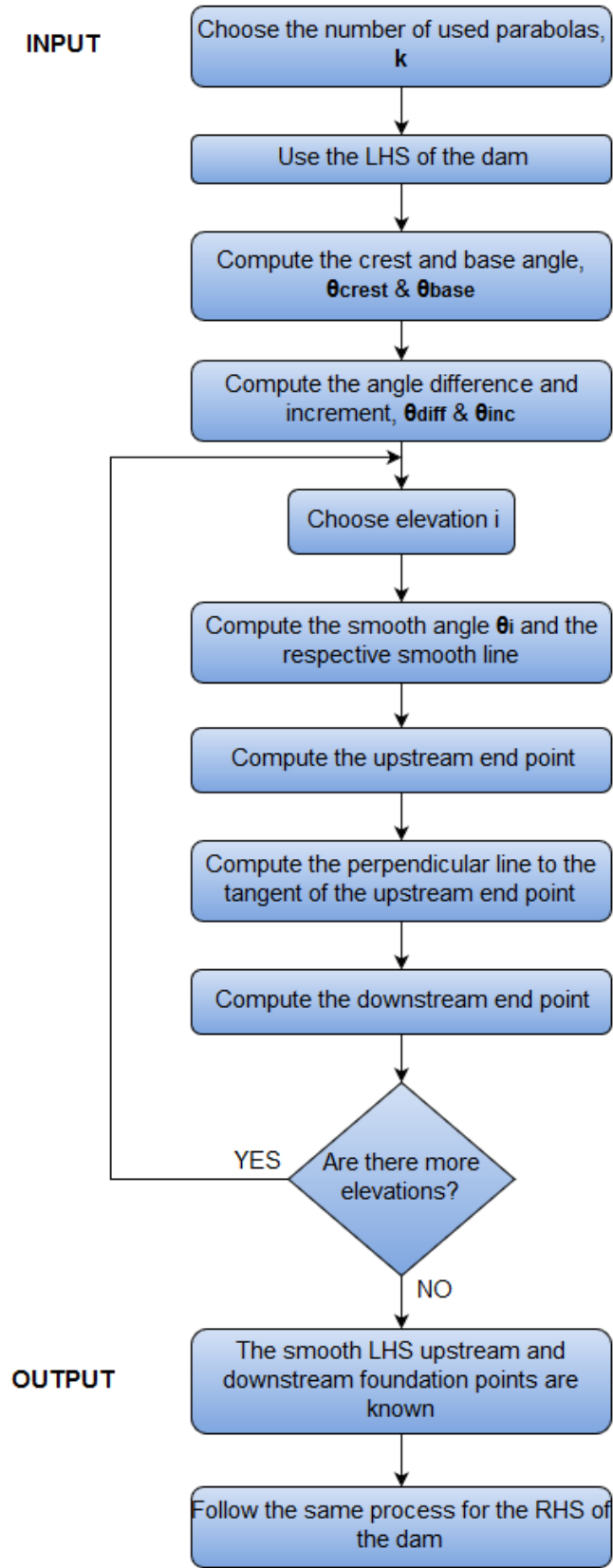


Figure 29: The workflow of the smooth dam shape method.

4.9. Review of the arches

The latter method can provide a good shaped profile for the dam but it does not guarantee that there are no gaps between the dam foundation and the surrounding topography. Hence, the foundation area must be reviewed detecting and redefining the defective arches until an acceptable profile is obtained.

The main goal of this section is to propose an efficient way that can redefine the entire foundation area of the dam adding the least essential concrete volume. It is also mentioned, the parabolic equations which are used for the upstream and downstream face are constant and only their end points are altered.

There are two basic criteria that the end points of the parabolas must satisfy.

- The horizontal length between the end point and the respective original topographic point must be always positive, which means that the parabolas must terminate “inside” the topography. Figure 30 is used to give an example, $x_{diff}^{up,i} = x_S^{down,i} - x_S^{up,i} > 0$, as $0 < x_S^{up,i} < x_S^{down,i}$.
- The horizontal length between the end point and the respective original topographic point must be larger than the minimum excavation length, $L_{excavation}^{min}$. Figure 30 is used to give an example, $L_S^{up,i} = x_S^{down,i} - x_S^{up,i} > L_{excavation}^{min}$, as $0 < x_S^{up,i} < x_S^{down,i}$

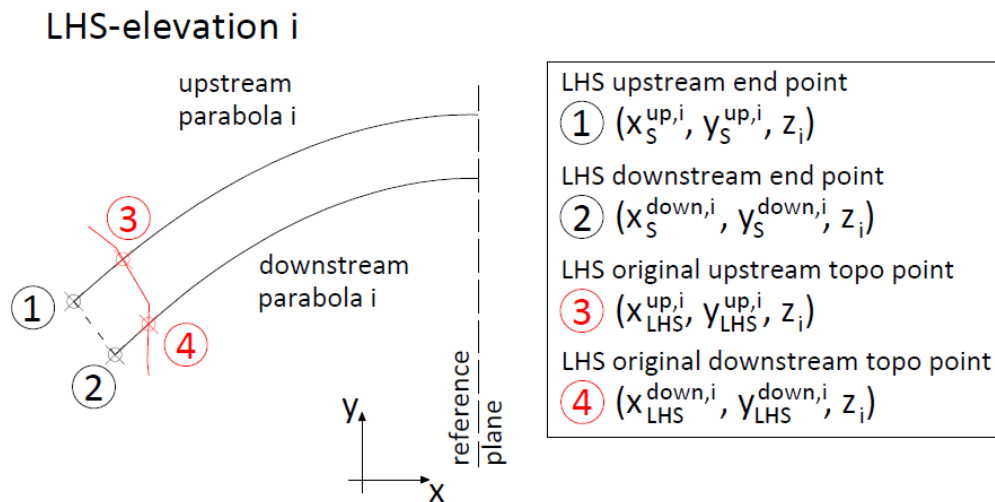


Figure 30: Left Hand Side of the arch i (plan view).

It was concluded that the downstream parabolas contain the most probable defective points. For this reason, an iterative process was developed which checks the downstream end points starting from the base to the crest elevation at each side.

When a defective point is located the process stops and the downstream end point is redefined taking into account the minimum excavation length criterion. The redefined upstream point is calculated and the new increment is found. To use the new increment one of the main angles, the crest angle θ_{LHS}^{crest} or

the base angle θ_{LHS}^{base} , must be changed. It was concluded that it is more efficient to change the base angle, keeping the uniform excavation length at the crest elevation as this is the initial assumption. The new angles can be recomputed at every elevation and the end points (upstream and downstream) can be redefined, eliminating the found defective point.

Afterwards, the redefined downstream end points are checked again and if another defective point is detected, the latter process is repeated. This process stops when all the points satisfy the two criteria. If all the end points satisfy the criteria from the beginning there is no need to be redefined and they are accepted neglecting the aforementioned process.

Using this method a valid dam, based on the two criteria, is always generated. It should be mentioned that this process is depended on the neighboring topographic points at every elevation. So, if the profile of the valley is not appropriate, then a valid dam with high concrete and excavation volume is generated.

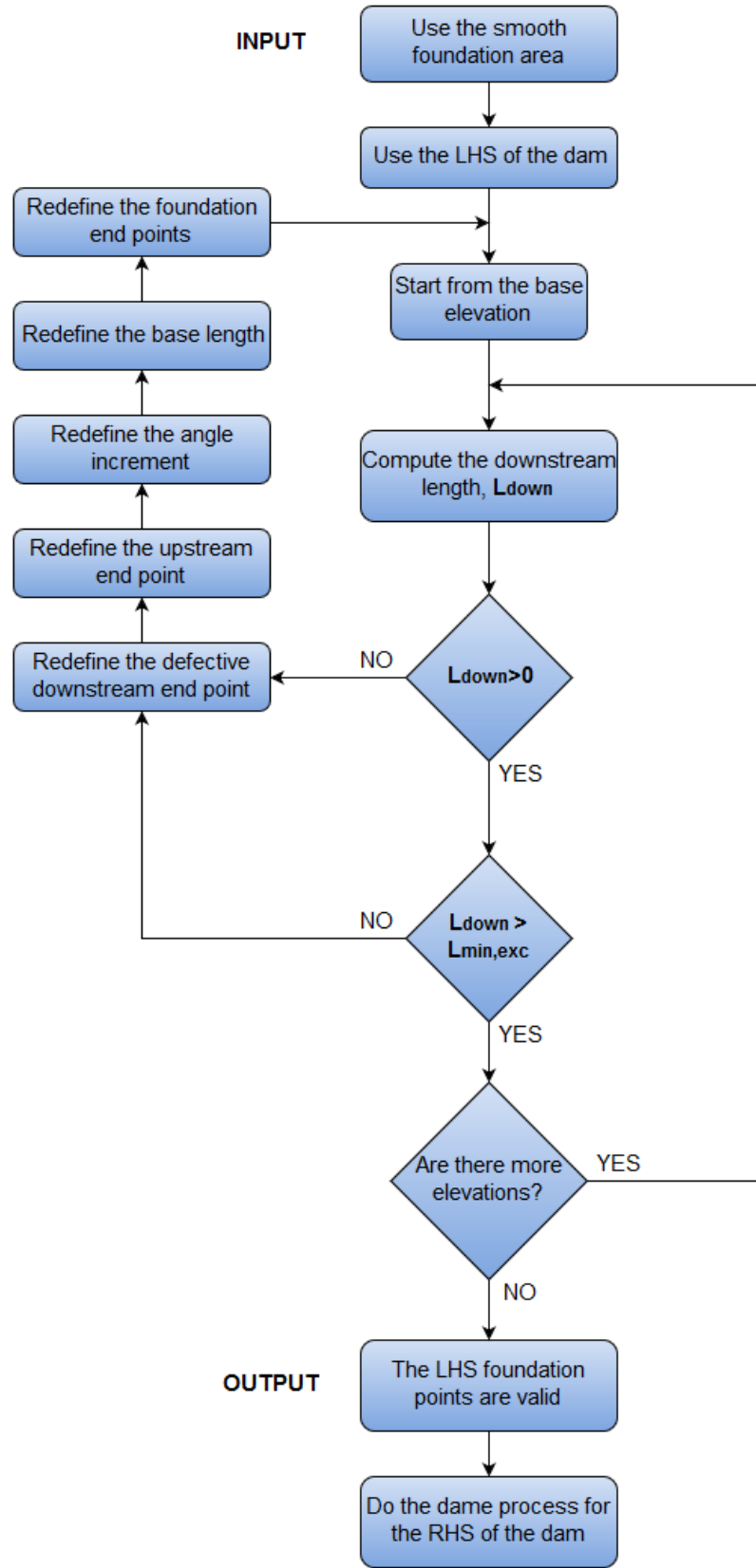


Figure 31: The workflow of the review of the arches.

4.10. Developed profile view

The developed profile view is used to examine the excavation volume that a particular layout has induced. It consists of a developed elevation of the upstream or downstream face of the dam (looking downstream) with the foundation topography shown. Note that a developed view is not the projection of the upstream face onto a flat plane [Figure 32, Figure 33].

In the context of this master project, the developed profile view is not used due to its complexity. However, the process is thoroughly described for integrity purposes and being the basis for future research. The developed view for the pre-processing stage is developed to validate the following method.

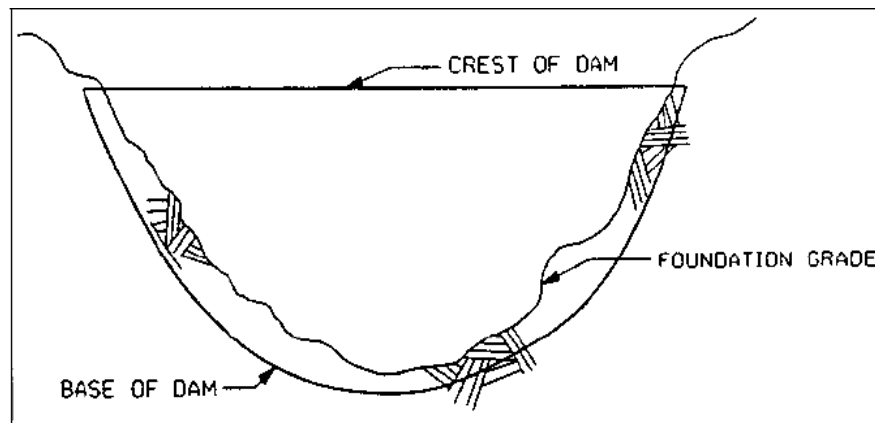


Figure 32: Valid developed profile view [1].

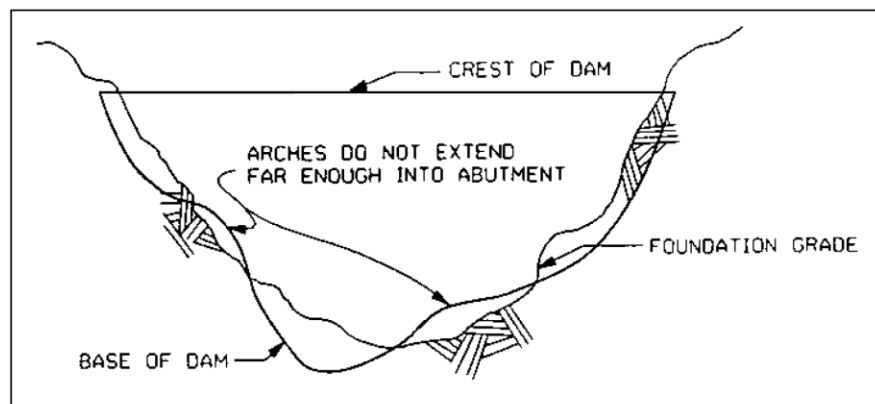


Figure 33: Invalid developed profile view [1].

To create the developed profile view the developed cylinder is introduced and it is used to map the essential points. The dimensions of the developed cylinder must be close to the largest parabola of the dam, which is the upstream crest elevation parabola (reference cylinder). For this reason, the developed cylinder is calculated using the focus point and the symmetry point of the reference cylinder.

Note that the developed cylinder is not the same with the reference cylinder which is the upstream crest elevation parabola.

All the upstream or downstream parabolas are projected on the developed cylinder and the cylindrical coordinates are defined using the arc length and the real height. The main goal for this step is to examine if there are gaps between the foundation grade and the dam base after reviewing the arches. For this reason, only the parabolas' corner points and the respective original topographic points should be transformed [Figure 34].

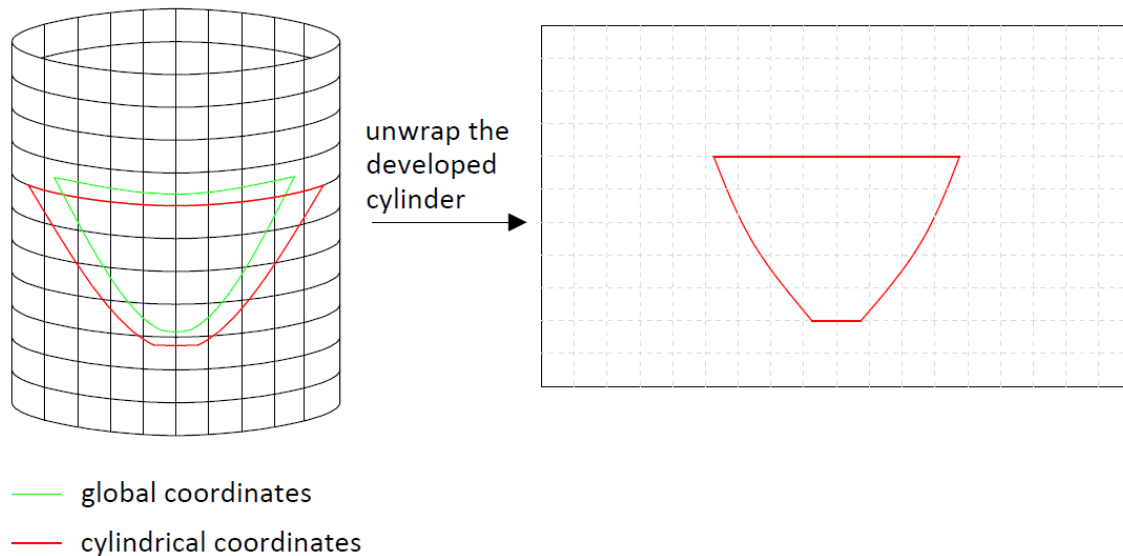


Figure 34: Cylindrical projection method (developed view).

In Figure 35 the transformation of the global coordinates to cylindrical coordinates in the the projection view is shown. Using the following formulas the developed cylinder can be unwrapped to a planar surface:

$$\tan \theta = \frac{x}{y} \longrightarrow \theta = \arctan\left(\frac{x}{y}\right) \quad (4.22)$$

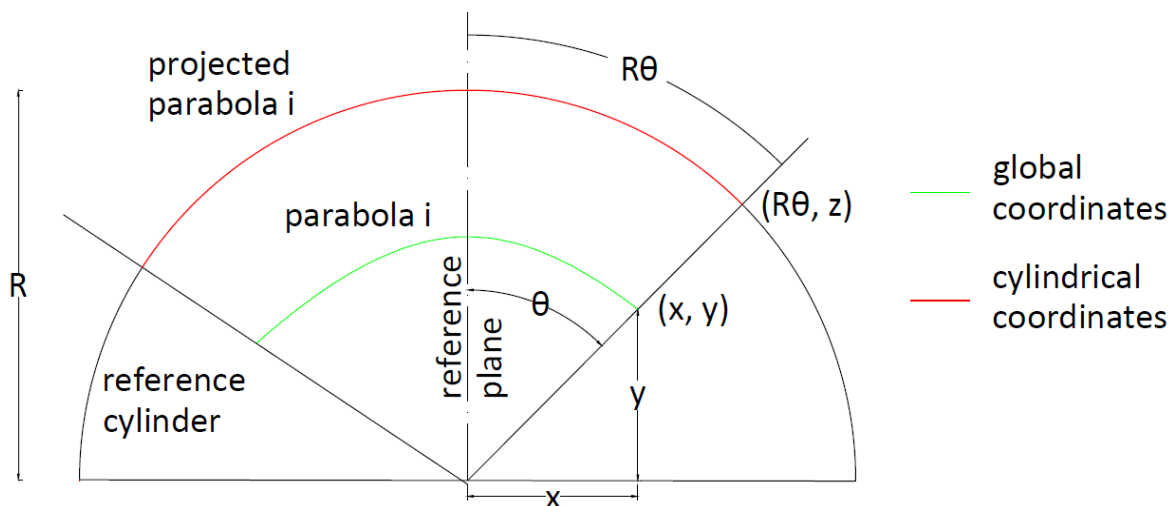


Figure 35: Transformation from global to cylindrical coordinates (plan view).

Using the transformed coordinates two sets of points are defined which describe the foundation grade and the dam base respectively. Connecting the points from each set two polylines can be computed and they are checked for intersections [Figure 36].

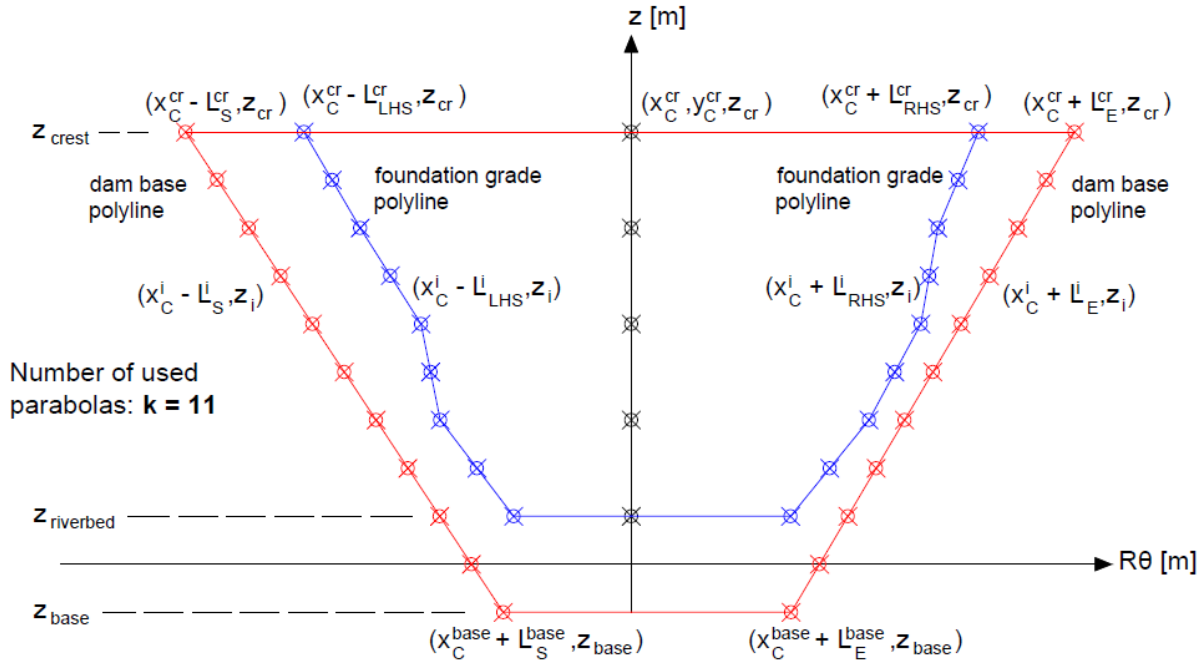


Figure 36: Polylines of the foundation grade and the dam base (developed profile view).

Point $(x_c^i - L_S^i, z_i)$, represents the LHS end points

Point $(x_c^i - L_{LHS}^i, z_i)$, represents the LHS original topographic points

Point $(x_c^i - L_E^i, z_i)$, represents the RHS end points

Point $(x_c^i - L_{RHS}^i, z_i)$, represents the RHS original topographic points

Where, $L_S^i = R\theta_S^i$ is the developed length of the LHS endpoint. (4.23)

$L_{LHS}^i = R\theta_{LHS}^i$ is the developed length of the LHS original topographic point. (4.24)

$L_E^i = R\theta_E^i$ is the developed length of the RHS endpoint. (4.25)

$L_{RHS}^i = R\theta_{RHS}^i$ is the developed length of the RHS original topographic point. (4.26)

z_i is the elevation i .

If the two polylines do not intersect then there are no gaps between the dam base and the foundation grade. Otherwise, the gaps and the affected parabolas must be detected and reshaped using the process described in Section 4.9. Afterwards, the polyline of the dam base is recomputed and checked again for intersections with the foundation grade. This process must be repeated until there are no gaps in the developed profile view.

To avoid stress singularities at the interface between the dam and foundation, it is important the developed excavated profile line remains “smooth”. Otherwise, further adjustments to the excavated profile line may be required. This requirement is satisfied from the process described in Section 4.8.

It is noted that the the dam-rock interface (to be modelled by DIANA geometric groups or interface finite elements) is also important for the abutment stability analyses (static and dynamic). Hence, the global stability of the dam and its abutments can be handled consistently in the iterative design process.

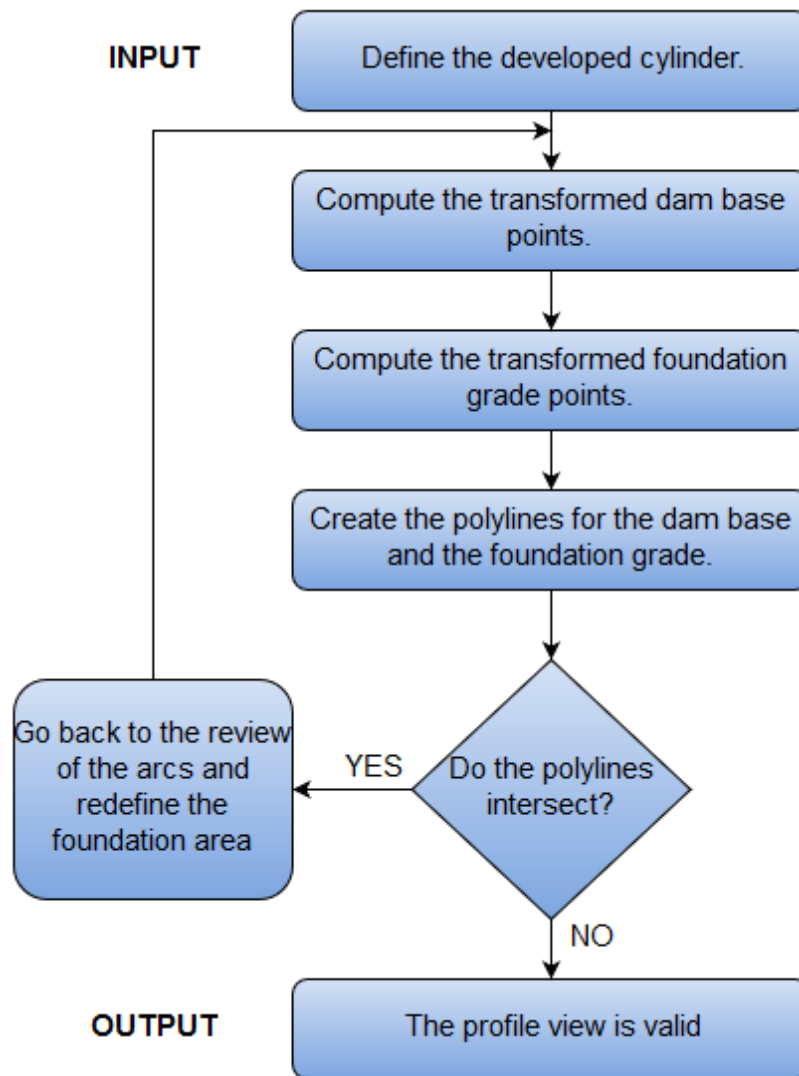


Figure 37: The workflow of the profile view using the developed cylinder.

4.11. Contraction joints

Concrete arch dams are built in alternate blocks to control the concrete shrinkage; the joints between the blocks are referred to contraction joints and must be grouted to form the monolith structure [2]. They are very important as they divide the dam into cantilevers and they create the surfaces where interface elements are applied. In this section the geometry of the contraction joints is explained.

In the Engineer Manual [1] no information is given for the definition of the contraction joints and for this reason a method is proposed that is based on the document reported by R.M. Gunn [2]. Contraction joints are an integral part of the dam design process and with today's computing facilities, they can be modelled automatically using iterative processes. It is mentioned that, contraction joints are not planar, but rather warped or helical in shape. Their definition is also critical in the design and analysis process.

First the joint centers are defined at the upstream crest elevation parabola. This parabola is divided into constant distance segments of 18-20 m. The maximum allowed distance is used to show the next steps of the method. The first two centers must be +10 m and -10 m from the crown cantilever section. Having these two points all the other segments can be defined [Figure 38].

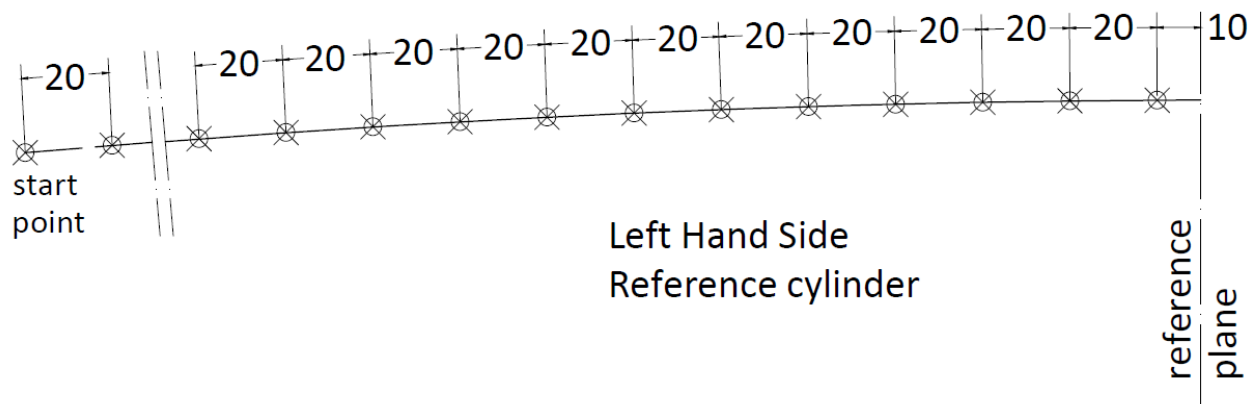


Figure 38: LHS joint centers at the reference cylinder (plan view).

Using the following formula to compute the length of the parabola the location of the joint centers can be found.

$$L_{segm} = \int_{x_0}^{x_1} \sqrt{1 + f'(x)^2} dx \quad (4.27)$$

Where, $f(x) = a_1^{crest} x^2 + b_1^{crest} x + c_1^{crest}$ is assumed to be the parabolic equation of the reference cylinder (main upstream parabola at the crest elevation).

It is assumed that the lower limit is provided and the upper limit x_1 must be defined.

$$L_{segm} = \int_{x_0}^{x_1} \sqrt{1 + f'(x)^2} dx \longrightarrow 20 = \int_{x_0}^{x_1} \sqrt{1 + (2a_1^{crest} x + b_1^{crest})^2} dx$$

The general solution of the upper integral is.

$$\int \sqrt{1 + (2a_1^{crest} x + b_1^{crest})^2} dx =$$

$$\frac{1}{16(a_1^{crest})^2} \left(8(a_1^{crest})^2 x + 4a_1^{crest} b_1^{crest} \right) \sqrt{4(a_1^{crest})^2 x^2 + 4a_1^{crest} b_1^{crest} x + (b_1^{crest})^2 + 1}$$

$$+ \frac{1}{4a} \left(\ln \left(\frac{1}{2a} \left(4(a_1^{crest})^2 x + 2a_1^{crest} b_1^{crest} \right) + \sqrt{4(a_1^{crest})^2 x^2 + 4a_1^{crest} b_1^{crest} x + (b_1^{crest})^2 + 1} \right) \right)$$

The analytical solution of the integral is very complex, so the unknown x_1 is computed numerically using an iterative process which provides the desirable solution with high accuracy. Afterwards, the respective y-coordinate must be computed by substituting x_1 into the parabolic equation of the reference cylinder.

$$y_1 = a_1^{crest} x_1^2 + b_1^{crest} x_1 + c_1^{crest}$$

Having computed the joint centers, their projection on the downstream crest elevation parabola must be found. For this reason, lines which are perpendicular to the upstream parabola and pass through the joint centers are being defined. Afterwards, the intersection points between these lines and the downstream crest elevation parabola are being computed [Figure 39].

The joint center $C(x_c, y_c)$ is assumed to show the mathematical background for this part.

$$\left. \begin{aligned} f'(x) = 2a_1^{crest} x_c + b_1^{crest} \perp a_{perline,i} &= -\frac{1}{2a_1^{crest} x_c + b_1^{crest}} \\ b_{perline,i} = y_c + \frac{1}{2a_1^{crest} x_p + b_1^{crest}} x_c \end{aligned} \right\} \text{perpendicular line: } L_{per,i} = a_{perline,i} x + b_{perline,i}$$

Using the perpendicular line $L_{per,i}$ the respective intersection point with the downstream crest elevation parabola is found.

$$\left. \begin{aligned} \text{perpendicular line: } L_{per,i} &= a_{perline,i} x + b_{perline,i} \\ \text{downstream crest elevation parabola: } g(x) &= a_2^{crest} x^2 + b_2^{crest} x + c_2 \end{aligned} \right\} a_{perline,i} x + b_{perline,i} = a_2^{crest} x^2 + b_2^{crest} x + c_2^{crest}$$

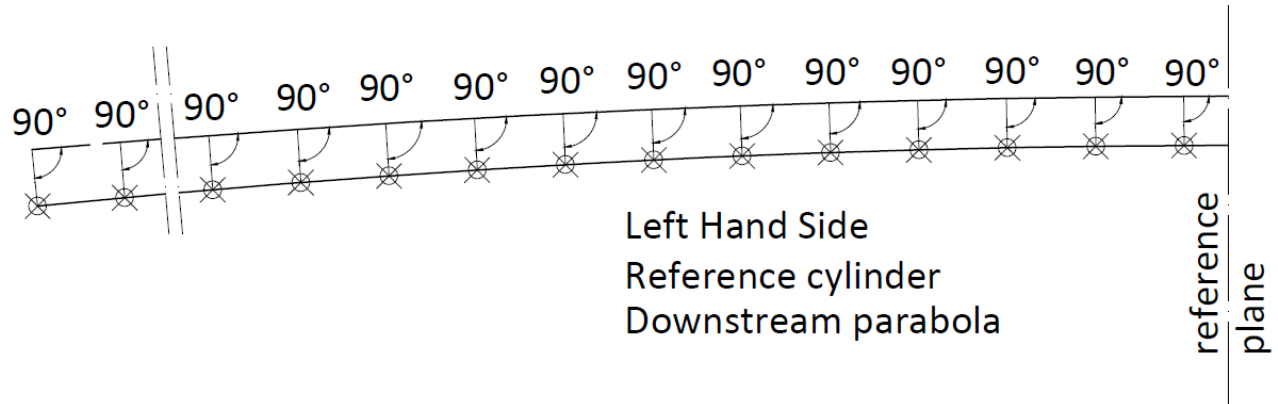


Figure 39: LHS contraction joints of the reference cylinder (plan view).

The joint centers are used for the lower arches as well. The upstream contraction joints are defined by using the joint centers and the points of the upstream parabola that are closest to them. Afterwards, lines are computed using the joint centers and their respective upstream contraction joints. Finally, the downstream contraction joints are the intersections between these lines and the downstream parabola. [Figure 40, Figure 41, Figure 42]

Assuming a joint center $C(x_c, y_c)$ the minimum distance from the upstream parabola i is computed.

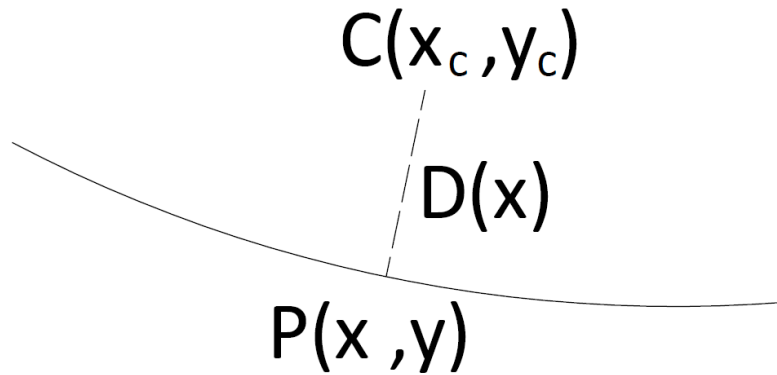


Figure 40: Minimum distance between a point and a parabola.

$$PC^2 = (y - y_c)^2 + (x - x_c)^2 = (a_1^i x^2 + b_1^i x + c_1^i - y_c)^2 + (x - x_c)^2$$

$$D(x) = (a_1^i x^2 + b_1^i x + c_1^i - y_c)^2 + (x - x_c)^2 \rightarrow D'(x) = 2(a_1^i x^2 + b_1^i x + c_1^i - y_c)(2a_1^i x + b_1^i) + 2(x - x_c)$$

$$D'(x) = 0 \rightarrow 3 \text{ roots} \rightarrow \text{pick the real } x \text{ which is closest to the joint center} \rightarrow x_p$$

Having computed the x_p coordinate the y_p can be found by substituting x_p into the parabolic equation.

$$y_p = a_1^i x_p^2 + b_1^i x_p + c_1^i$$

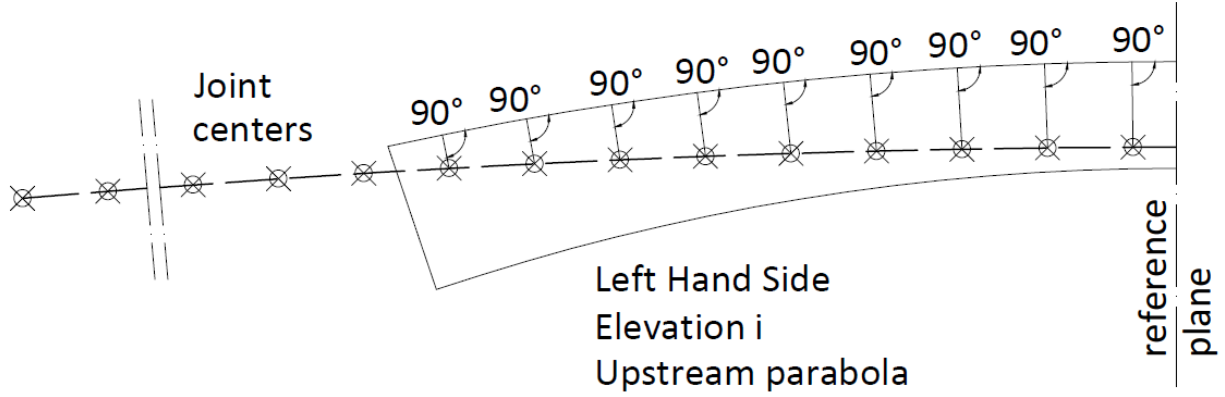


Figure 41: Upstream contraction joints at elevation i (plan view).

The line that passes through the points C and P can be found.

$$\left. \begin{aligned} y_p &= a_{\text{int},i}x_p + b_{\text{int},i} \\ y_c &= a_{\text{int},i}x_c + b_{\text{int},i} \end{aligned} \right\} \text{intersection line } i: L_{\text{inter},i} = a_{\text{int},i}x + b_{\text{int},i}$$

The intersection points with the downstream parabola i are found.

$$\left. \begin{aligned} \text{intersection line } i: L_{\text{inter},i} &= a_{\text{int},i}x + b_{\text{int},i} \\ \text{downstream parabola } i: g_i(x) &= a_2^i x^2 + b_2^i x + c_2^i \end{aligned} \right\} a_{\text{int},i}x + b_{\text{int},i} = a_2^i x^2 + b_2^i x + c_2^i$$

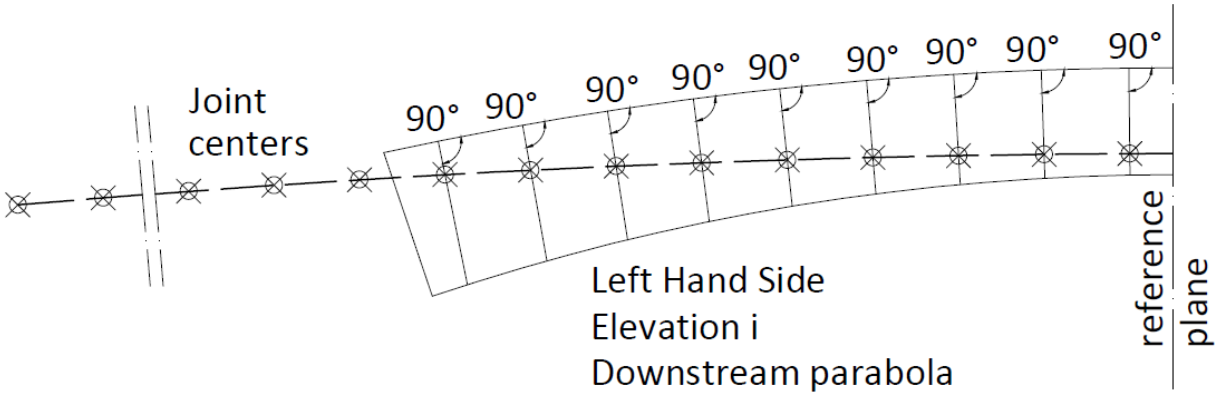


Figure 42: Downstream contraction joints at elevation i (plan view).

Point $(x_{\text{top},RHS}^i, y_{\text{top},RHS}^i)$

$$g_i(x) = a_2^i x^2 + b_2^i x + c_2^i \rightarrow y_{\text{top},RHS}^i = a_2^i x_{\text{top},RHS}^i + b_2^i x_{\text{top},LHS}^i + c_2^i$$

Point (x_p^i, y_p^i)

$$g_i'(x_p^i) = 2a_2^i x_p^i + b_2^i$$

$$\text{tangent } \perp \text{ reference plane } \rightarrow 2a_2^i x_p^i + b_2^i = 0$$

The intersection points of the downstream parabola i with the lines y_1^i and y_2^i are the end points of the downstream parabola i . The lines y_1^i and y_2^i connect the respective upstream parabola with its center.

$$g_i(x_{LHS}^i) = y_1^i(x_{LHS}^i) \rightarrow a_2^i x_{i,LHS}^2 + b_2^i x_{i,LHS} + c_2^i = d_1^i x_{i,LHS} + e_1^i$$

$$g_i(x_{RHS}^i) = y_2^i(x_{RHS}^i) \rightarrow a_2^i x_{i,RHS}^2 + b_2^i x_{i,RHS} + c_2^i = d_2^i x_{i,RHS} + e_2^i$$

In the same manner the upstream and downstream contraction joints at every elevation can be defined.

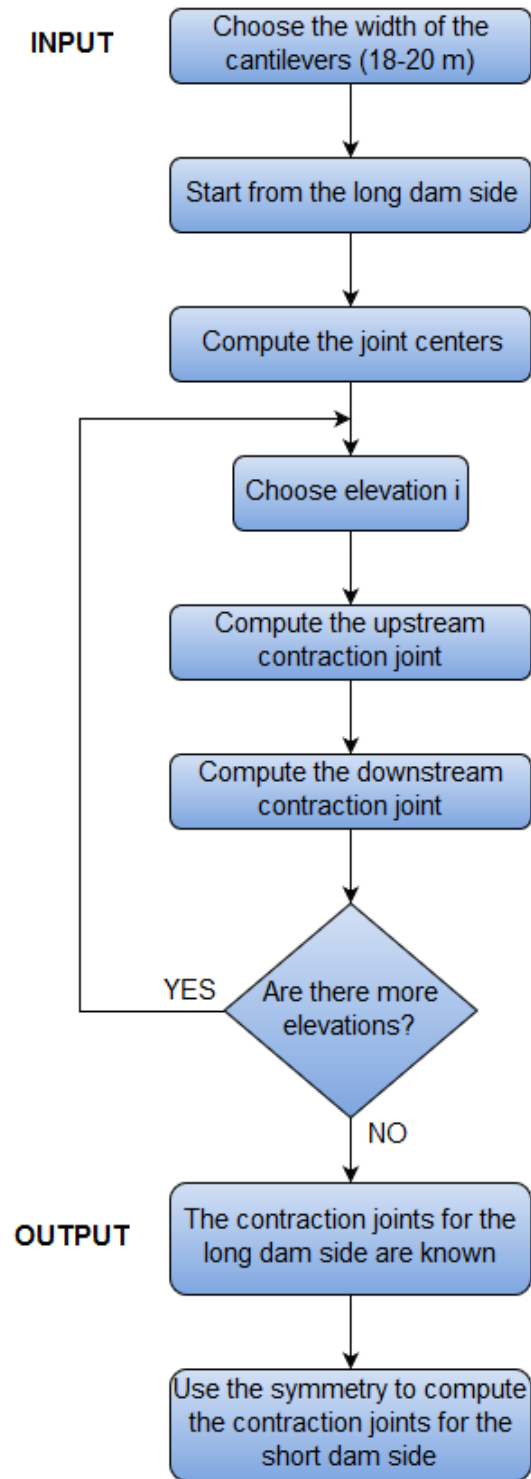


Figure 43: The workflow of the contraction joints.

4.12. Diana Interactive Environment (DianaIE) Model

At this stage the main parts of the dam are described by sets of parabolic equations. These sets are used to generate clouds of points so they can be fitted by Bezier Surfaces, which is one of the new features of Diana Interactive Environment Software.

It is mentioned that, Bezier Surfaces are a very powerful tool which can describe abnormal surfaces, using a very large number of points. However, possible distance errors from the given points can occur due to their sensitivity. For this reason, a good point grid is essential as through this simple rule the errors can be minimized and become negligible. Each surface must be investigated separately so the optimal grid can be found.

First, the designer must choose the number of the used elevations and then the cloud of points are defined. The number of the elevations should be chosen based on the aforementioned rule regarding the sensitivity of Bezier Surfaces.

4.12.1. Preliminary upstream cloud of points

The upstream face consists of one set of parabolas, the main upstream parabolas. Using this set the respective cloud of points is generated. For each elevation a set of x-values is defined representing the x-coordinates of the upstream points.

The x-values are generated using the x-coordinates of the upstream and downstream point adding a small tolerance at each side, so the final points can extend the borders of the dam. This tolerance is very useful for Section 4.12.4 where the final shape of the dam is obtained using a specific process. Furthermore, the number of the x-values is defined by the designer and it is very important to be in accordance with the number of the used elevations.

In Figure 44, it is shown the cloud of points and of the upstream dam face using 25 elevations and 21 points for each elevation.

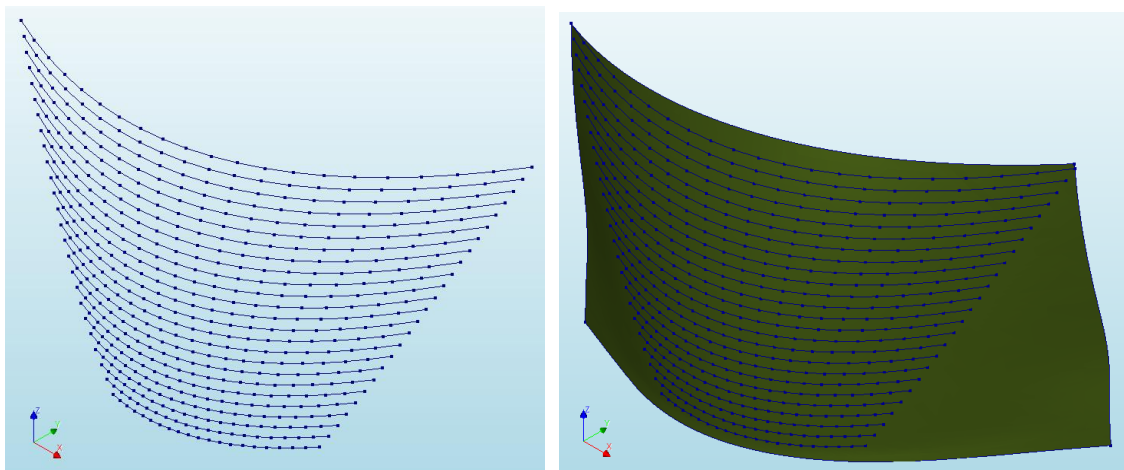


Figure 44: Cloud of points of the upstream face (left). Bezier Surface of the upstream face (right).

4.12.2. Preliminary downstream cloud of points

In the preliminary design stage the downstream face consists of one set of parabolas as well, the main downstream parabolas. The process to define the essential points is identical to upstream face and for this reason it is not repeated.

Similarly as before, in Figure 45, it is shown the cloud of points of the downstream dam face using again 25 elevations and 21 points for each elevation.

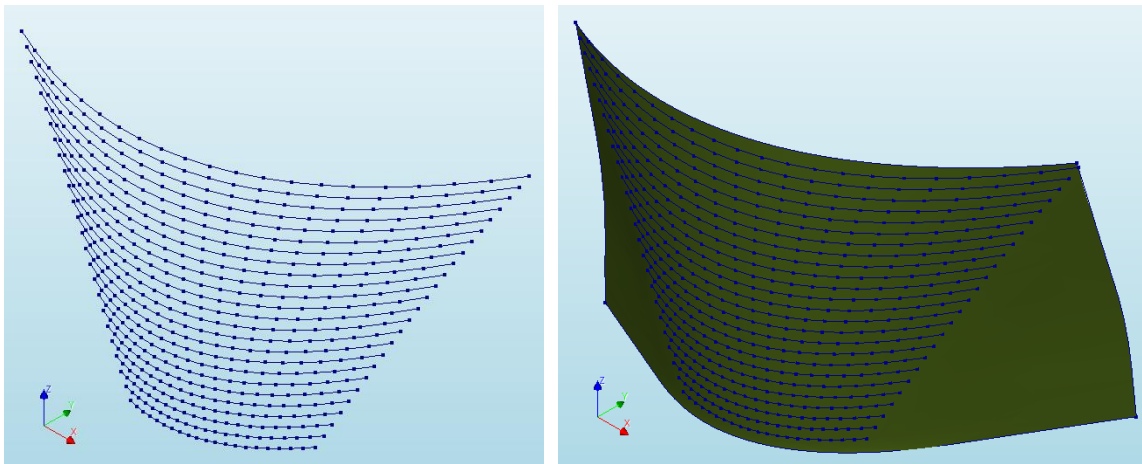


Figure 45: Cloud of points of downstream face (left). Bezier Surface of downstream face (right).

4.12.3. Preliminary foundation clouds of points

Two clouds of points, one for each side, are essential to describe the entire foundation area of the dam, using the respective upstream and downstream end points and their middle points.

Furthermore, for each end point an additional point is generated which uses the same x and z-coordinates while in the y-coordinate a large tolerance is added. The sign of the tolerance is dependent on the end point. For the upstream points the tolerance is negative, while for the downstream points the tolerance is positive.

Finally, at the base and the crest elevation additional points are computed also deviating now on the z-coordinate using a different tolerance which is proportional to the height of the dam. In this way, the Bezier Surface passes smoothly through all the end points, while at the same time it always extends from the borders of the dam.

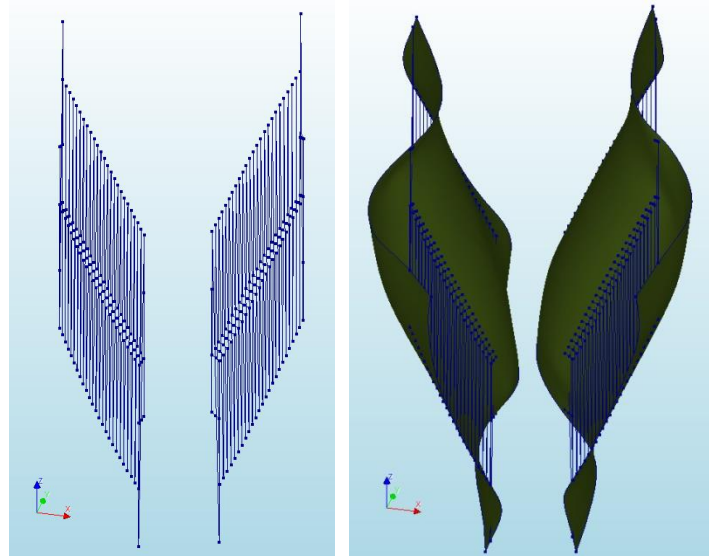


Figure 46: Clouds of points of foundation area (left). Bezier Surfaces of foundation area (right).

4.12.4. Preliminary solid shape of the dam

A solid block is created to represent the arch dam. For this purpose, the maximum coordinates of the dam points are used for the lateral dimensions while the height of the block is equal to the real height of the dam [Figure 47].

To obtain the solid shape of the arch dam the Bezier surfaces for the upstream and downstream face and the foundation area are used, subtracting the solid block following a specific order. First the foundation surfaces subtract the solid block [Figure 48] and afterwards the upstream and downstream surface [Figure 49]. The solid shapes which do not contain the dam geometry are removed and the solid shape of the dam is obtained [Figure 50].

Finally, the dam solid is imprinted on the topographic surface and a line is generated on each face which shows the area of the connection of the dam with the rock, or the volume of the dam which is “inside” the rock.

It is mentioned that, the subtraction between a solid shape and a surface is only successful when the borders of the surface are larger than the borders of the solid as Diana Interactive Environment (DianaIE) does not support partially sectioned bodies. In addition the surface must intersect each side of the solid only once, creating an intersection line for each side [7]. For this reason, all the used tolerances and additional points are so important and in this way a good-shaped dam is generated as far as a proper topographic surface is given.

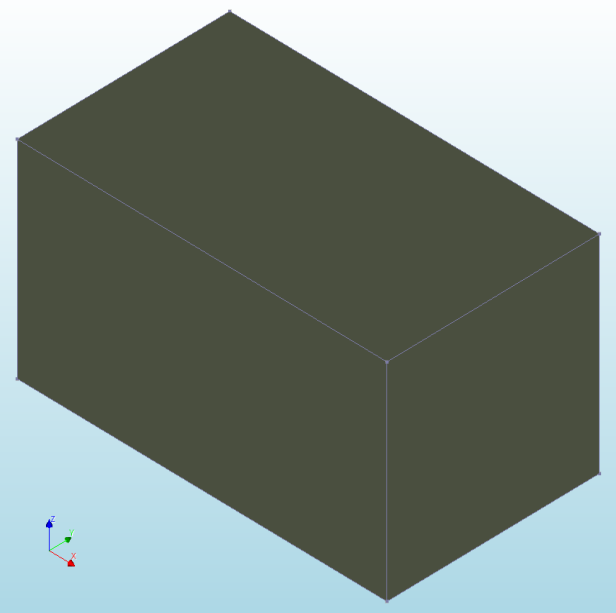


Figure 47: Solid block of the arch dam.

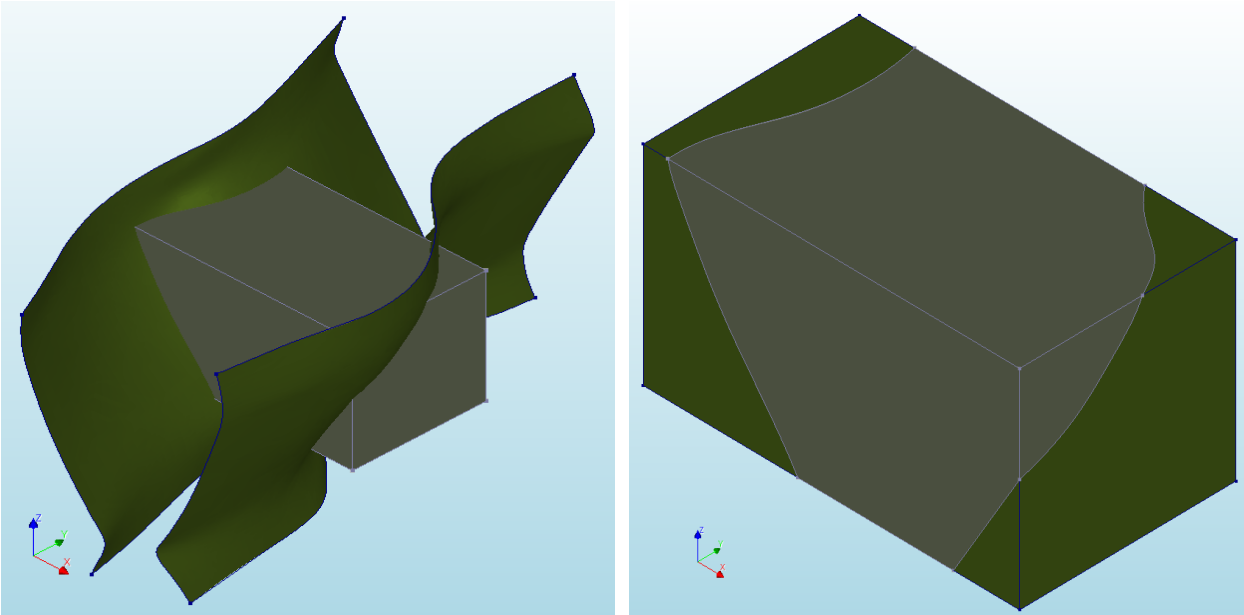


Figure 48: The dam solid before (left) and after (right) the subtraction with the foundation surfaces.

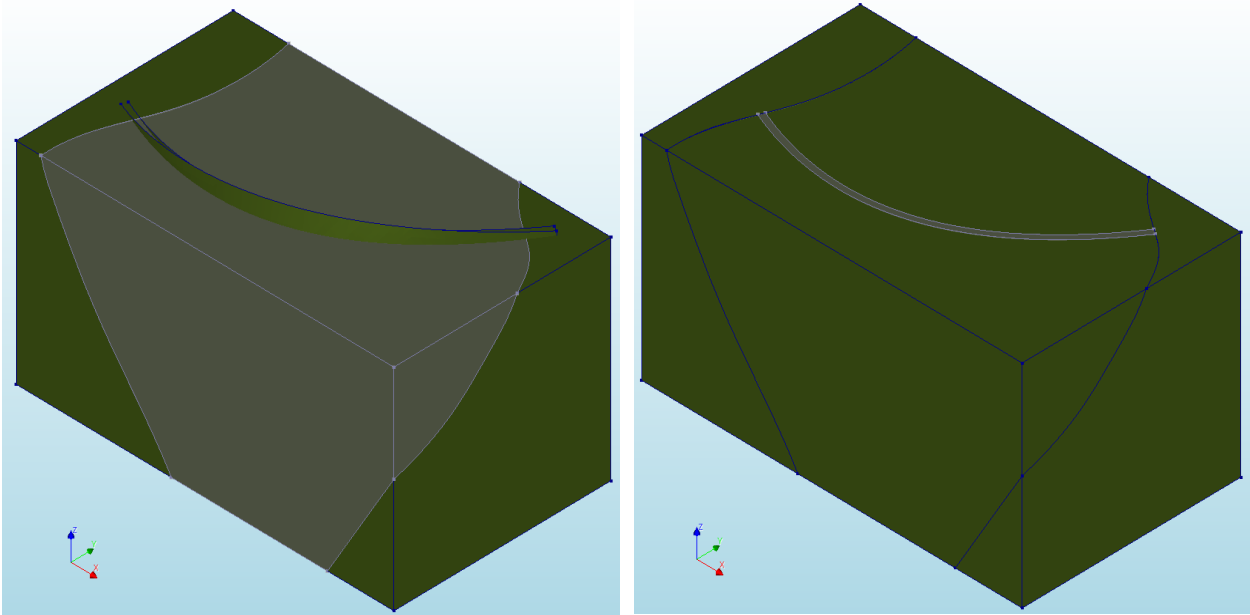


Figure 49: The dam solid before (left) and after (right) the subtraction with the upstream and downstream surfaces.

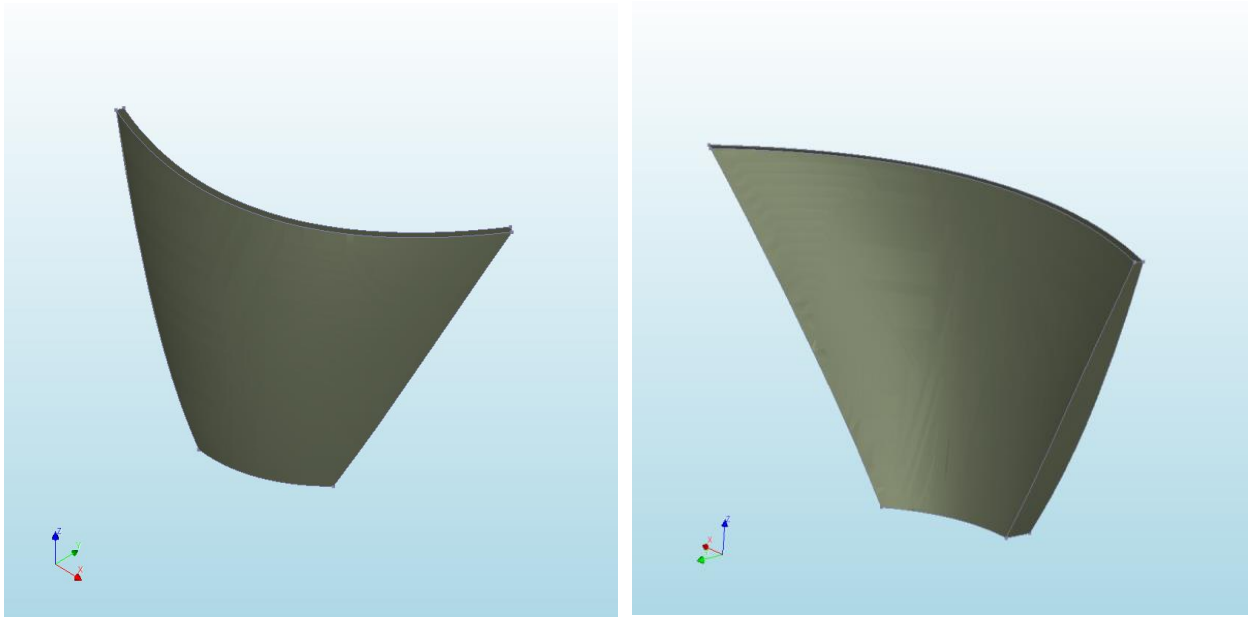


Figure 50: Solid shape of the dam removing the unsuitable solids.

4.12.5. Preliminary solid shape of the topography

To create the solid shape of the topography a tolerance and the extreme coordinates of the topographic points are used to define the dimensions of a solid block. The depth of the block is defined by the designer as well [6]. The value of the tolerance should be in accordance with Section 4.1 and not exceed the dimensions of the given topographic surface, or else a partially sectioned body occurs which it is not allowed.

The topographic surface sections the solid block and the upper part is removed [Figure 51]. Afterwards, the dam solid is subtracted from the topography solid and the footprint of the dam on the topography, or the excavation area, is generated [Figure 52].

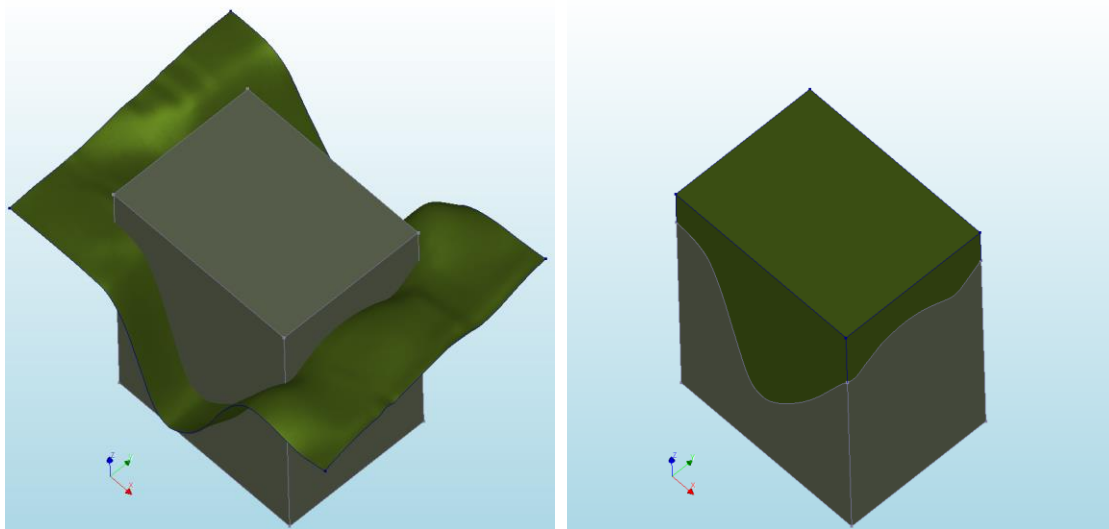


Figure 51: The topography solid before (left) and after (right) the subtraction with the topographic surface.

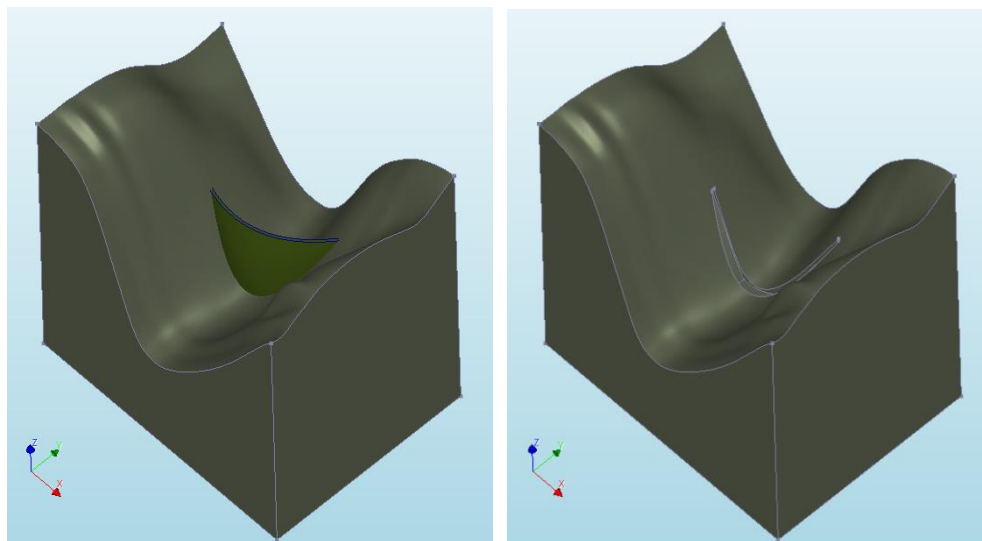


Figure 52: The topography solid before (left) and after (right) the subtraction with the dam solid.

4.12.6. Preliminary contraction joints

The contraction joints follow the method described in Section 4.11 and for this reason it is not explained again. In this section the contraction joints are visualized so the reader can understand how they are generated in Diana Interactive Environment.

Using the solid shape of the dam with the imprinted topography the geometry of the contraction joints is computed automatically based on the given cantilever width, which can be from 18 to 20 meters [Figure 53].

The same strategy from Section 4.12.3 is used, where additional points are used to generate good-shaped Bezier Surfaces. It is mentioned that, for every location a list is generated including the contraction joints and the additional points. The number of the occurred cantilevers is arbitrary and it is dependent on the length of the reference cylinder (upstream crest elevation parabola) [Figure 54].

The point of attention that should be taken into account is that the contraction joints create helical surfaces between the cantilevers and not planar surfaces. Choosing a random cantilever from the dam, its top view is visualized [Figure 55].

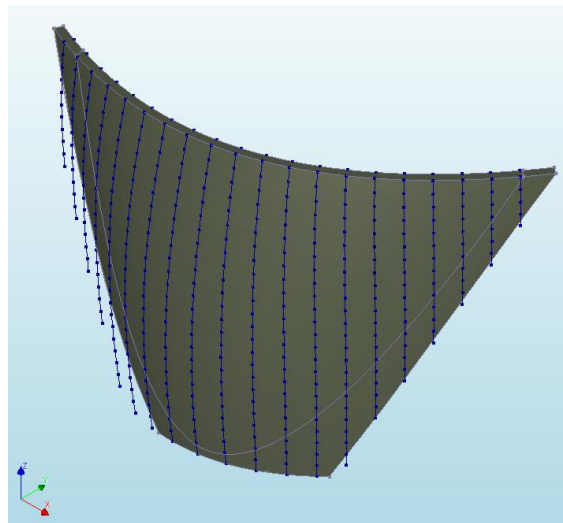


Figure 53: Geometry of the contraction joints.

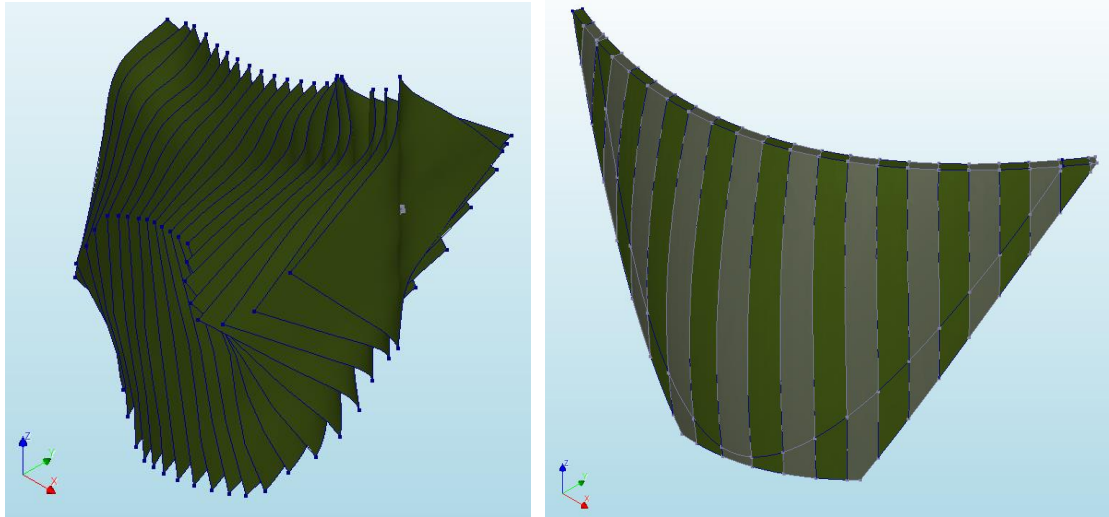


Figure 54: Bezier Surfaces of the contraction joints (left). The dam cantilevers after the subtraction (right).

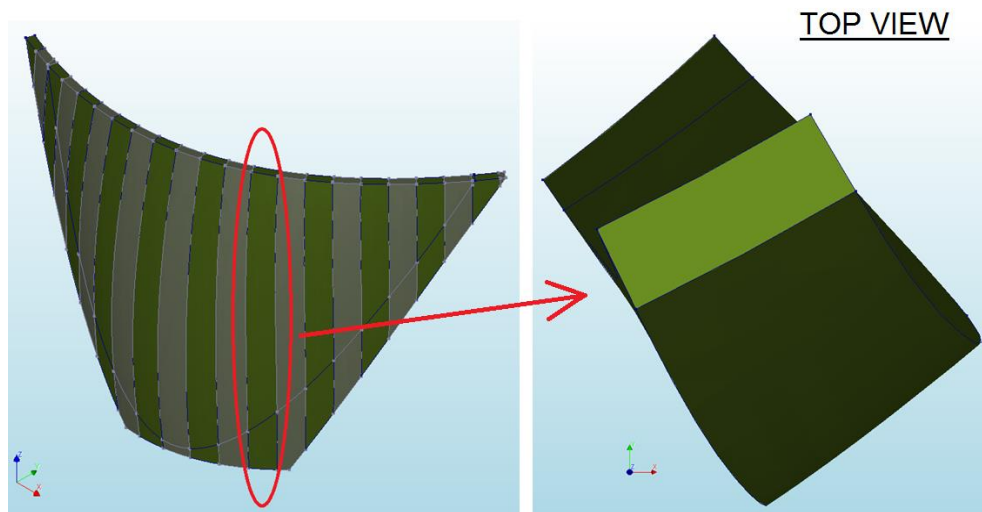


Figure 55: Visualization of the helical surfaces of a cantilever.

4.12.7. Preliminary boundary conditions

In this section the boundary conditions and the load combinations are defined for the preliminary design stage.

The boundary conditions are formulated as follows. The bottom face of the solid of the topography is supported in the vertical direction (z-axis) and the four side faces are supported in the horizontal directions (x and y-axis) [Figure 56].

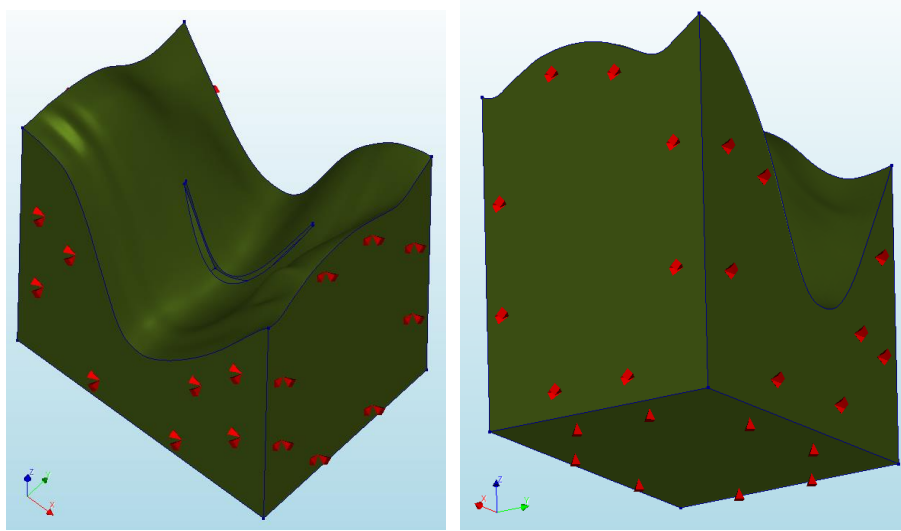


Figure 56: Boundary conditions of the model.

A preliminary stress analysis is performed to determine the state of stress of the dam under various loading conditions. Only static loading conditions are analyzed like hydrostatic, thermal, silt, ice tail water loads and dead weight.

In the context of this master project only the self-weight and the hydrostatic pressure on the dam are taken into account. The main reason for selecting the aforementioned load combination is that they are applied automatically through the code in the present product version of Diana Interactive Environment (DianaIE). This is not the case for the temperature load as at this stage it must be applied manually after meshing the dam. Furthermore, the hydrostatic pressure on the topographic surface is neglected on the valley. Stresses due to the rock self-weight should be avoided.

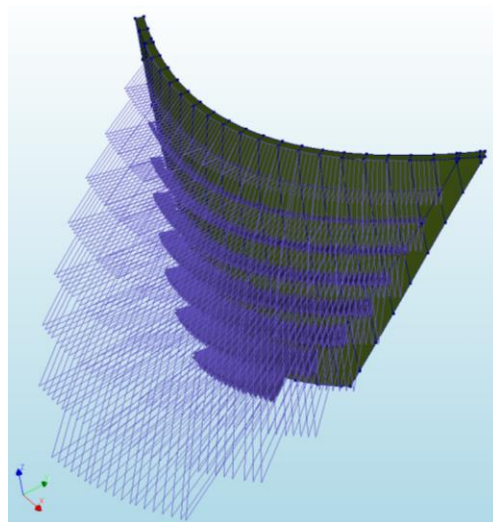


Figure 57: Hydrostatic load on the upstream face of the dam.

4.12.8. Preliminary mesh guidelines

A proper mesh size must be defined for the model so it can be analyzed. There are two solid shapes, the dam and the topography, and a different mesh size is defined for each of them.

The topography solid shape is not of high importance and as the value of 100 meters is chosen for its mesh size.

Regarding the mesh of the dam, the guidelines from the document [3] are used to compute the limit of the dam mesh size. For linear elastic analyses, the largest size of the finite element must be limited to one fifth of the shortest wave length.

$$G = \frac{E}{2(1+\nu)} \quad (4.28)$$

Where, E is the Young's modulus of the concrete.

ν is the Poisson's ratio of the concrete.

G is the shear modulus of the concrete.

$$V_s = \sqrt{\frac{G}{\rho}} \quad (4.29)$$

Where, ρ is the density of the concrete.

V_s is the wave travelling speed to travel across an element of characteristic dimension h such

$$\text{that } \Delta t \leq \frac{h}{V_s}.$$

$$\lambda_{\min} = \frac{V_s}{f_{\max}} \quad (4.30)$$

Where, $f_{\max} = 20 \text{ Hz}$ is the maximum frequency of the seismic signal.

λ_{\min} is the shortest wave length.

Having the dam mesh size limit the most appropriate mesh should be selected for the model. Consequently, more than one dam mesh sizes may be checked which should be equal or smaller than the limit.

In the context of this master project, only Hexa/Quad linear elements [7] are used for two reasons. The first one is that a fine mesh is used for the dam and the integration points of a linear element are sufficient. The second is that Hexa/Quad quadratic elements may generate bad shaped elements with negative volume and as a result the analysis is not completed.

4.13. Selection of the best alternative

This step can be divided into two parts so the best alternative can be chosen based on the geometric constraints. First, each dam site must be thoroughly investigated so the dam with the least concrete and excavation volume is generated, checking the orientation of the dam axis. Afterwards, all the different dam sites are compared and the best alternative is chosen.

Regarding the first step, it is very important to follow the guidelines from Section 4.5, where the angles of incidence β should approximately be equal for each side and larger than 30 degrees in the upper half [Figure 17] [1]. The allowable deviation between the angles is assumed 10 degrees. One more simple but very effective rule is that the dam axis should be approximately parallel to the axis of the riverbed. In other words, the dam should be perpendicular to the riverbed.

Having found the best alternative the final design stage can take place where the final shape of the dam is defined taking into account the allowable stress level.

It is mentioned again that, stress peaks during the preliminary design stage are not of high importance due to the stress singularities occurring around the connection area of the dam with the rock. Furthermore, the script does not take into account the size of the reservoir which is a significant factor for the selection of the best alternative in practice.

5. Final design stage

In the final design stage the optimization techniques are applied using the preliminary best alternative. The main goal is to add the least essential concrete and excavation volume to reduce the principal stresses to allowable levels. Hence, the geometry of the best alternative must be redefined by changing the used equations and adding new ones.

5.1. Design improvement

Through the design improvement the initial dam is reshaped so a more efficient shape in terms of stress levels can be generated. The side parabolas are used to thicken the abutment. Furthermore, the crown cantilever section and the line of main centers may be redefined so the dam can be thickened along its height.

It is mentioned that, the final dam must be reshaped until allowable stress levels are reached. For this reason, an iterative process is followed where the following variables are altered progressively till the final dam design is found.

Based on the document [3] the most important areas (key points), in terms of stress levels, of a double-curvature arch dam are visualized [Figure 58]. This section focuses on these areas and how they can be reshaped so smaller stresses can be obtained. This master project focuses on the green and the red circles as only static analyses are performed.

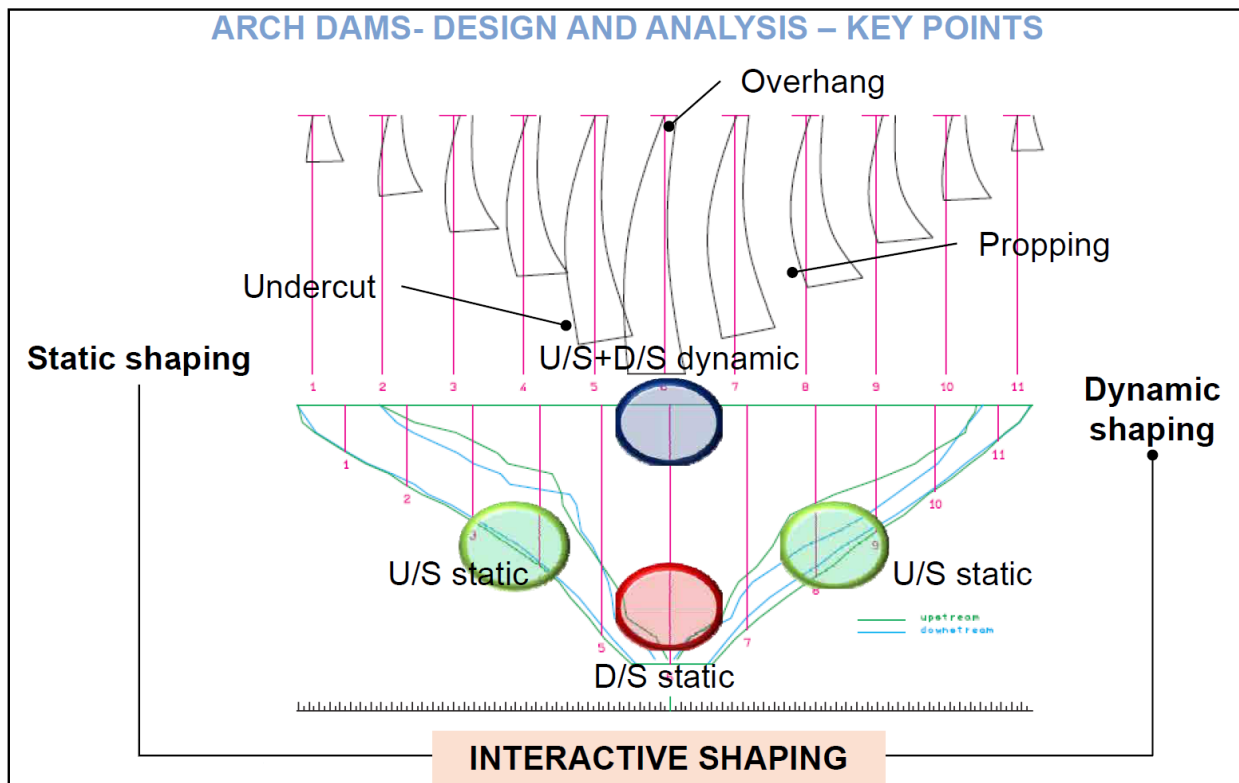


Figure 58: Key stress points of a double-curvature arch dam [3].

5.1.1. Definition of side parabolas

Side parabolas are the additional parabolic sets that describe the thickening in the downstream face of the dam. They consist of two different sets, one for each side, and they are correlated to each other as they use the same parameters.

They are defined based on the document [2] and their assumptions were thoroughly discussed so they can be as realistic as possible. One of the most dominant design factors was that they must be applicable to all different sites without generating abnormal dam shapes.

Four basic variables are introduced which describe the entire geometry of the side parabolas. Due to their high dependency with the main downstream parabolas they work using proportions.

$control_angle[-]$, is the proportion which defines the side angles. For this reason the variable is multiplied with the main angles along the dam height and its range is from 0 to 1. Note that, the main angles are computed by the end points and the reference plane. Using the side angles the respective lines are computed, which pass through the main center points, so the intersection points between the lines and the main downstream parabolas are computed. These points are the transition (tangent) points. Furthermore, both sides use the same proportion so a smooth downstream face can be generated based on the dam boundaries [Figure 59, Figure 62].

$control_crest[-]$, is the proportion which defines the side center point at the crest elevation, its range is from 0 to 1. At crest elevation, the y-coordinate of the side center point is defined by using the horizontal length between the respective tangent point and the main center point. This length is multiplied by this proportion and it is added to the y-coordinate of the tangent point. Afterwards, the x-coordinate of the side center point is defined by the equation of the line which connects the transition point with the main center point [Figure 59, Figure 61].

$control_050H[-]$, is the proportion which defines the side center point at elevation 050H above the base, its range is from 0 to 1. The same process described for the variable $control_crest$ is used and only the target elevation is changed [Figure 59, Figure 61].

$control_base[-]$, is the proportion which defines the side center at the base elevation, its range is from 0 to 1. The same process described for the variable $control_crest$ is used and only the target elevation is changed [Figure 59, Figure 61].

Using the three side centers points a parabola is calculated, which described the line of side centers. Consequently, the side center point at each elevation can be computed. In this way the abutment thickening is calculated along the height of the dam creating a smooth downstream face, eliminating possible geometric anomalies [Figure 62].

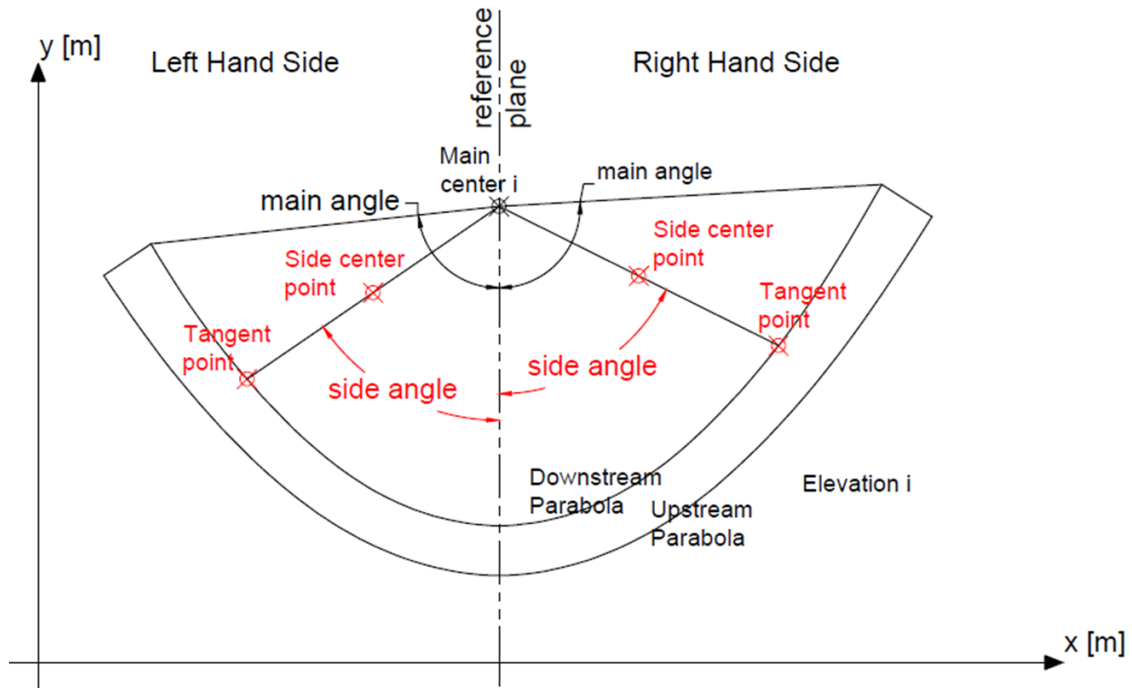


Figure 59: Transition (tangent) and side center point at elevations i (plan view) [2].

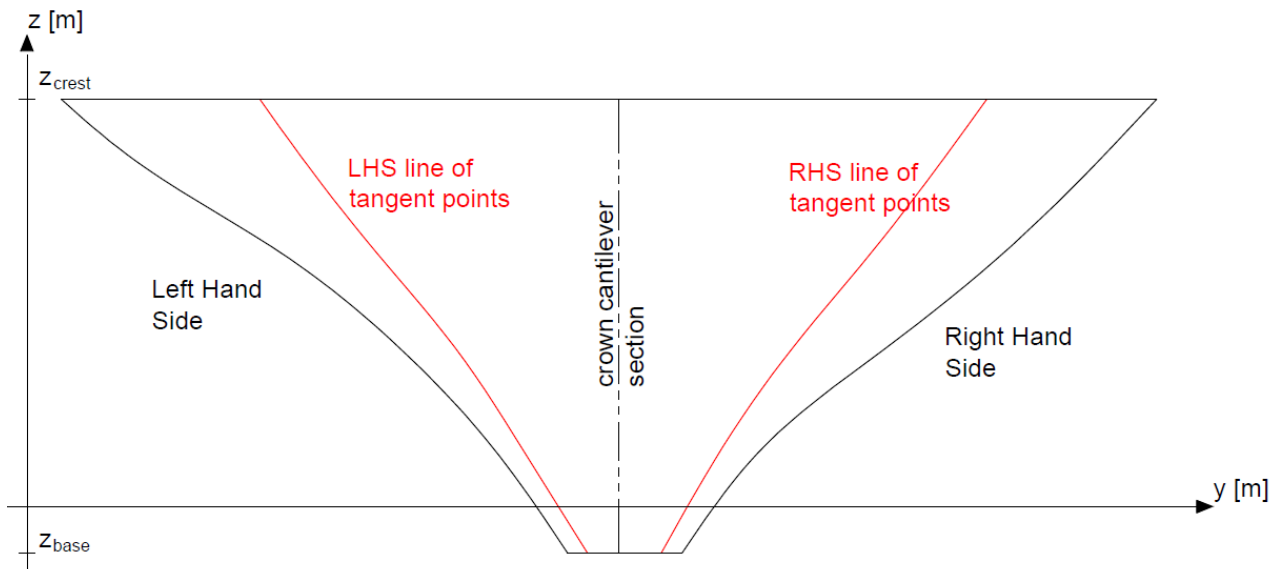


Figure 60: Lines of transition (tangent) points along the dam height (front view) [2].

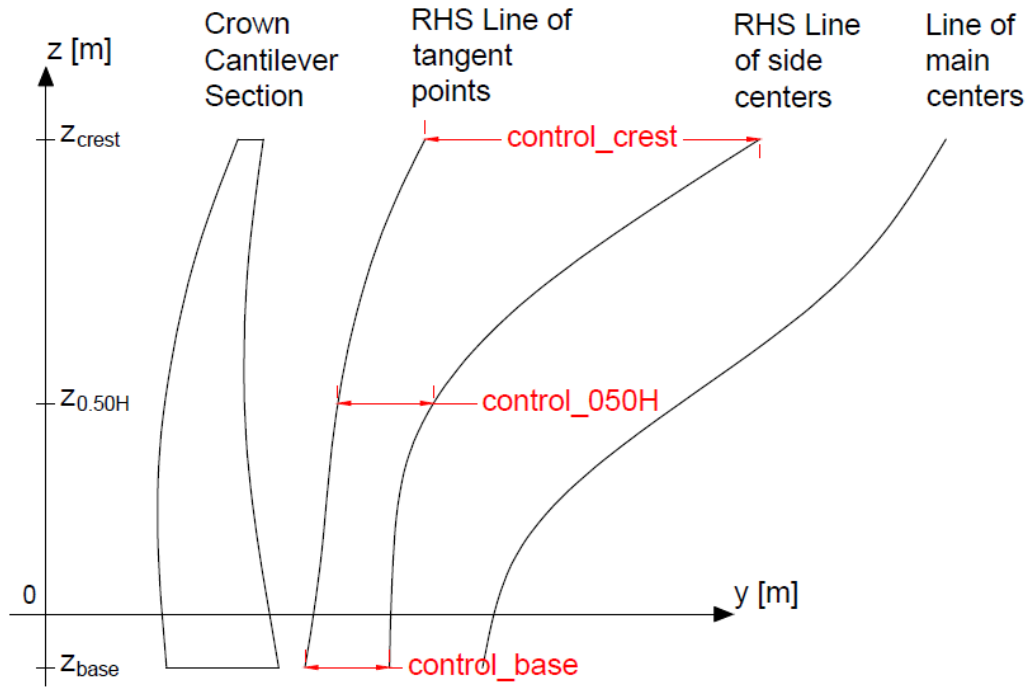


Figure 61: RHS line of side centers (side view) [2].

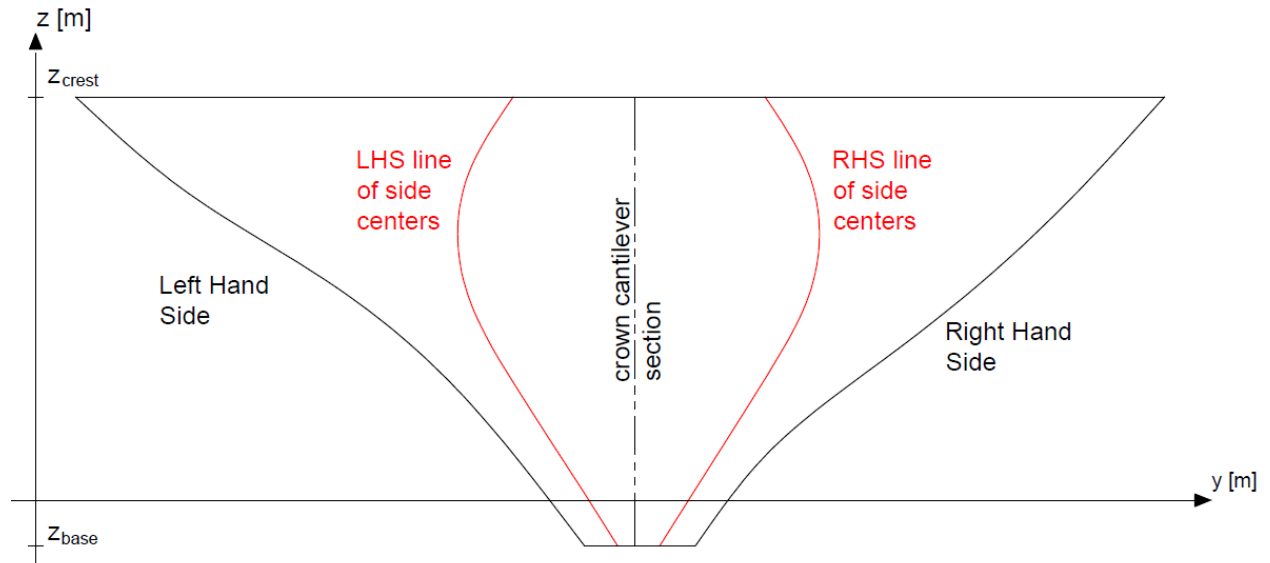


Figure 62: Lines of side centers along the dam height (front view) [2].

In the context of this master project the value of the *control_angle* is set to 0.667 as this value is concluded to be an efficient approximation for the transition points, based on the document [2], which describes a real dam.

Regarding the variables *control_crest*, *control_050H* and *control_base* the determination of their values must be checked separately using trials. It is mentioned that, if their value is small, close to 0, then the side center point is close to the transition point and a steeper (narrower) side parabola is generated, which means that more abutment is added. The exactly opposite happens when a large value, close to 1, is chosen where the side center point is close to the main center point. Consequently, the generated side parabola is broader (wider), which means that less abutment is added. In addition, the least concrete volume should be added so the best alternative remains the most economical one.

Abutment thickening is used to reduce areas with high tensile stresses. The areas of the dam with the highest tensile stresses are normally on the upstream face, above the base near the foundation area. These areas are visualized in Figure 58 described by the green circles. Furthermore, abutment thickening reduces the compressive stresses around the foundation area.

For this reason, sharper side parabolas are more essential for the elevations close to the base compared to the elevations close to the crest. In this way, the variable *control_crest* should have a large value so the least abutment thickening is added at the crest, while the variables *control_050H* and *control_base* should have a small value so more abutment thickening is added around the base.

5.1.2. Redefinition of crown cantilever section

In this section it is described how the crown cantilever section is reshaped, so the uniform thickness along the height can be smoothly changed.

The geometry of the crown cantilever section is defined in Section 4.6 and it consists of the upstream and downstream crown cantilever lines. For integrity purposes, the upstream line remains intact while the downstream line is redefined using three new variables which move the downstream projection points along the reference plane. Afterwards, a new parabola is computed based on the redefined points, which describes the redefined downstream line.

cc_down_tol_crest[meters], is the tolerance that is added in the y-coordinate of the downstream crown cantilever point at the crest elevation [Figure 63].

cc_down_tol_045H[meters], is the tolerance that is added in the y-coordinate of the downstream crown cantilever point at $0.45H$ above the base elevation [Figure 63].

cc_down_tol_base[meters], is the tolerance that is added in the y-coordinate of the downstream crown cantilever point at the base elevation [Figure 63].

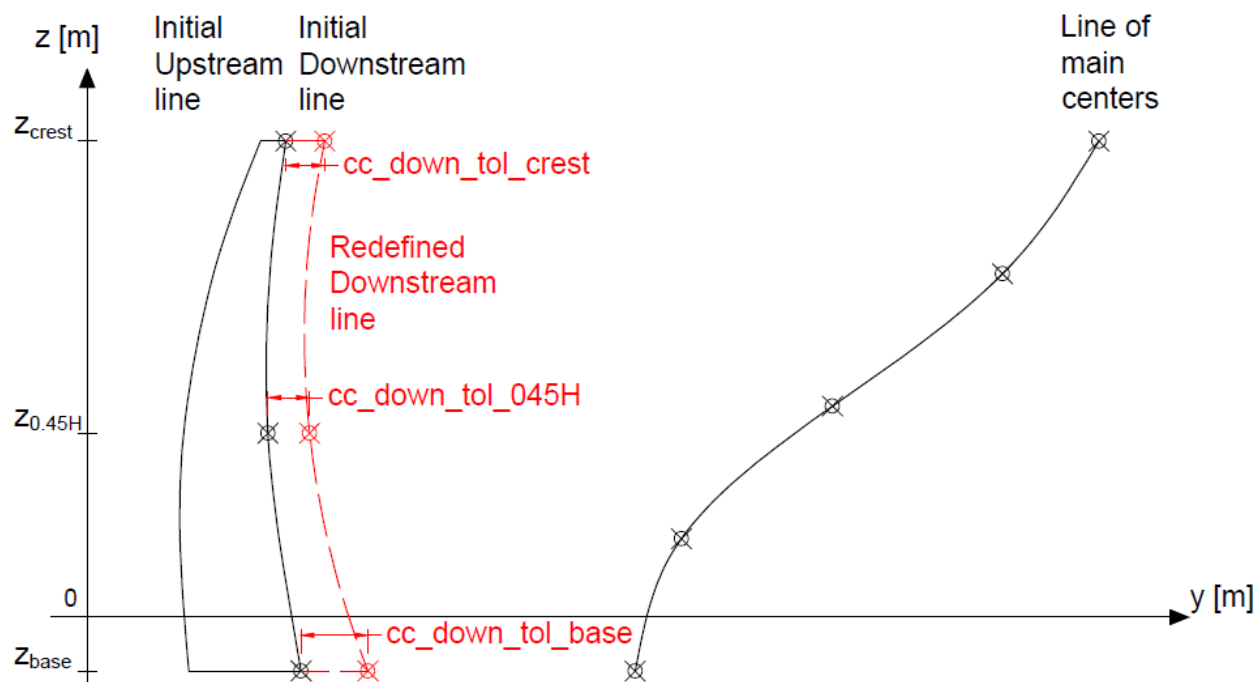


Figure 63: Redefinition of the crown cantilever section (side view) [2].

In this way, the uniform thickness of the dam at each elevation is altered. The values of the variables can be negative, meaning that a thinner dam is generated, or positive, meaning that a thicker dam is generated. However, if the given values are negative, they must not be larger than the initial thickness at this elevation as the dam volume becomes negative.

The main goal of this section is to reduce the maximum tensile stresses located in the middle dam area above the base. The values of the variables must be defined by trials adding the least needed concrete volume. Furthermore, the shape of the downstream line should be similar to the initial line, or else a completely different dam will be generated. In other words, the values of the variables should be chosen so the thickness change along the height remains approximately the same.

5.1.3. Redefinition of line of main centers

The line of main centers can be redefined as well so a more efficient dam is generated. In this way, the main upstream and downstream parabolas are narrowed or widened, so they can fit better on the surrounding topography.

The definition of the line of main centers is described in Section 4.7 and in the context of this master project five points are used. For this reason, five variables are used so each of these points can be redefined moving them along the reference plane.

$center_tol_z_crest$ [meters], is the tolerance that is added in the y-coordinate of the initial main center point at the crest elevation [Figure 64].

$center_tol_z_075H$ [meters], is the tolerance that is added in the y-coordinate of the initial main center point at $0.75H$ above the base elevation [Figure 64].

$center_tol_z_050H$ [meters], is the tolerance that is added in the y-coordinate of the initial main center point at $0.50H$ above the base elevation [Figure 64].

$center_tol_z_025H$ [meters], is the tolerance that is added in the y-coordinate of the initial main center point at $0.25H$ above the base elevation [Figure 64].

$center_tol_z_base$ [meters], is the tolerance that is added in the y-coordinate of the initial main center point at the base elevation [Figure 64].

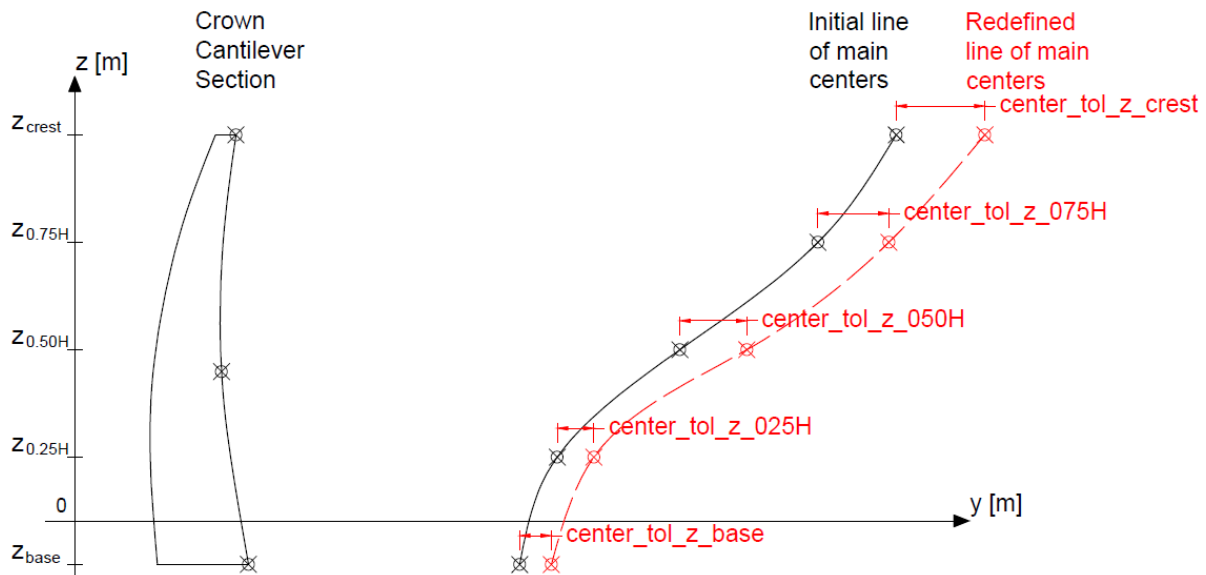


Figure 64: Redefinition of the line of main centers (side view) [2].

If the variables have a positive value then their distance from the crown cantilever section becomes larger. Consequently, the redefined parabola becomes wider. It is mentioned that, a wider parabola usually leads to an increase of the respective tensile stresses.

These variables are very efficient in reducing the tensile stresses of the green circle [Figure 58], located on the downstream face. However, special attention should be given so the shape of the line remains smooth as it directly affects the entire shape of the dam.

Their values should be modified in accordance with the other variables from the crown cantilever section, so local anomalies are avoided, like dimples on Bezier Surfaces. Around the anomalies bad-shaped elements may occur which significantly affect the principal stresses.

5.2. Interface elements

Interface elements must be used for the common surfaces of the dam and the rock to simulate possible openings. In his way, the stress singularities are drastically reduced and a more realistic model is obtained.

Two different types of interface elements are used to reduce the stress singularities. The first one connects the common surfaces of the dam cantilevers, while the other one connects the common surfaces of the dam cantilever with the surrounding rock.

Non-linear elastic interface elements are used and their stiffness should depend on the stiffness of adjacent material. For this reason, the normal and tangential stiffness moduli are defined through the following rule of thumb.

$$K_n = 100 \sim 1000 \frac{E}{l^{el}} [N/m^3] \quad (5.1)$$

$$K_t = \frac{K_n}{10 \sim 100} [N/m^3] \quad (5.2)$$

Where, $K_n [N/m^3]$ is the normal stiffness modulus-z*.

$K_t [N/m^3]$ is the tangential stiffness modulus-y*.

$E [N/m^2]$ is the highest elastic modulus of the connected solids.

$l^{el} [m]$ is the characteristic length of the smallest element.

It is recommended that, the highest possible material values should be used such that overlapping is avoided.

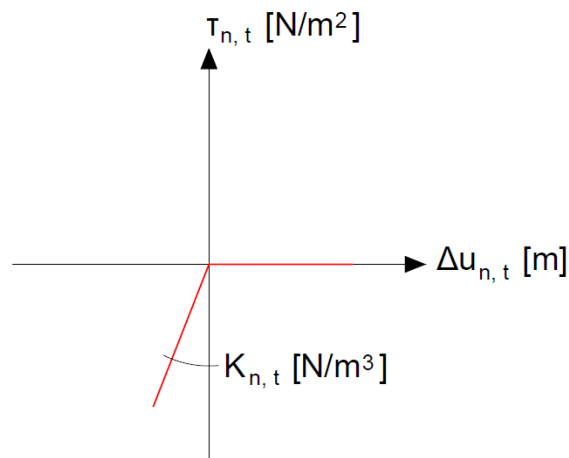


Figure 65: Constitutive model for interfaces in normal and tangential direction.

5.2.1. Concrete-concrete connection

Concrete-concrete interfaces use the geometry of the contraction joints, described in Section 4.11, simulating possible sliding between the dam cantilevers. In this way, the cantilever joints can partly or fully open and close during a seismic excitation [Figure 66].

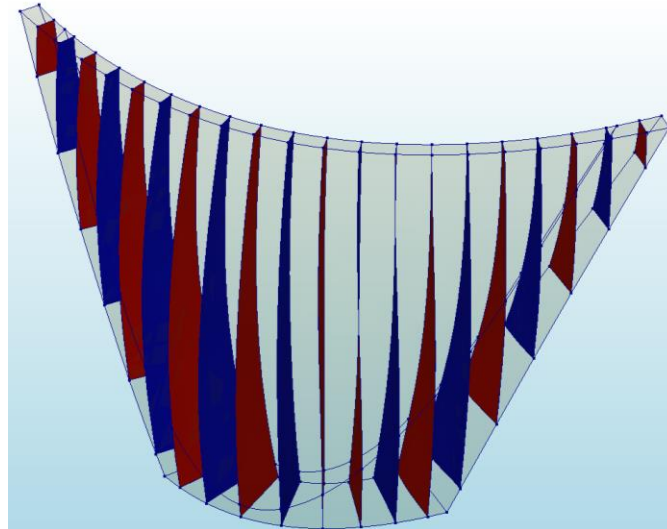


Figure 66: Concrete-concrete interfaces (3D view).

5.2.2. Concrete-rock connection

The common surfaces of the dam and the rock are split into two types of interface elements. The first one contains the upstream and downstream cantilever surfaces [Figure 67], while the second one the cantilever surfaces of the foundation area [Figure 68]. They are called side and base interfaces respectively.

The side interfaces remove the connection between the dam and the rock [Figure 67]. In this way the two solid shapes can act independently and the stress singularities are eliminated from these surfaces. This is very important as these surfaces contain the stress key points that have to be checked [Figure 58, green circles].

The base interfaces connect the dam to the rock [Figure 68]. Hence, the stress singularities are located around them and a more realistic model is obtained where openings between the dam and rock can happen.

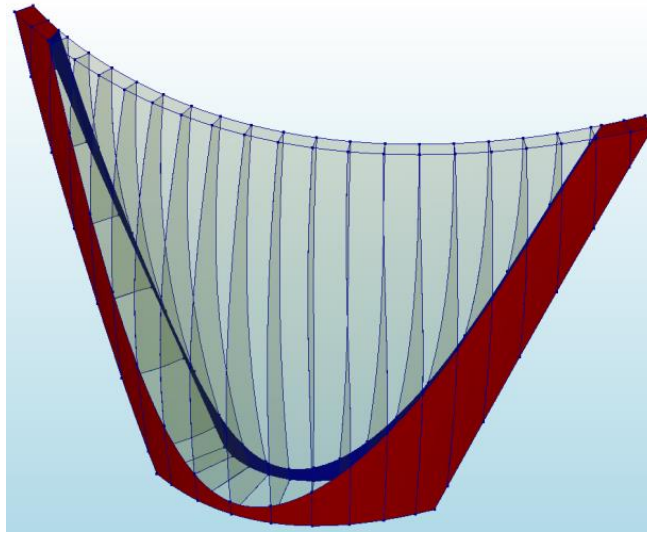


Figure 67: Side concrete-rock interfaces (3D view).

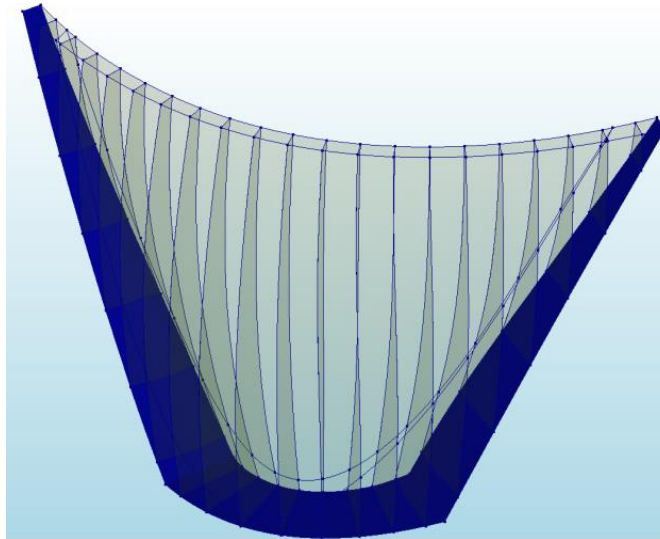


Figure 68: Base concrete-rock interfaces (3D view).

5.3. Final stress analysis

Having defined the new parabolic sets that describe the geometry of the final dam, the model is generated and a non-linear static analysis is performed.

To create the model in Diana Interactive Environment (DianaIE) the same process from Section 4.12 is used taking into account the final variables. Consequently, the redefined downstream face consists of three different types of parabolas as the side parabolas for each side are taken into account. The foundation area is affected too as the side parabolas describe the downstream end points. In the end, the dam and the topography solid shapes are generated based on the final variables.

In the context of this master project, a non-linear static analysis is performed and the non-linearity is located only on the interface elements.

5.4. Evaluation of results

The results for the final model must be evaluated so it can be concluded if the stress constraints are satisfied. The principal stresses on the dam must be below 1 MPa in tension and below the compressive strength of the used concrete [6]. The principal stresses on the rock are neglected as they are assumed to be of secondary importance.

Using interface elements, the stress singularities are drastically reduced but they are not eliminated. Hence, the key stress points must be located based on Figure 58 neglecting the stresses around the foundation area which contains the stress singularities.

If the key point stresses satisfy the constraints then this is the final dam. Otherwise, the final variables [Section 5.1] must be modified adding a small amount of concrete volume where is needed. The way that the variables should be redefined is based on the designer's judgement and the found results.

The process stops when the stress constraints are satisfied. In this way, a "manual" optimization takes place where the final solution is dependent on the designer's experience. Further research is essential for this part and it is out of the context of this report.

An alternative to the aforementioned process is to use only a scalar as an optimization target which simplifies the treatment of the principal stress vectors $(\sigma_1, \sigma_2, \sigma_3)$ a scalar is defined which combines all of them into one value. For dam mass concrete, the biaxial stress state is used for the upstream and downstream surfaces of the dam.

The scalar represents a safety factor for concrete under static and dynamic loading conditions with reference to a biaxial failure envelope. Hence, the designer must define the static uniaxial compressive strength of the concrete f_c , the transformation factor from static to dynamic strength X_{rate} ($X_{rate} = 1.30$), and the transformation factor from apparent to actual stiffness X_{spec} ($X_{spec} = 0.44$) [7].

The static compressive strength can be defined either by a constant value or as a function of time or maturity, using a multilinear diagram. In the context of this master project, only the first situation is taken into account. In addition, the two transformation factors are used to calculate the static tensile strength and the dynamic compressive and tensile strength [7].

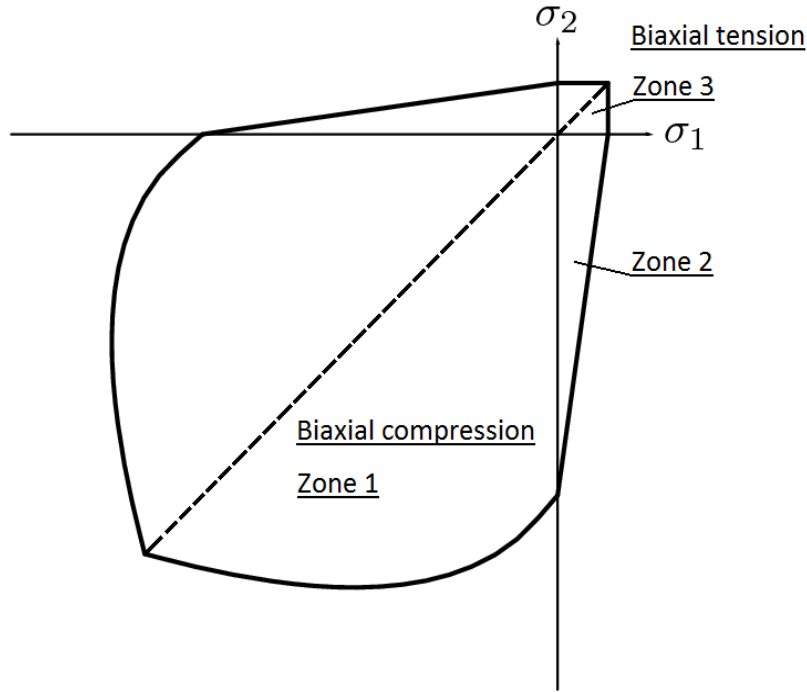


Figure 69: Static (inner) and dynamic (outer) concrete biaxial failure envelope [7].

In Figure 69 the biaxial failure envelope for concrete under static loading and under dynamic loading is defined in the stress surface which is expanded by the maximum principle stress σ_1 and the minimum principle stress σ_2 [7].

There are three different zones which are defined by the ratio α between the maximum principal stress σ_1 and the minimum principal stress σ_2 , ($\alpha = \sigma_1/\sigma_2$) [7].

For Zone 1 ($0 < \alpha < 1$):

$$R = \frac{(1 + 3.65\alpha)\sqrt{(1 + \alpha^2)}f_c}{(1 + \alpha^2)f_{sc}}$$

For Zone 2 ($\alpha < 0$):

$$R = \frac{\sqrt{(1 + \alpha^2)}f_c}{\left(1 - \alpha \frac{f_c}{f_t}\right)f_{si}}$$

For Zone 3 ($\alpha > 1$):

$$R = \frac{\sqrt{(1 + \alpha^2)} f_t}{\alpha f_{st}}$$

Where, R is the distance from the origin to the failure envelope.

f_{sc} is the compressive strength safety factor.

f_{st} is the tensile strength safety factor.

f_{si} is the intermediate safety factor.

There are four different load cases and only the first one is taken into account [7].

- Static Usual (FSstus)
- Static Unusual (FSstun)
- Dynamic Unusual (FSdyun)
- Dynamic Extreme (FSdyex)

Note that, the value of the safety factor R must be larger than one so it can be accepted. Otherwise the static uniaxial compressive strength of the concrete f_c must be increased so the biaxial failure envelope can be expanded. Consequently, the dam is reshaped while at the same time the best fitting concrete strength class is investigated. Note that, a normal range for concrete strength should be from 15 to 45 MPa.

This process is not investigated in this master project and only some characteristic plots are going to be shown.

6. Application of the code

To demonstrate the aforementioned process and validate its efficiency a realistic dam design is simulated in the following sections.

6.1. Selection of the topographic surface

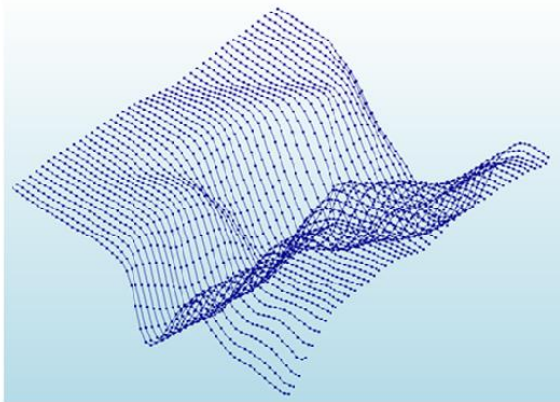
First a realistic topographic surface based on Section 4.2 is obtained. The main aim is to find a valley that is high, narrow and long enough, so a sufficient number of potential dam sites can be picked. For this reason, a small part of Vikos Gorge is chosen.

Vikos Gorge (Φαράγγι του Βίκου) is a gorge in the Pindus Mountains of northern Greece. It lies on the southern slopes of Mount Tymfi, with a length of about 20 km, depth ranging from 450 to 1600 m and a width ranging from 400 m only a few meters at its narrowest part. The picked surface is 2 km long and satisfies the general criteria to design a dam [9].

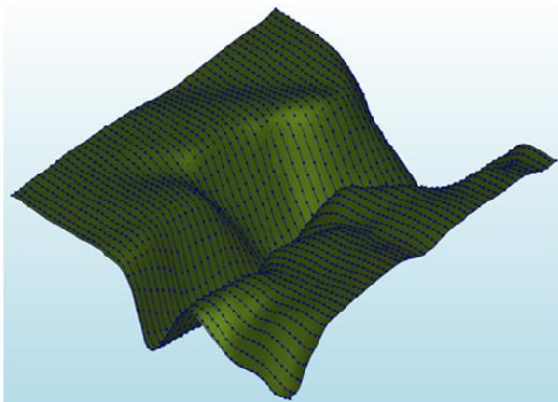
Picture of Vikos Gorge



Cloud of points (3D view)



Bezier surface (3D view)



Bezier surface (top view)

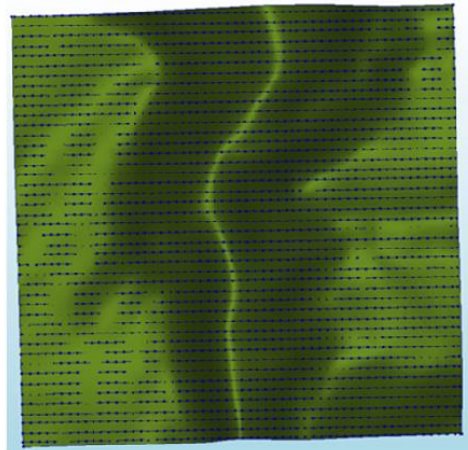


Figure 70: Vikos Gorge surface from Sketchup2015 to DianaIE.

6.2. Selection of the potential dam sites

Three different locations are investigated which are chosen based on the general shape of the dam so all the potential dam shapes can be compared [Figure 71].

- Location A should generate an unsymmetrical dam where Right Hand Side (RHS) is longer.
- Location B should generate a symmetrical dam.
- Location C should generate an unsymmetrical dam where Left Hand Side (LHS) is longer.

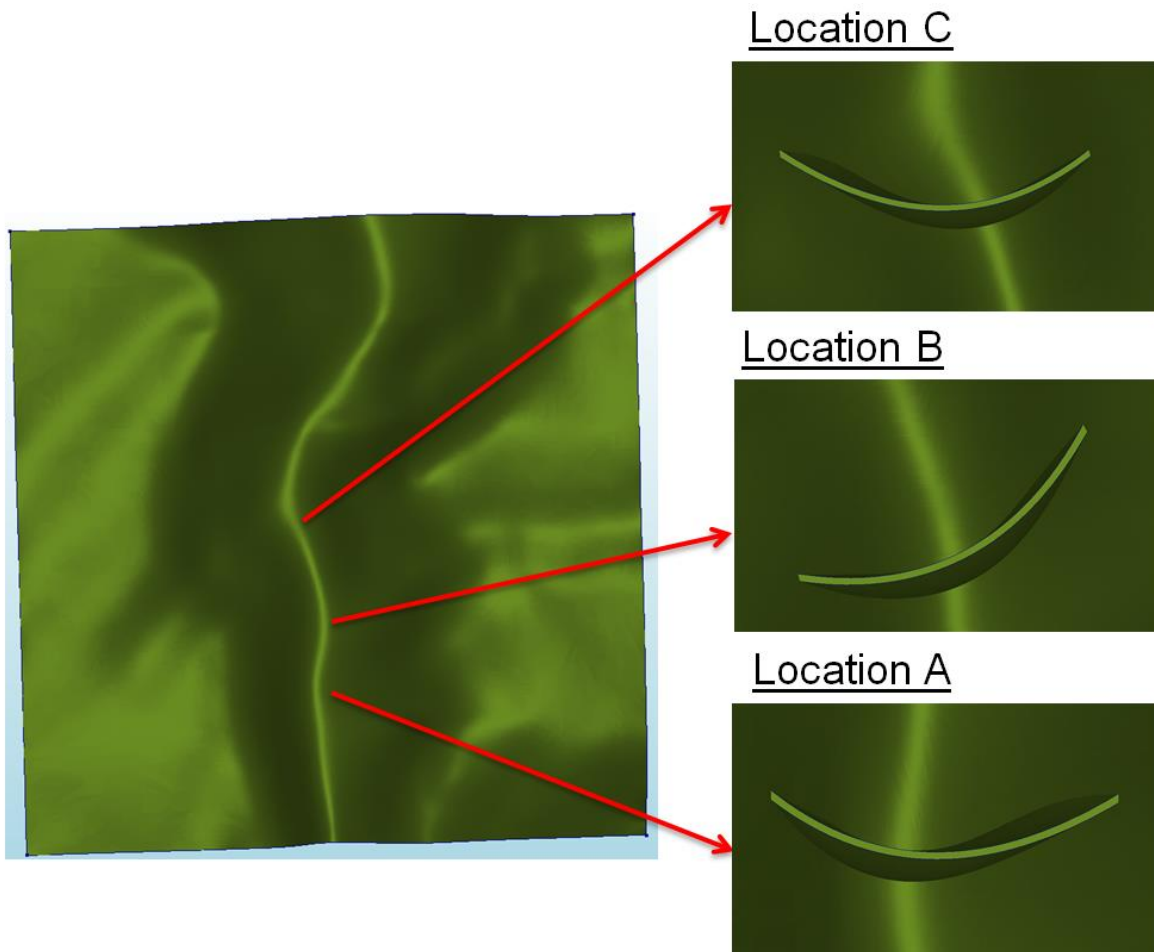


Figure 71: The chosen locations on the topographic surface (plan view).

6.3. Selection of the basic variables

To generate dams using the script, the basic variables must be defined. The following values for each location are not based on a real dam but they are assumed. If one of the variables changes then a totally new dam is generated and it is not comparable with the previous one.

To obtain the desirable locations more than one hundred different sites were tested and the best three were chosen based on the guidelines of Section 0 [Figure 71].

The basic variables of the dam height, the uniform excavation length and the minimum excavation length have the same values for all the locations and as a result the generated dam models are comparable with each other. As mentioned before, the dam base elevation is assumed to be 8 meters below the lowest contour in riverbed [6].

The value of the axis angle must be checked for each location so the most economical dam is generated. Therefore, each location is checked for a range of angle values and then the most efficient one is chosen, based on the least concrete (dam) and excavation volume. A table and the respective graph, containing the essential information, are shown for each location in the following sections.

The range of the axis angle is highly dependent on the used topography. If the topography is smooth enough then the range is large as well and vice versa.

6.3.1. Location A-Selection of the best fitting dam

$$y_{start} = -400 m$$

$$H = 250 m$$

$$z_{base} = 42 m$$

$$\theta_{axis} = -25^\circ .. 6^\circ \rightarrow \theta_{axis} = -10^\circ$$

$$L_{excavation} = 30 m$$

$$L_{excavation}^{\min} = 10 m$$

Location A			
axis angle (°)	equal angles β (°)	V_{conc} (m ³)	V_{exc} (m ³)
6	NO	1.557E+06	4.368E+05
4	NO	1.527E+06	3.641E+05
2	NO	1.487E+06	3.547E+05
0	NO	1.476E+06	3.586E+05
-2	NO	1.466E+06	3.599E+05
-4	YES	1.460E+06	3.626E+05
-6	YES	1.455E+06	3.644E+05
-8	YES	1.450E+06	3.629E+05
-10	YES	1.447E+06	3.611E+05
-12	NO	1.441E+06	3.545E+05
-14	NO	1.435E+06	3.234E+05
-16	NO	1.596E+06	3.021E+05
-18	NO	1.687E+06	3.185E+05
-20	NO	1.789E+06	3.384E+05
-22	NO	1.904E+06	3.673E+05
-24	NO	2.019E+06	4.058E+05
-26	NO	2.156E+06	4.931E+05

	$\beta_{LHS} > 30^\circ$ and $\beta_{RHS} > 30^\circ$	$\beta_{LHS} = \beta_{RHS}$
NO	FALSE	FALSE
NO	TRUE	FALSE
YES	TRUE	TRUE

Table 1: Location A, concrete and excavation volume vs axis angle.

In Table 1 there are different colors in the columns of angles β . The definition of the angle of incidence is explained in Section 4.5. **NO** means that, the angles are not equal and at least one of them is smaller than 30 degrees. **NO** means that, the angles are not equal and both of them are larger than 30 degrees. **YES** means that, the angles are equal and both of them are larger than 30 degrees.

Only the results with **YES** are suitable, based on the initial criteria. Furthermore, the best fitting solution is pointed out in each table.

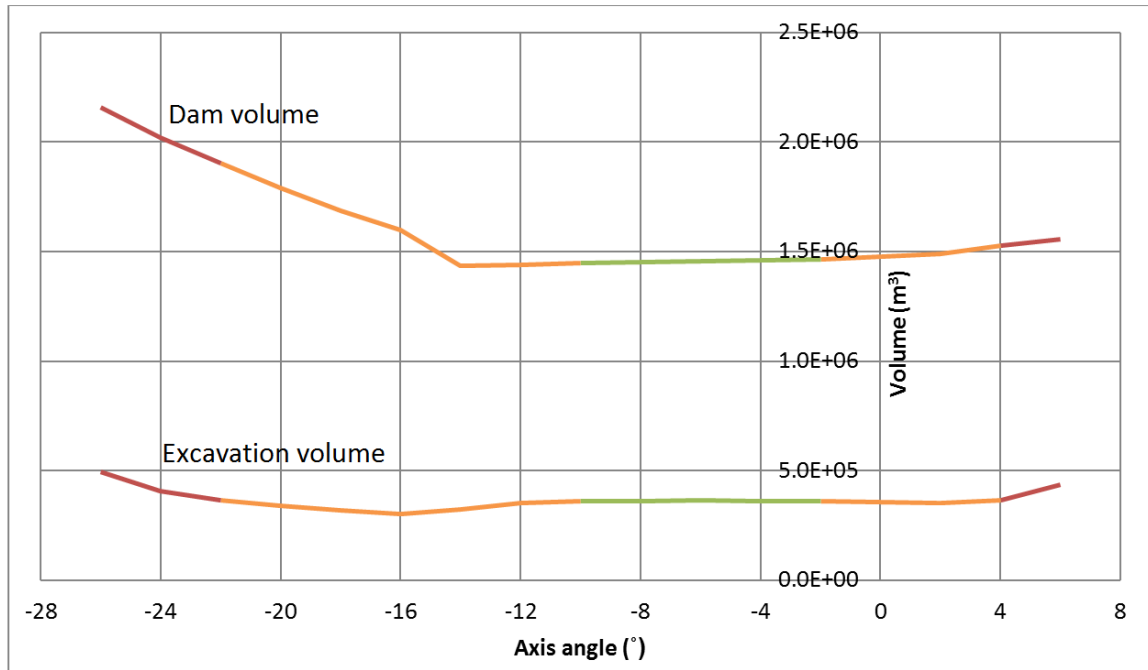


Figure 72: Location A, concrete and excavation volume vs axis angle.

In Figure 72 it is shown how the change of the axis angle influences the dam (concrete) and excavation volume. The different colors that are used have the same meaning as in Table 1.

6.3.2. Location B-Selection of the best fitting dam

$$y_{start} = -240m$$

$$H = 250m$$

$$z_{base} = 38m$$

$$\theta_{axis} = -14^\circ \dots 40^\circ \rightarrow \theta_{axis} = 24^\circ$$

$$L_{excavation} = 30m$$

$$L_{excavation}^{\min} = 10m$$

Location B			
axis angle (°)	equal angles β (°)	V_{conc} (m ³)	V_{exc} (m ³)
40	NO	1.275E+06	2.965E+05
38	NO	1.192E+06	2.607E+05
36	NO	1.163E+06	2.495E+05
34	NO	1.155E+06	2.472E+05
32	NO	1.152E+06	2.474E+05
30	NO	1.152E+06	2.482E+05
28	NO	1.155E+06	2.499E+05
26	NO	1.165E+06	2.551E+05
24	YES	1.173E+06	2.591E+05
22	YES	1.181E+06	2.612E+05
20	YES	1.192E+06	2.632E+05
18	YES	1.207E+06	2.657E+05
16	YES	1.224E+06	2.688E+05
14	YES	1.244E+06	2.709E+05
12	NO	1.264E+06	2.706E+05
10	NO	1.283E+06	2.657E+05
8	NO	1.310E+06	2.664E+05
6	NO	1.340E+06	2.698E+05
4	NO	1.368E+06	2.708E+05
2	NO	1.391E+06	2.704E+05
0	NO	1.421E+06	2.794E+05
-2	NO	1.453E+06	2.955E+05
-4	NO	1.469E+06	3.066E+05
-6	NO	1.465E+06	3.082E+05
-8	NO	1.468E+06	3.229E+05
-10	NO	1.455E+06	3.249E+05
-12	NO	1.440E+06	3.271E+05
-14	NO	1.429E+06	3.308E+05

	$\beta_{LHS} > 30^\circ$ and $\beta_{RHS} > 30^\circ$	$\beta_{LHS} = \beta_{RHS}$
NO	FALSE	FALSE
NO	TRUE	FALSE
YES	TRUE	TRUE

Table 2: Location B, concrete and excavation volume vs axis angle.

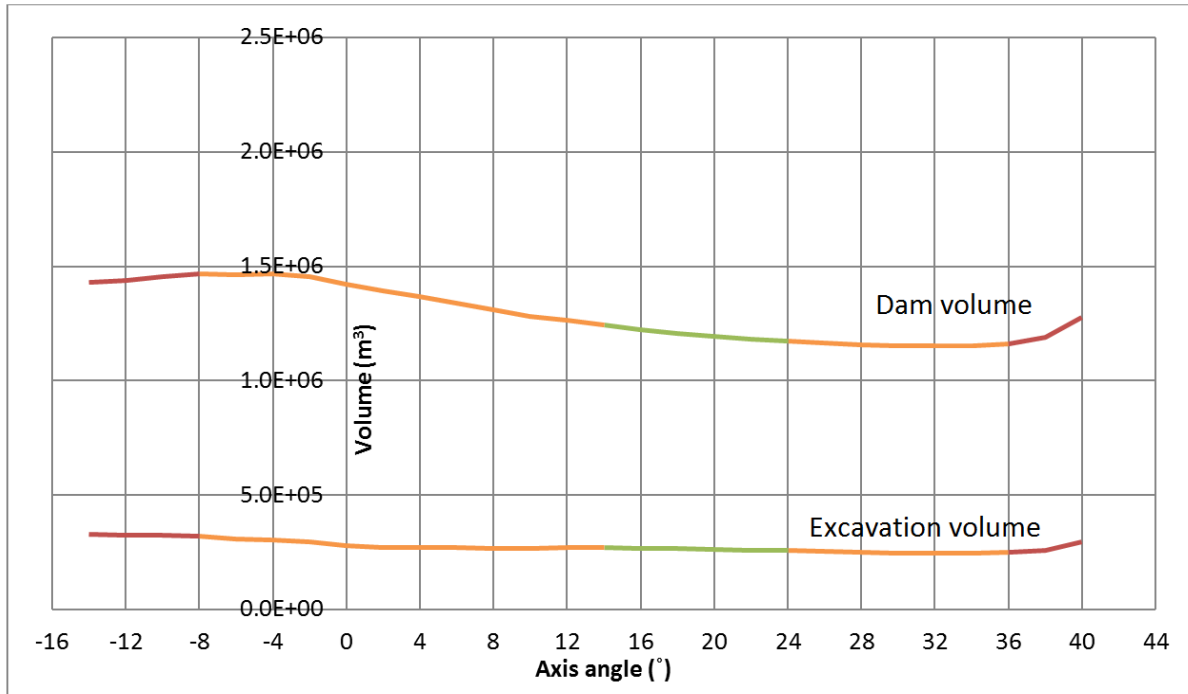


Figure 73: Location B, concrete and excavation volume vs axis angle.

6.3.3. Location C-Selection of the best fitting dam

$$y_{start} = 60m$$

$$H = 250m$$

$$z_{base} = 38m$$

$$\theta_{axis} = -6^\circ \dots 20^\circ \rightarrow \theta_{axis} = 8^\circ$$

$$L_{excavation} = 30m$$

$$L_{excavation}^{\min} = 10m$$

Location C			
axis angle (°)	equal angles β (°)	V_{conc} (m ³)	V_{exc} (m ³)
20	NO	1.696E+06	4.069E+05
18	NO	1.630E+06	3.834E+05
16	NO	1.609E+06	3.853E+05
14	NO	1.610E+06	3.988E+05
12	NO	1.622E+06	4.189E+05
10	NO	1.644E+06	4.466E+05
8	YES	1.705E+06	5.039E+05
6	YES	1.799E+06	5.807E+05
4	NO	1.870E+06	6.257E+05
2	NO	1.949E+06	6.938E+05
0	NO	2.005E+06	7.413E+05
-2	NO	2.068E+06	7.918E+05
-4	NO	2.139E+06	8.488E+05
-6	NO	2.211E+06	9.024E+05

	$\beta_{LHS} > 30^\circ$ and $\beta_{RHS} > 30^\circ$	$\beta_{LHS} = \beta_{RHS}$
NO	FALSE	FALSE
NO	TRUE	FALSE
YES	TRUE	TRUE

Table 3: Location C, concrete and excavation volume vs axis angle.

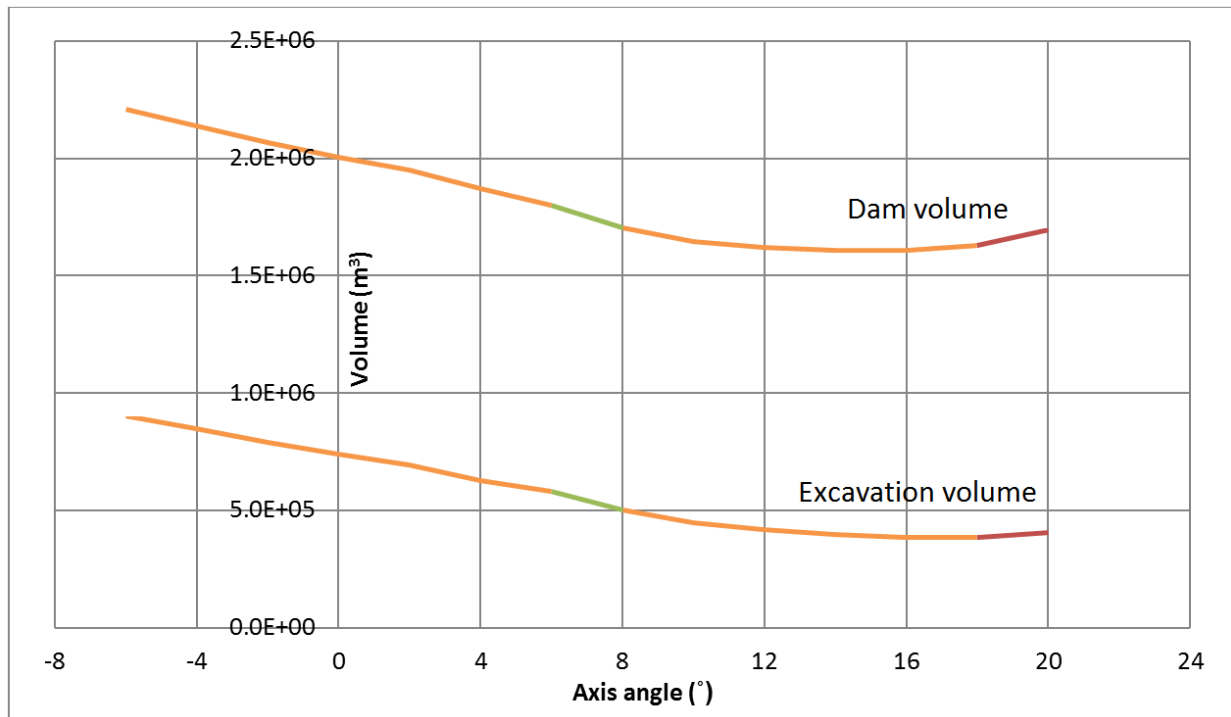


Figure 74: Location C, concrete and excavation volume vs axis angle.

6.4. Preliminary model properties

During the preliminary design stage only linear analyses are performed. So, the elastic properties of the materials, concrete and rock, must be defined.

For the rock, the following properties are chosen.

- Young's modulus: $E_{rock} = 18 \text{ GPa}$
- Poisson ratio: $\nu_{rock} = 0.27$
- Mass density: $\rho_{rock} = 0 \text{ kg/m}^3$

For the concrete, the following properties are chosen.

- Young's modulus: $E_{conc} = 25.5 \text{ GPa}$
- Poisson ratio: $\nu_{conc} = 0.20$
- Mass density: $\rho_{conc} = 2400 \text{ kg/m}^3$

	E (GPa)	ν	ρ (kg/m ³)
Rock	18.0	0.27	0
Concrete	25.5	0.20	2400

Table 4: Preliminary material properties.

The density of the rock is assumed to be zero, as the stresses due to the rock self-weight should be avoided. The focus is on the arch dam and not on the surrounding topography.

6.5. Preliminary results

The preliminary results are visualized for each location. The used boundary conditions are explained in Section 4.12.7 and they are the same for every model.

The determination of the mesh sizes is based on Section 4.12.8, where the topography mesh size is always fixed at 100 m. For the dam three different mesh sizes are tested, the first one is the limit size 21 m, the second one is the intermediate mesh size 10 m and the third one is the fine mesh size 5 m.

The reason for using three mesh sizes is to point out the influence of the stress singularities around the connection area of the dam with the rock. In the following three sections the results for the intermediate mesh are shown, while the other results are in Appendix 1: Preliminary results. The results for the displacement field $DtXYZ$ and the in-plane principal components at the upstream and downstream face of the dam are shown.

The topography solid shape is not of high importance and as a result it is not visualized.

6.5.1. Location A-Dam mesh size 10

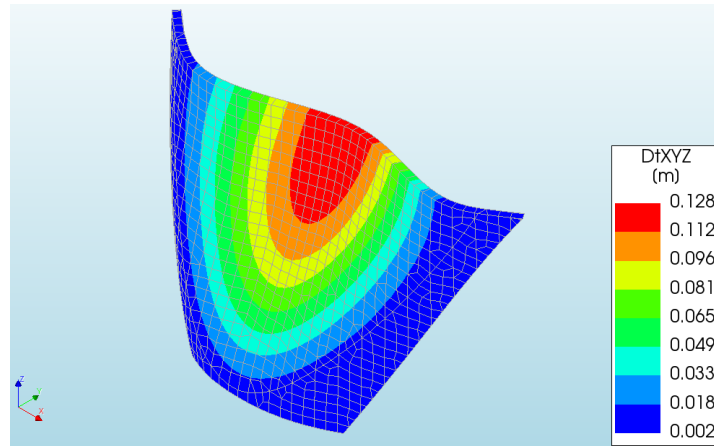


Figure 75: Location A-Mesh 10-Displacement field DtXYZ (3D view).

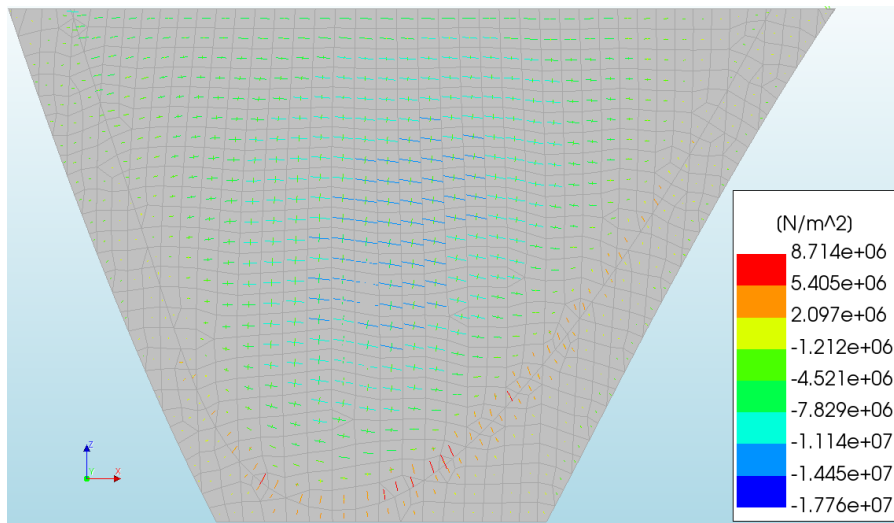


Figure 76: Location A-Mesh 10-In plane principal stresses (Upstream view).

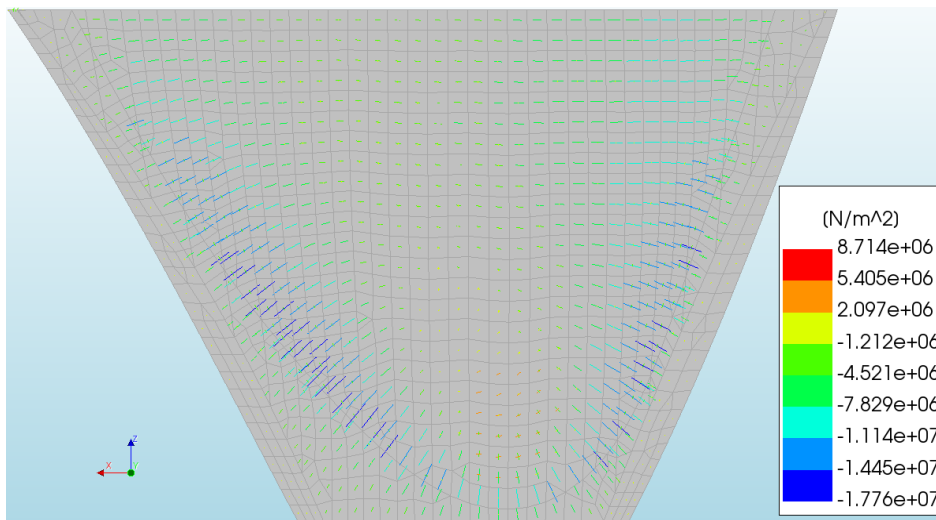


Figure 77: Location A-Mesh 10-In plane principal stresses (Downstream view).

6.5.2. Location B-Dam mesh size 10

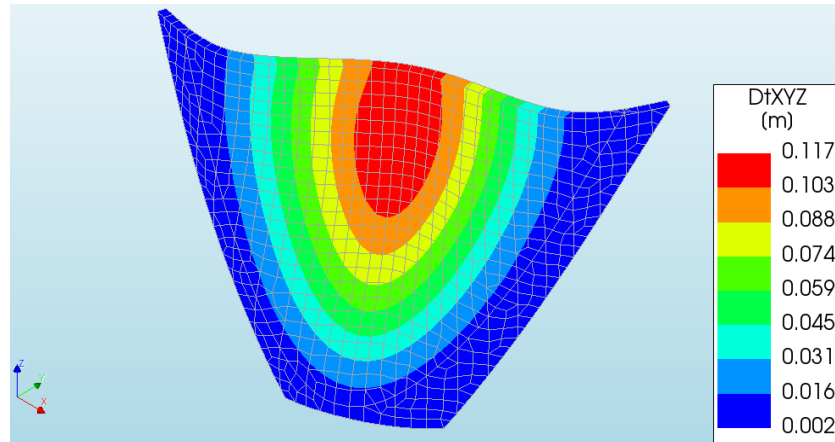


Figure 78: Location B-Mesh 10-Displacement field DtXYZ (3D view).

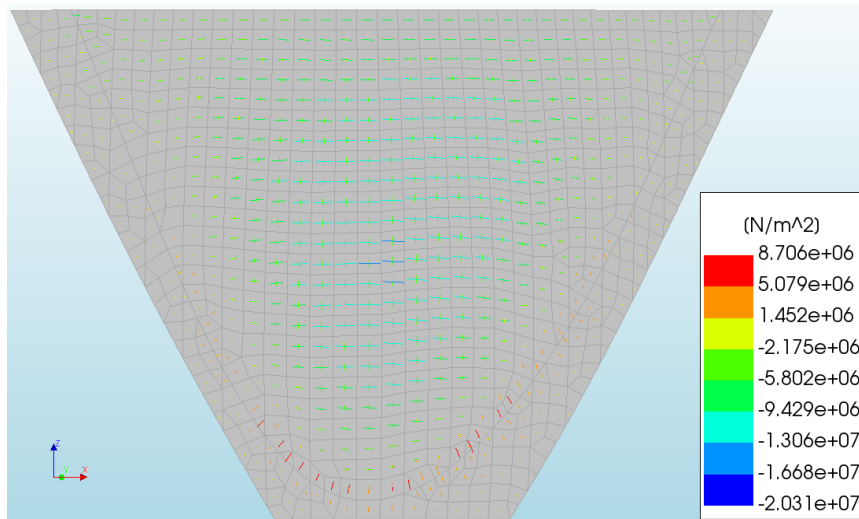


Figure 79: Location B-Mesh 10-In plane principal stresses (Upstream view).

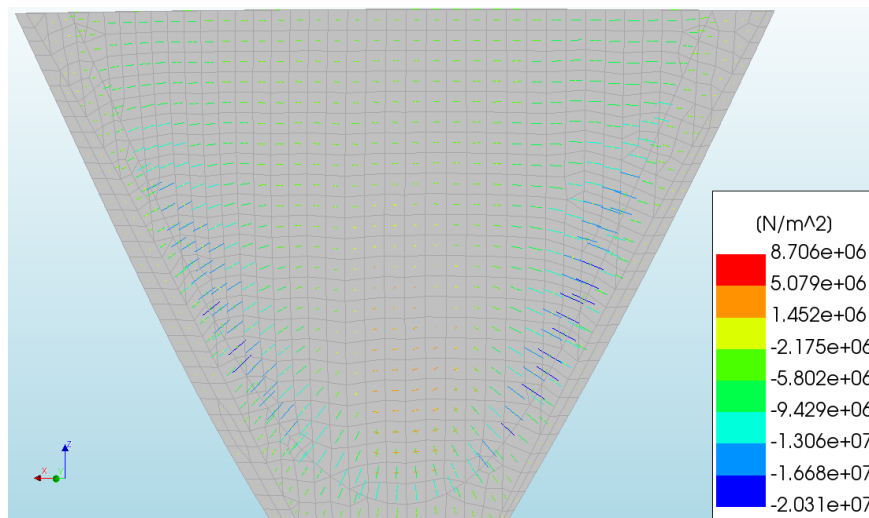


Figure 80: Location B-Mesh 10-In plane principal stresses (Upstream view).

6.5.3. Location C-Dam mesh size 10

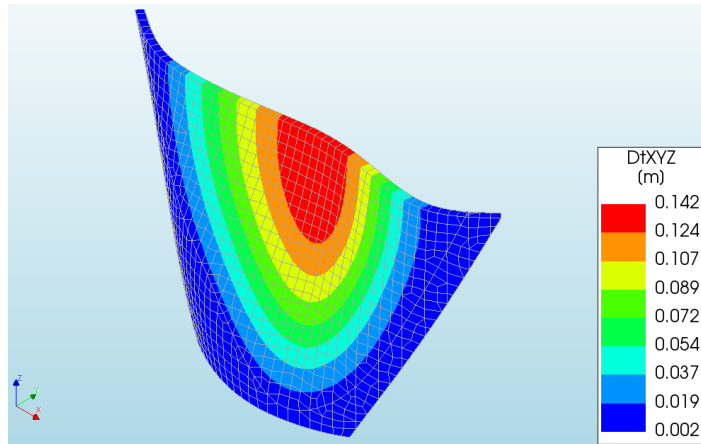


Figure 81: Location C-Mesh 10-Displacement field DtXYZ (3D view).

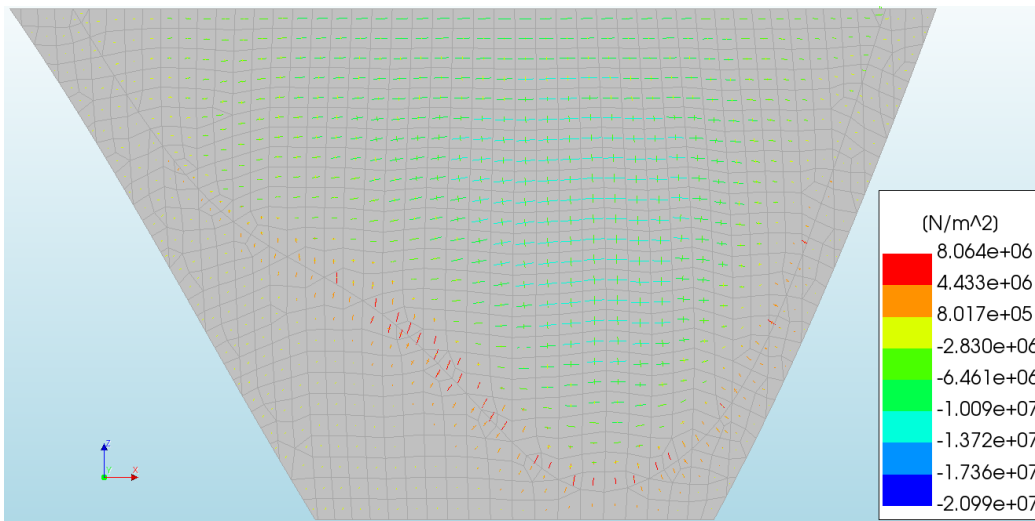


Figure 82: Location C-Mesh 10-In plane principal stresses (Upstream view).

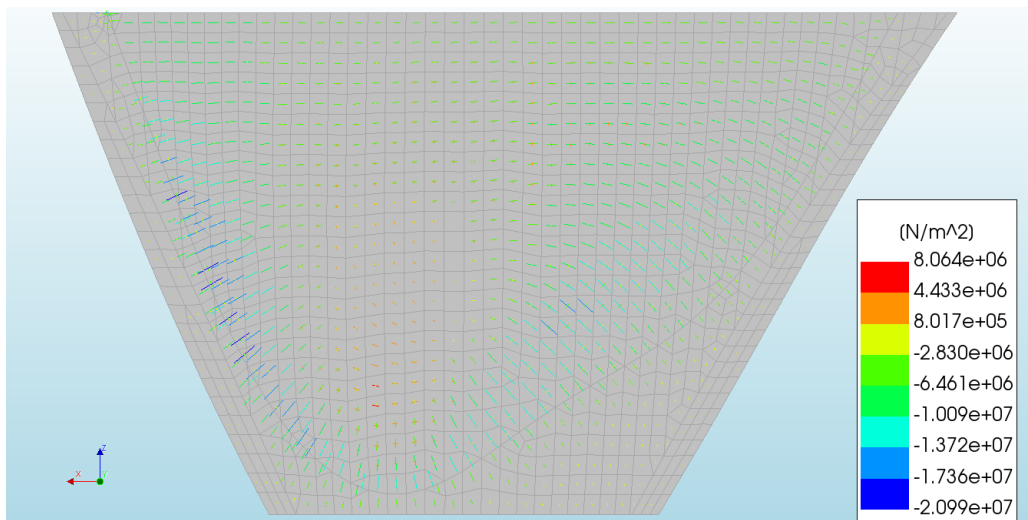


Figure 83: Location C-Mesh 10-In plane principal stresses (Upstream view).

6.6. Selection of the best alternative

The best fitting dam for each location is compared, so the best alternative is chosen. The predominant factors are the concrete (dam) and the excavation volume. Based on Table 5 and Figure 84 it is concluded that Location B gives the best alternative. Consequently, the most symmetrical dam gives the most economical solution and this is not just a coincidence.

Location	axis angle (°)	equal angles β (°)	V_{conc} (m ³)	V_{exc} (m ³)
A	-10	YES	1.447E+06	3.611E+05
B	24	YES	1.173E+06	2.591E+05
C	8	YES	1.705E+06	5.039E+05

Table 5: Concrete and excavation volume for the fitting dams for the chosen locations.

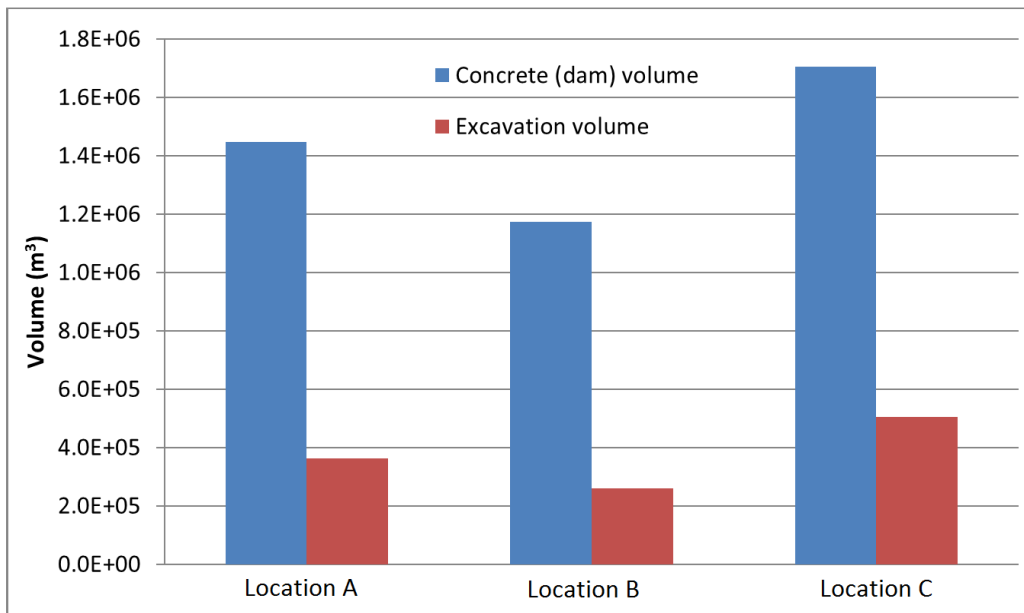


Figure 84: Concrete and excavation volume for the fitting dams for the chosen locations.

In the Engineer Manual [1] it is pointed out that it is important to design a dam as symmetrical as possible, because it helps to use the least concrete volume and to have stresses distributed as uniformly as possible. However, at this stage of the design the stress levels cannot be evaluated properly due to the stress singularities as shown in Section 6.4.

6.7. Final results

Location B is reshaped till the optimal dam in terms of stress levels is obtained. The same dam mesh size (10 m) is used as for the preliminary design stage.

The material properties for concrete are modified to use more reasonable values. As mentioned in Section 5.4 a normal range for concrete strength can be between 15 and 40 MPa and as a result the concrete class C 30/37 is used. The material properties for the rock remain the same. Their details are shown in Table 6.

The interface properties are computed based on Section 5.2.

$$K_n = 1000 \frac{E_{conc}}{l^{el}} = 1000 \frac{32}{10} = 3200 \text{ GPa}$$

$$K_t = \frac{K_n}{10} = 320 \text{ GPa}$$

	E (GPa)	f _c (MPa)	v	ρ (kg/m ³)
Rock	18.0	-	0.27	0
Concrete (C 30/37)	32.0	30	0.20	2400
	K _n (GPa)	K _t (GPa)		
Interface	3200	320		

Table 6: Final material properties.

The preliminary variables remain constant, while the final variables, which are described in Sections 5.1.1, 5.1.2 and 5.1.3, are modified till the best solution is found. The final variables are increased progressively adding each time a small amount of concrete. In this way, the optimal solution will satisfy the stress and geometric constraints at the same time.

More than sixty different combinations were tested to obtain the optimal final dam for Location B. Four characteristic iterations are visualized so the process can be described. Iteration 0 [Section 6.7.1] shows the results of the initial model, Iterations 1 and 2 [Sections 6.7.2, 6.7.3] display two intermediate models and Iteration 3 [Section 6.7.4] shows the final model which is concluded to be the optimal solution.

In Table 7 the essential information regarding the final variables, the respective volumes and the maximum tensile/compressive stresses are given. The areas with stress singularities which are located on the dam-rock interface are neglected.

In Sections 6.7.1, 6.7.2, 6.7.3 and 6.7.4 the respective results are shown. Regarding the figures for the principal stresses, the key point stresses are pointed out with the respective color from Figure 58. The red and green circles refer to the upstream and downstream tensile areas respectively. Note that, the

green areas were chosen to be wider in these figures below in order to show the areas that are redefined by the side parabolas.

In addition, the relative interface displacements DUN_z are visualized, so openings of the interface elements can be located. It is obvious that there are no openings between the dam cantilevers as a static analysis is performed and they can only open in a dynamic analysis. As expected, the openings are located on the dam-rock interfaces around the base, as this area contains the highest tensile stresses.

The figures regarding the interface tractions show the areas of the tensile and compressive stresses. In this way, the dam locations that require more concrete volume are detected and help the designer to choose more efficient variables, leading to the final dam shape faster.

Note that, the principal compressive stresses are of secondary importance as they usually satisfy the respective constraint, which is based on the concrete strength class divided by a safety factor.

Finally, for each iteration the biaxial failure envelope for the upstream and downstream face are plotted. Only the usual static load case is taken into account and the safety factors are found by using a constant concrete strength of 30 MPa. The safety factor must be larger than one so it can be accepted. Otherwise the dam must be strengthened by using a higher concrete class. The red color represents the areas where the stress constraints are satisfied while the blue color shows the critical areas that have to be reshaped further. However, this process is out of the context of this master project.

Location B				
	Iteration 0	Iteration 1	Iteration 2	Iteration 3
Side parabolas				
control_angle (-)	-	0.667	0.667	0.667
control_crest (-)	-	0.875	0.875	0.750
control_050H (-)	-	0.750	0.625	0.500
control_base (-)	-	0.625	0.500	0.500
Crown cantilever section				
cc_down_tol_crest (m)	-	0	3	4
cc_down_tol_045H (m)	-	3	5	6
cc_down_tol_base (m)	-	10	20	30
Line of main centers				
center_tol_z_crest (m)	-	0	0	-5
center_tol_z_025H (m)	-	0	-5	-15
center_tol_z_050H (m)	-	-5	-5	-25
center_tol_z_075H (m)	-	-5	-15	-35
center_tol_z_base (m)	-	-10	-25	-45
Volumes				
V_conc (m ³)	1.173E+06	1.365E+06	1.564E+06	1.806E+06
V_exc (m ³)	2.590E+05	3.430E+05	4.191E+05	5.892E+05
Tensile stresses (Allowable tensile stress: 1.000E+06)				
U/S max (N/m ²)	1.861E+06	1.541E+06	1.107E+06	9.227E+05
D/S max (N/m ²)	3.517E+06	2.447E+06	1.695E+06	8.778E+05
Compressive stresses (Allowable compressive stress: concrete strength class)				
U/S-D/S min (N/m ²)	-23.710E+06	-21.040E+06	-19.870E+06	-14.320E+06

Table 7: Final results for the characteristic iterations.

6.7.1. Iteration 0

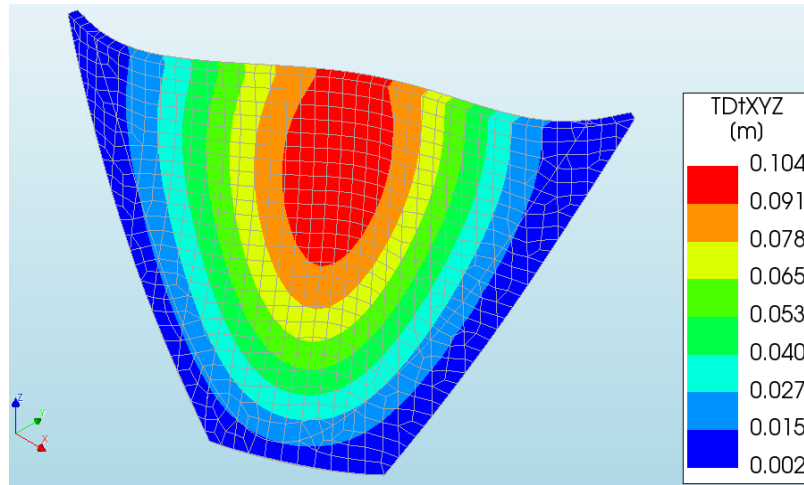


Figure 85: Iteration 0-Displacement field DtXYZ (3D view).

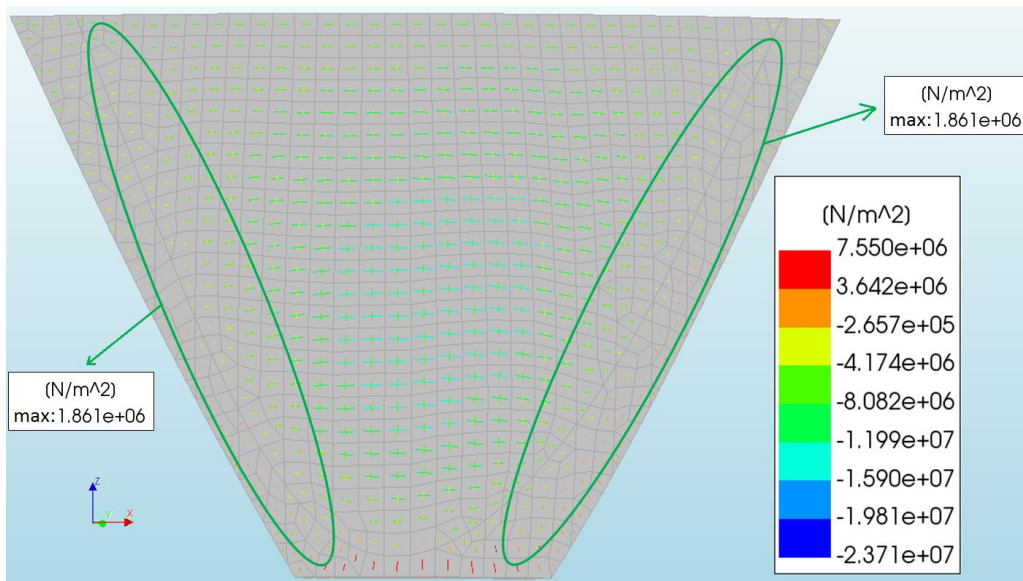


Figure 86: Iteration 0-In plane principal stresses (Upstream view).

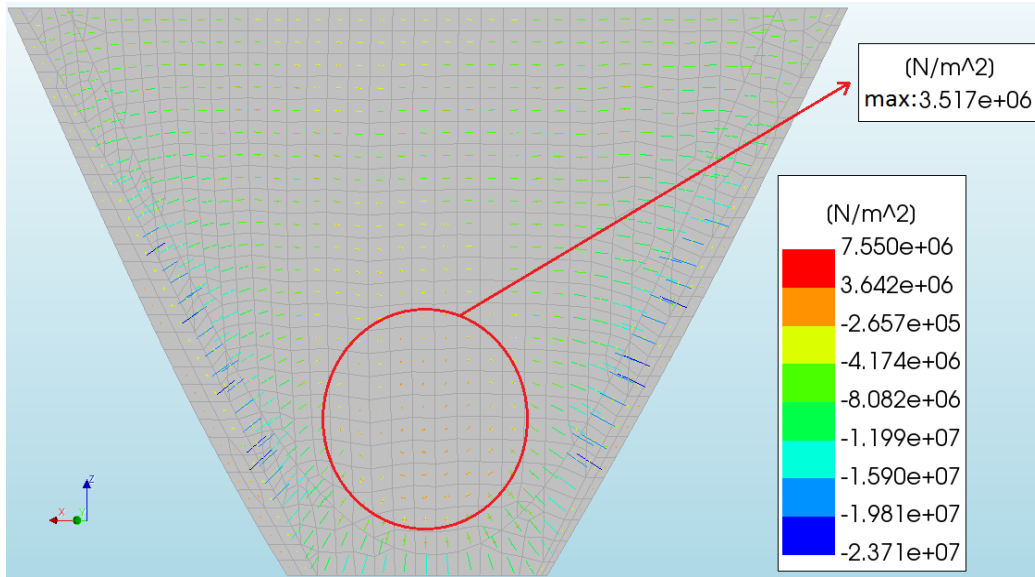


Figure 87: Iteration 0-In plane principal stresses (Downstream view).

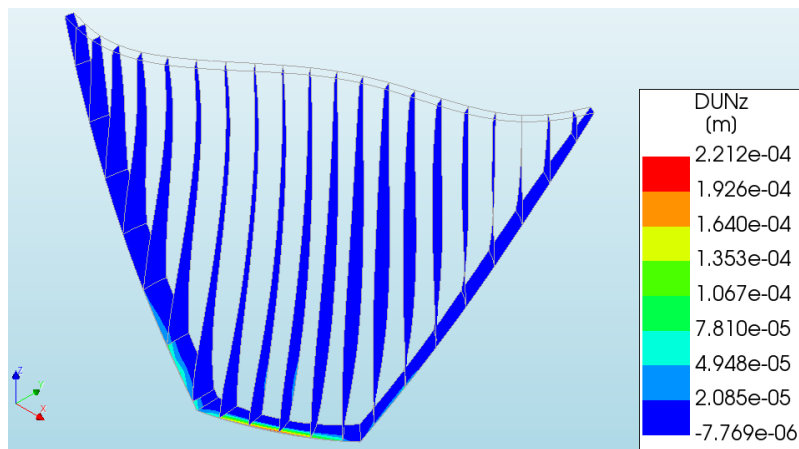


Figure 88: Iteration 0-Interface relative displacements DUN_z (3D view).

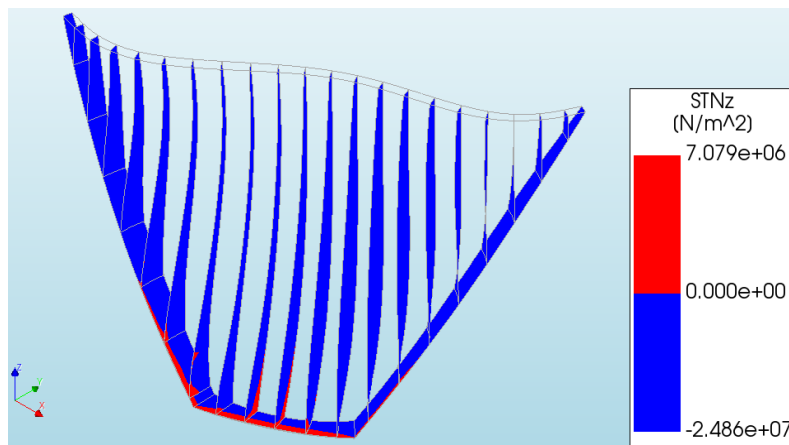


Figure 89: Iteration 0-Interface tractions STN_z (3D view).

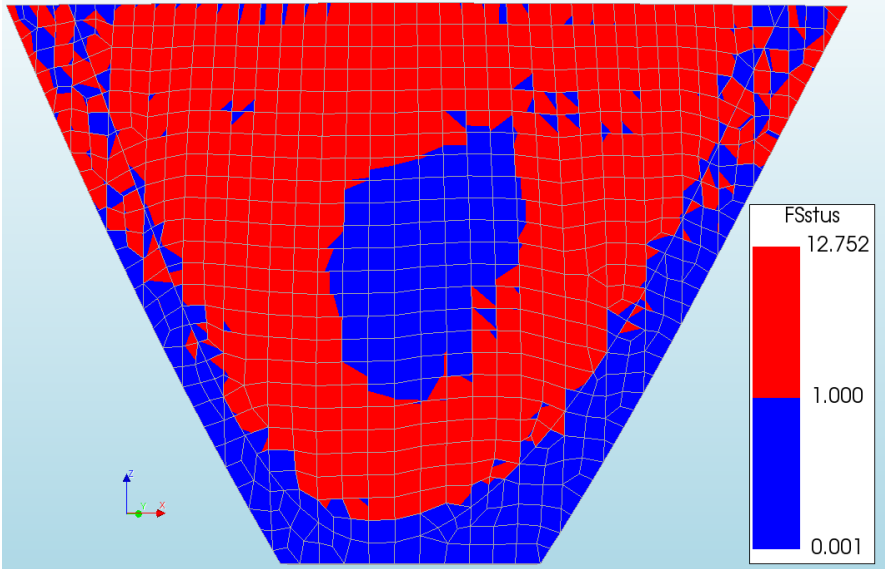


Figure 90: Iteration 0-Biaxial failure envelope-Static usual (FSstus) (Upstream view).

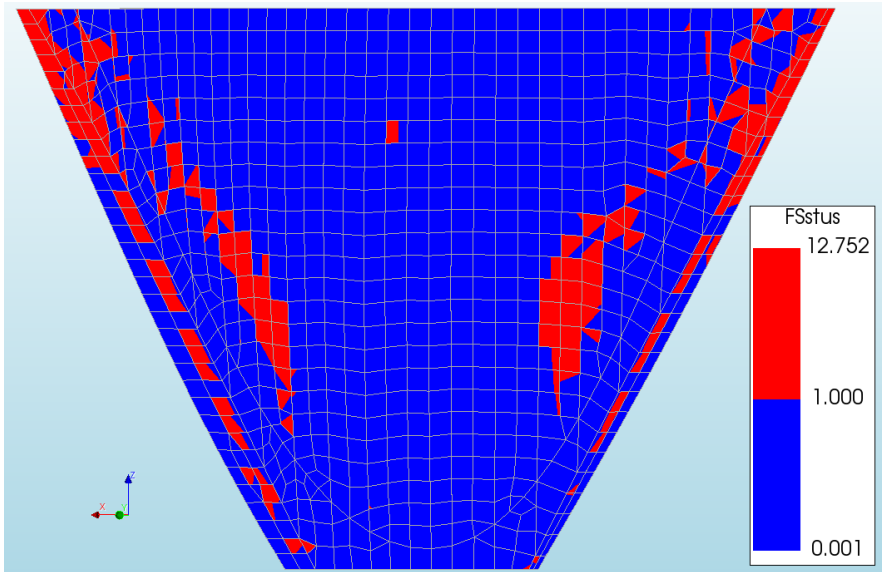


Figure 91: Iteration 0-Biaxial failure envelope-Static usual (FSstus) (Downstream view).

6.7.2. Iteration 1

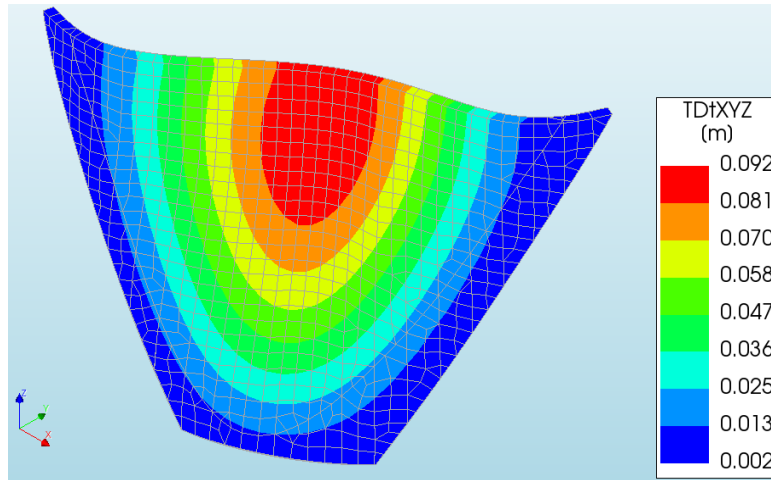


Figure 92: Iteration 1-Displacement field DtXYZ (3D view).

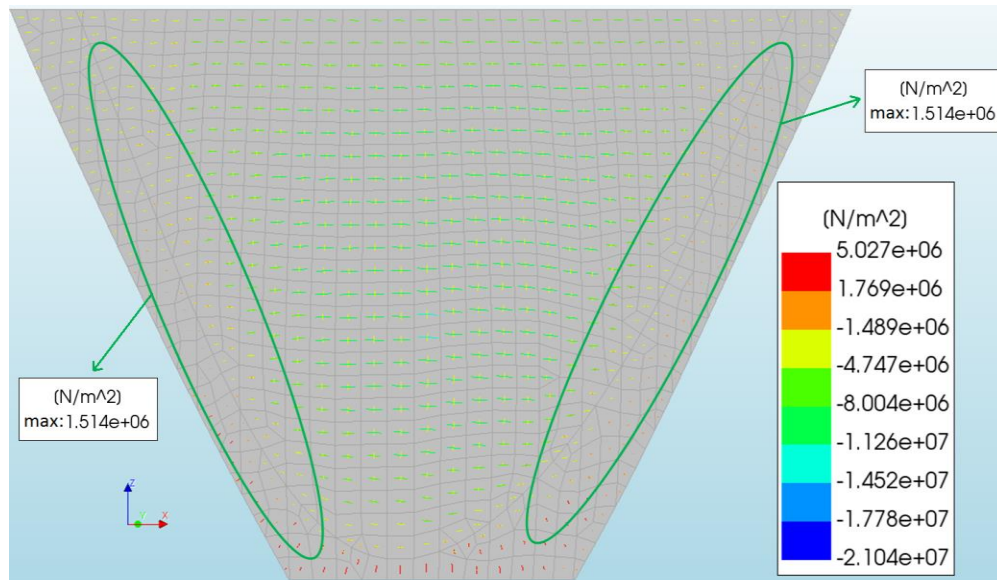


Figure 93: Iteration 1-In plane principal stresses (Upstream view).

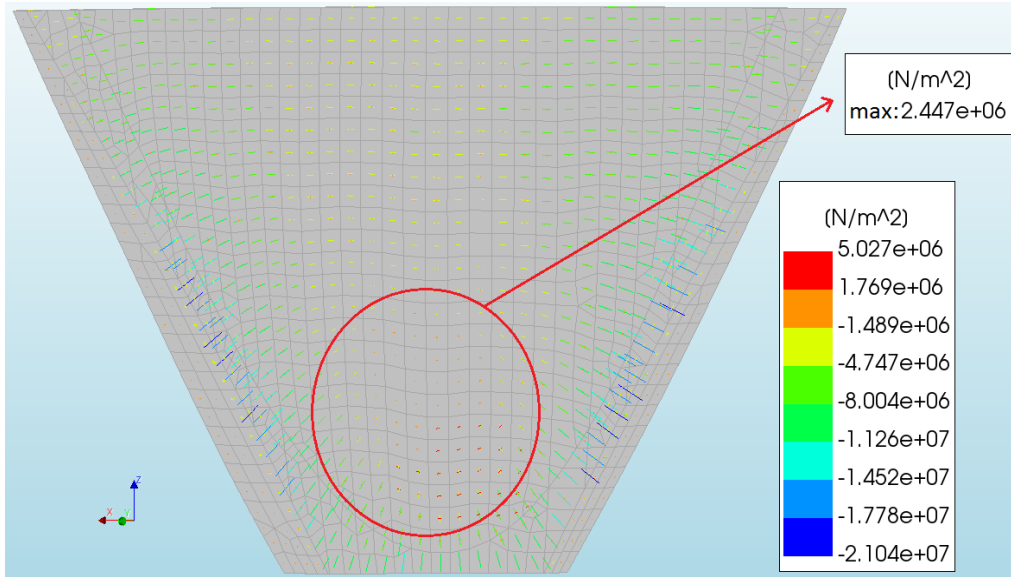


Figure 94: Iteration 1-In plane principal stresses (Downstream view).

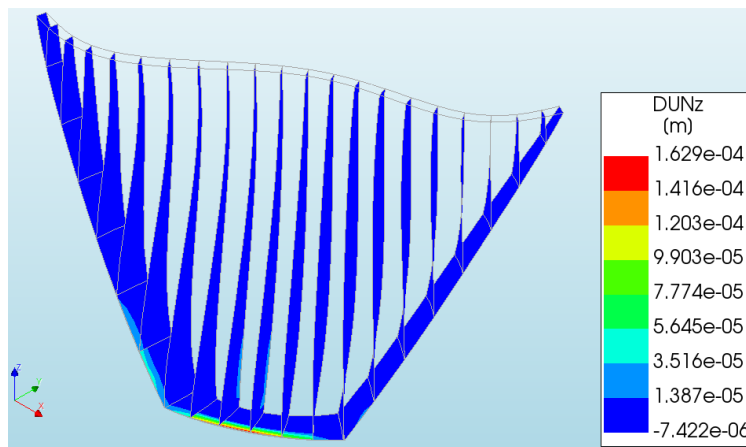


Figure 95: Iteration 1-Interface relative displacements DUNz (3D view).

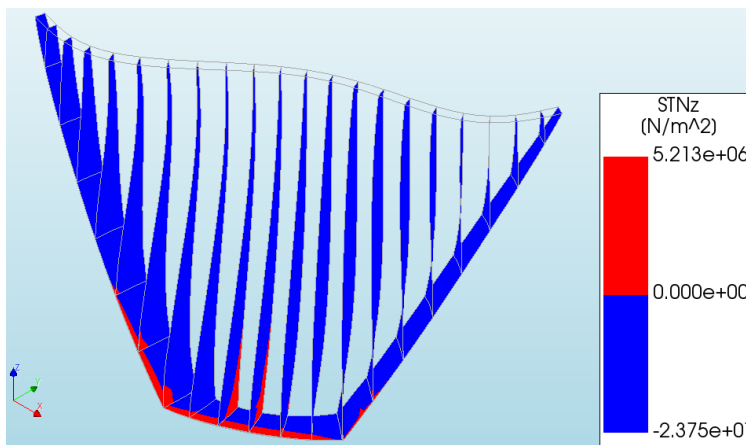


Figure 96: Iteration 1-Interface tractions STNz (3D view).

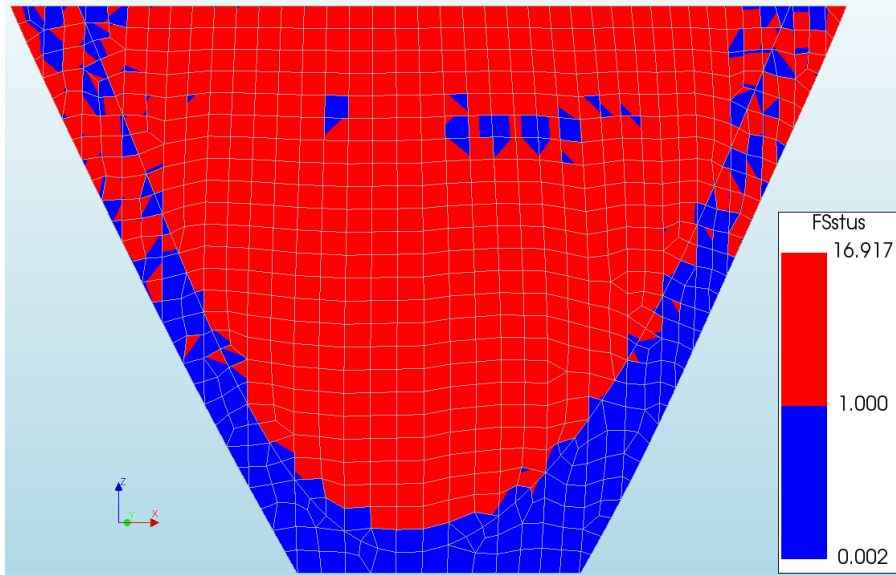


Figure 97: Iteration 1-Biaxial failure envelope-Static usual (FSstus) (Upstream view).

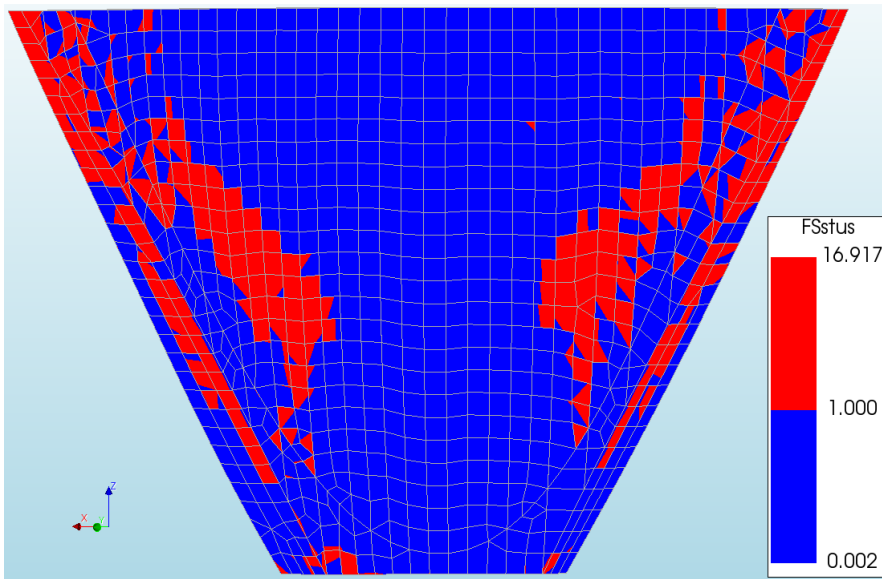


Figure 98: Iteration 1-Biaxial failure envelope-Static usual (FSstus) (Downstream view).

6.7.3. Iteration 2

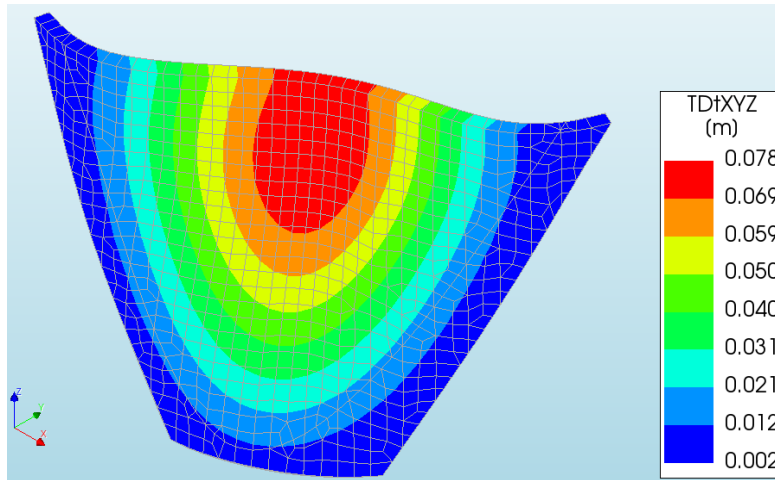


Figure 99: Iteration 2-Displacement field $DtXYZ$ (3D view).

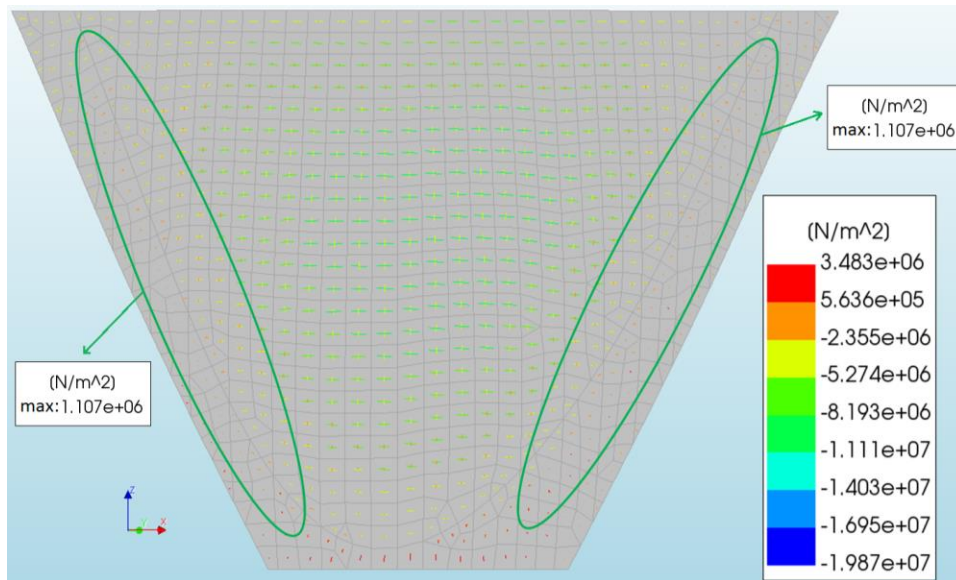


Figure 100: Iteration 2-In plane principal stresses (Upstream view).

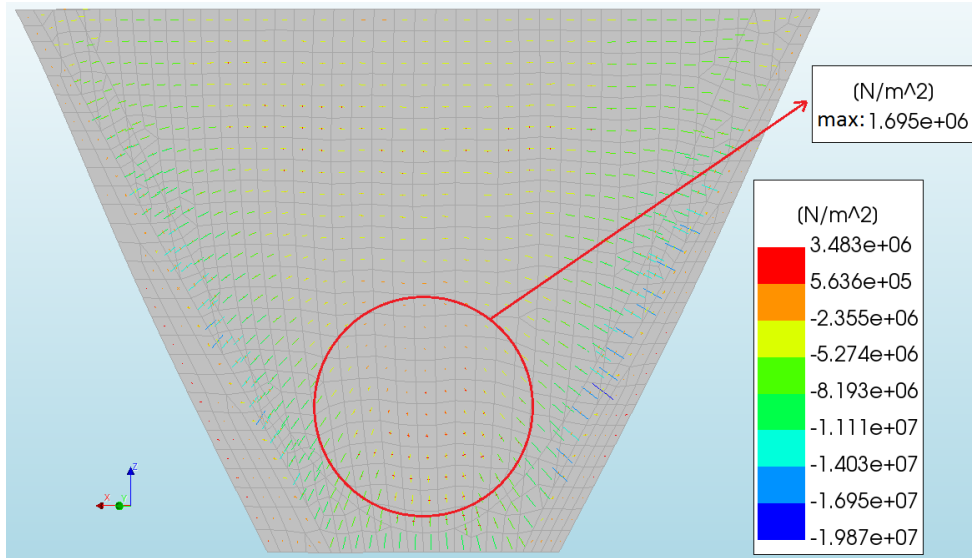


Figure 101: Iteration 2-In plane principal stresses (Downstream view).

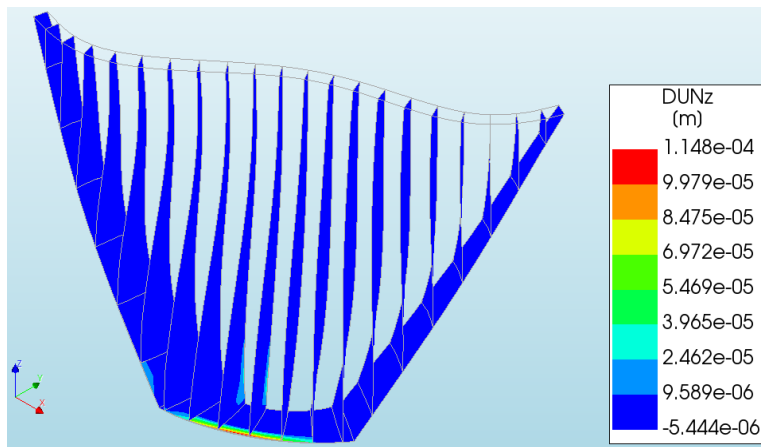


Figure 102: Iteration 2-Interface relative displacements DUN_z (3D view).

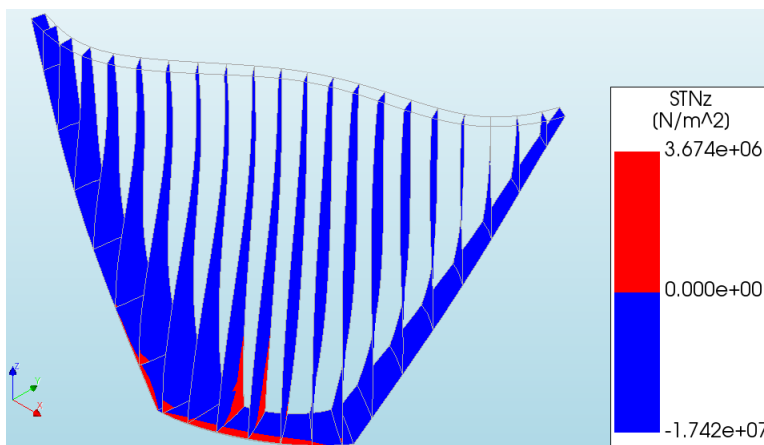


Figure 103: Iteration 2-Interface tractions STN_z (3D view).

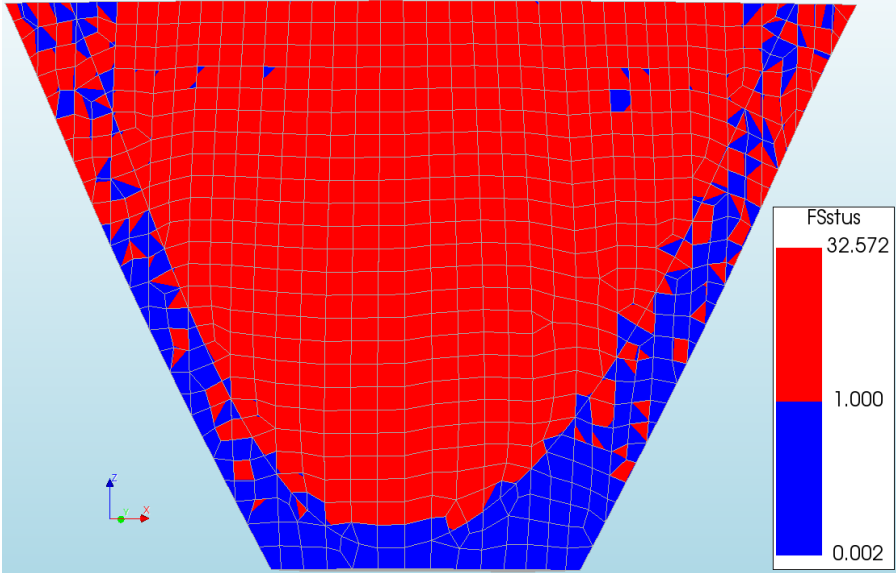


Figure 104: Iteration 2-Biaxial failure envelope-Static usual (FSstus) (Upstream view).

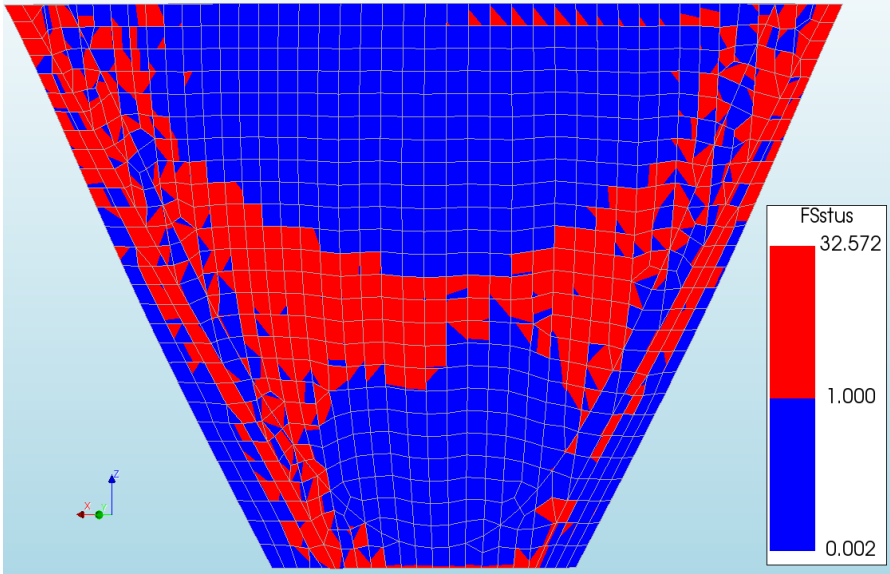


Figure 105: Iteration 2-Biaxial failure envelope-Static usual (FSstus) (Downstream view).

6.7.4. Iteration 3

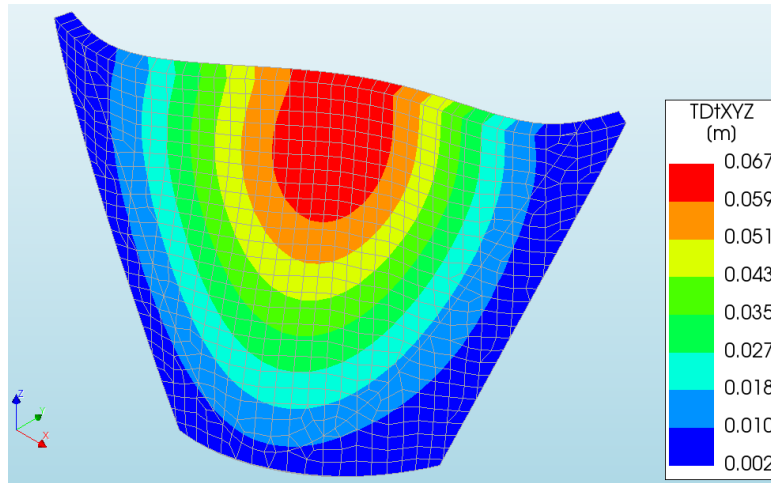


Figure 106: Iteration 3-Displacement field DtXYZ (3D view).

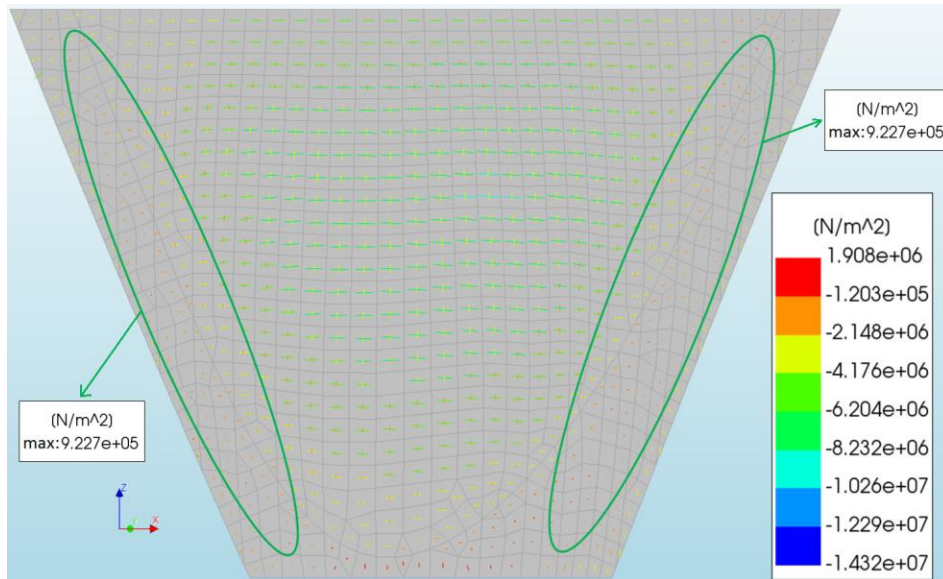


Figure 107: Iteration 3-In plane principal stresses (Upstream view).

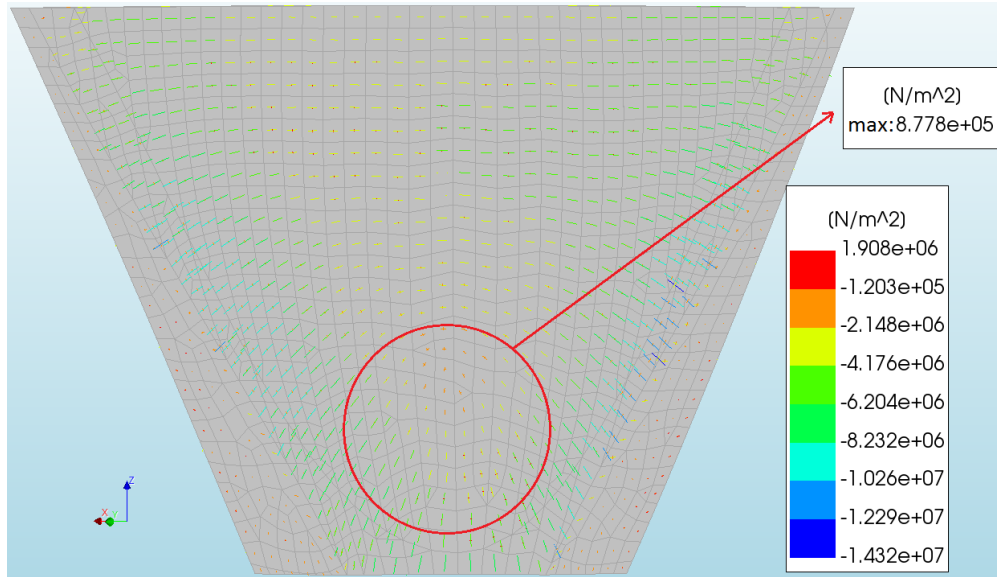


Figure 108: Iteration 2-In plane principal stresses (Downstream view).

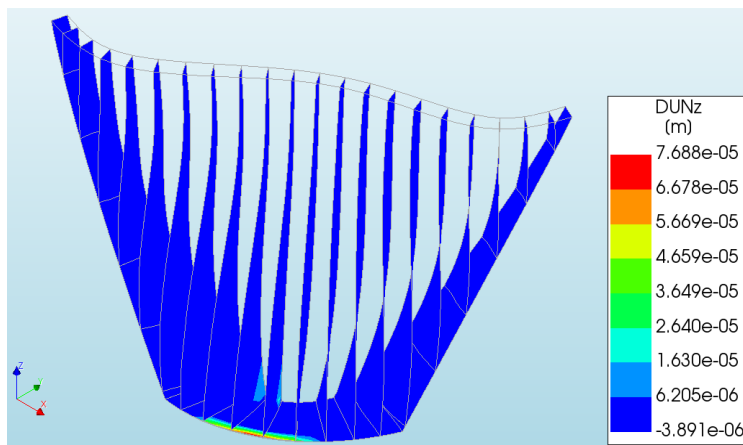


Figure 109: Iteration 3-Interface relative displacements DUN_z (3D view).

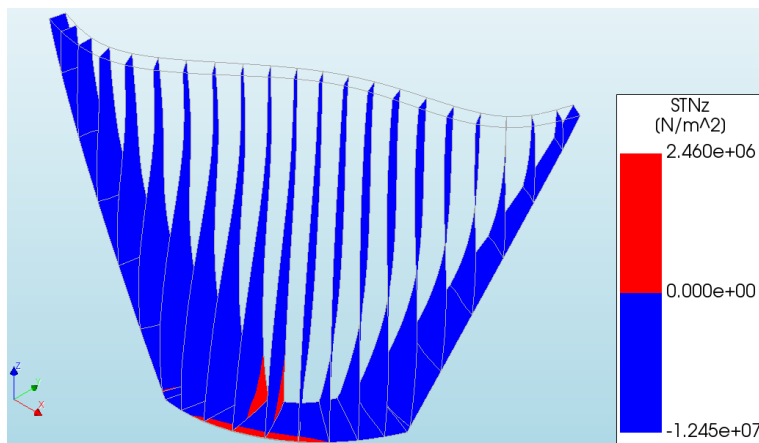


Figure 110: Iteration 3-Interface tractions STN_z (3D view).

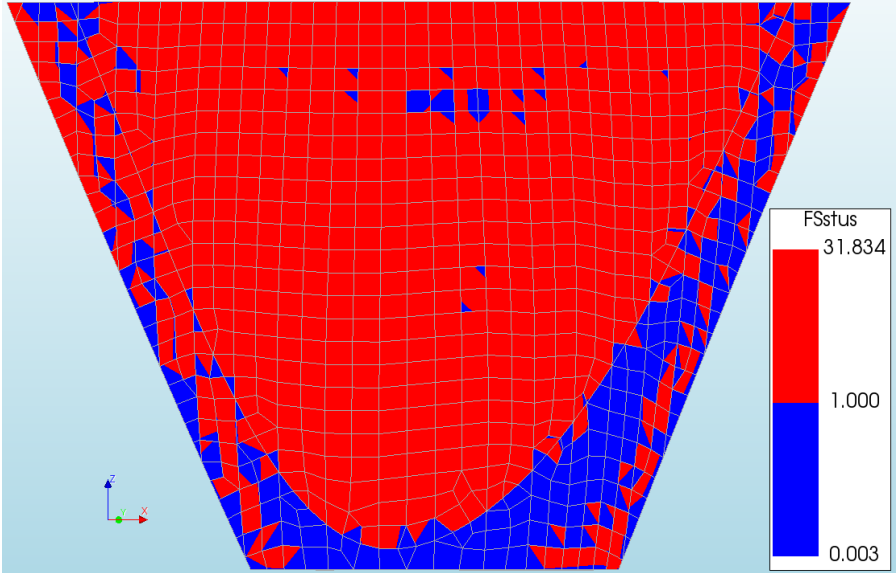


Figure 111: Iteration 3- Biaxial failure envelope-Static usual (FSstus) (Upstream view).

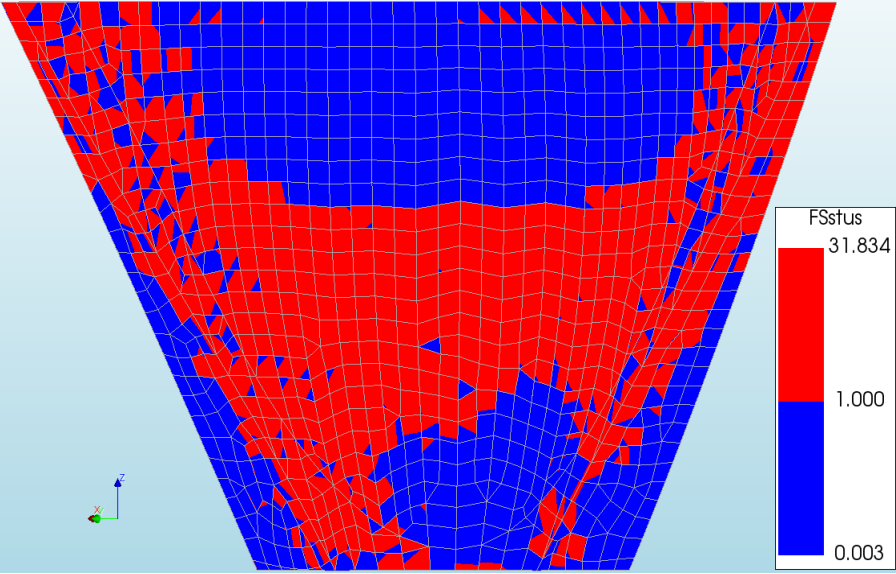


Figure 112: Iteration 3- Biaxial failure envelope-Static usual (FSstus) (Downstream view).

7. Discussion of research questions

As the script is developed and the entire process is validated, the secondary research questions from Section 1.2 can be discussed in detail.

7.1. Comparison of the theoretical with the numerical volume

Using the best alternative, Location B, the theoretical concrete (dam) volume is computed, based on equation 4.1, and compared to the respective numerical concrete (dam) volume from the preliminary design stage. The final design stage is not used as no relative information is contained in the Engineer Manual [1].

Furthermore, the excavation volume is not taken into account as the USBR method does not include it.

Location B			
axis angle (°)	equal angles β (°)	V_{theor} (m ³)	V_{num} (m ³)
40	NO	2.872E+06	1.275E+06
38	NO	2.761E+06	1.192E+06
36	NO	2.740E+06	1.163E+06
34	NO	2.773E+06	1.155E+06
32	NO	2.815E+06	1.152E+06
30	NO	2.862E+06	1.152E+06
28	NO	2.914E+06	1.155E+06
26	NO	2.985E+06	1.165E+06
24	YES	3.057E+06	1.173E+06
22	YES	3.124E+06	1.181E+06
20	YES	3.162E+06	1.192E+06
18	YES	3.205E+06	1.207E+06
16	YES	3.257E+06	1.224E+06
14	YES	3.307E+06	1.244E+06
12	NO	3.320E+06	1.264E+06
10	NO	3.291E+06	1.283E+06
8	NO	3.297E+06	1.310E+06
6	NO	3.316E+06	1.340E+06
4	NO	3.315E+06	1.368E+06
2	NO	3.339E+06	1.391E+06
0	NO	3.406E+06	1.421E+06
-2	NO	3.471E+06	1.453E+06
-4	NO	3.523E+06	1.469E+06
-6	NO	3.504E+06	1.465E+06
-8	NO	3.550E+06	1.468E+06
-10	NO	3.532E+06	1.455E+06
-12	NO	3.503E+06	1.440E+06
-14	NO	3.482E+06	1.429E+06

	$\beta_{LHS} > 30^\circ$ and $\beta_{RHS} > 30^\circ$	$\beta_{RHS} = \beta_{RHS}$
NO	FALSE	FALSE
NO	TRUE	FALSE
YES	TRUE	TRUE

Table 8: Location B, theoretical vs numerical concrete volume.

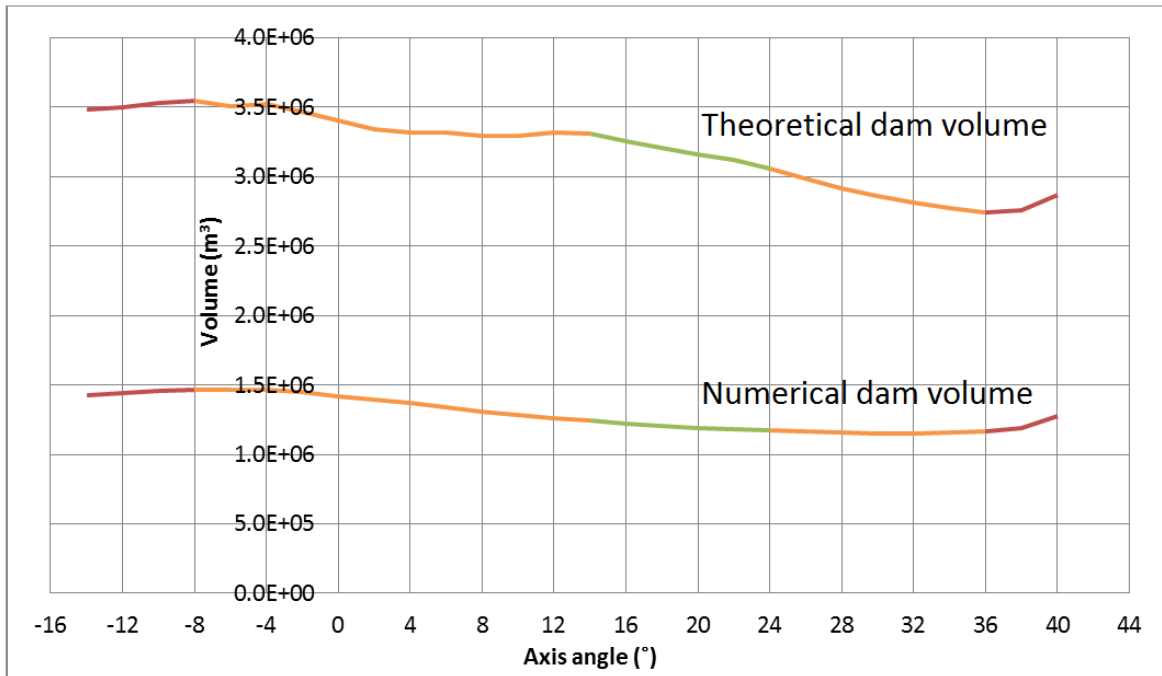


Figure 113: Location B, theoretical vs numerical concrete volume.

It is obvious that, the deviations between the two volumes are quite large. The theoretical volume is around three times larger than the numerical volume for all the different axis angles [Table 8, Figure 113]. The question that arrives is how these large differences can be justified. For this reason, the basic assumptions from Section 1.4 are used, as the proposed method is not identical to the USBR method [1].

First, the assumption of the uniform excavation length is very conservative for the theoretical volume as the same amount of rock is excavated at every elevation. This is not very realistic for the USBR method and in this way more volume is added from the variables L_1 and L_2 in equation 4.1.

One more important factor is that, the USBR method does not take into account a base length but only one point, which is the lowest crown cantilever point. On the other hand, the proposed method computes the optimal base length based on the neighboring valley so the least concrete is added. Consequently, the amount of the base length of the theoretical volume cannot be controlled by changing the base length.

The two volumes are obtained by different dam geometries, the theoretical and the numerical volumes use circular and parabolic equations respectively. Consequently, if the same variables are used for both of the volumes two different dams are going to be generated.

The empirical formula, equation 4.1, is just an initial judgement that helps the designer to choose a proper location so he/she can start the layout of the dam. Furthermore, the modifications during the dam layout are not taken into account, like reshaping the arches due to potential gaps. As a result, it is not that accurate as the numerical volume which gives the concrete volume for the best fitting dam in terms of geometric constraints based on the given variables.

7.2. The influence of the excavation length

For the best alternative, Location B, the influence of the excavation length on the generation of the dam is investigated, focusing on the preliminary parameters.

The excavation length is a first guess to simulate a reasonable amount of overburden so a dam is generated. The designer must choose this value based on borings or sound judgment [1]. In the upper sections this variable is assumed to be fixed and equal to 30 m.

In this section the relation of the excavation length with the concrete and excavation volume is investigated so it can be concluded if there is an optimal length that can be used. Consequently, the best alternative from the preliminary design stage is used, Location B, and the value of the excavation length is changed from 20 m to 120 m [Table 9]. Regarding the minimum excavation length, its value remains constant and equals to 10 m.

Looking at the empirical equations 4.5 and 4.6, the excavation length is fully correlated to the crest and base thickness. For this reason, their relation is expected to be linear and this is verified in Figure 115. In addition, the change of the base thickness is larger compared to the crest thickness and this is completely in agreement due to the formation of the empirical formulas.

Regarding the concrete and excavation volume, again a linear relation is expected as more volume due to the increase of the excavation length is added. In other words, the borders of the dam are extended when the excavation length is larger and vice versa, while at the same time the shape of the foundation area remains the same as the other variables are constant [Figure 114].

Furthermore, in Figure 114 the slope of the lines of the dam and excavation volume are very similar. This is because; the minimum excavation length is constant and only the value of the excavation length changes. Consequently, the main factor that adds volume on the dam and thickens the foundation area is only the excavation length.

Location B				
excavation length (m)	crest thickness (m)	base thickness (m)	V_{conc} (m ³)	V_{exc} (m ³)
20	6.75	21.94	1.106E+06	2.473E+05
25	6.87	22.68	1.137E+06	2.504E+05
30	6.98	23.40	1.173E+06	2.591E+05
35	7.10	24.11	1.209E+06	2.677E+05
40	7.21	24.80	1.248E+06	2.805E+05
45	7.33	25.47	1.290E+06	2.959E+05
50	7.45	26.12	1.332E+06	3.112E+05
55	7.56	26.75	1.372E+06	3.264E+05
60	7.68	27.38	1.413E+06	3.413E+05
65	7.79	27.99	1.454E+06	3.564E+05
70	7.91	28.60	1.501E+06	3.774E+05
75	8.02	29.19	1.549E+06	3.999E+05
80	8.14	29.78	1.598E+06	4.230E+05
85	8.25	30.37	1.650E+06	4.489E+05
90	8.37	30.95	1.702E+06	4.749E+05
95	8.49	31.53	1.755E+06	5.018E+05
100	8.60	32.10	1.809E+06	5.294E+05
105	8.72	32.67	1.864E+06	5.584E+05
110	8.84	33.22	1.920E+06	5.875E+05
115	8.96	33.78	1.978E+06	6.191E+05
120	9.08	34.34	2.038E+06	6.514E+05
125	9.20	34.89	2.099E+06	6.842E+05
130	9.32	35.43	2.160E+06	7.174E+05
135	9.44	35.98	2.223E+06	7.525E+05
140	9.57	36.51	2.289E+06	7.908E+05

Table 9: Location B, the influence of the excavation length.

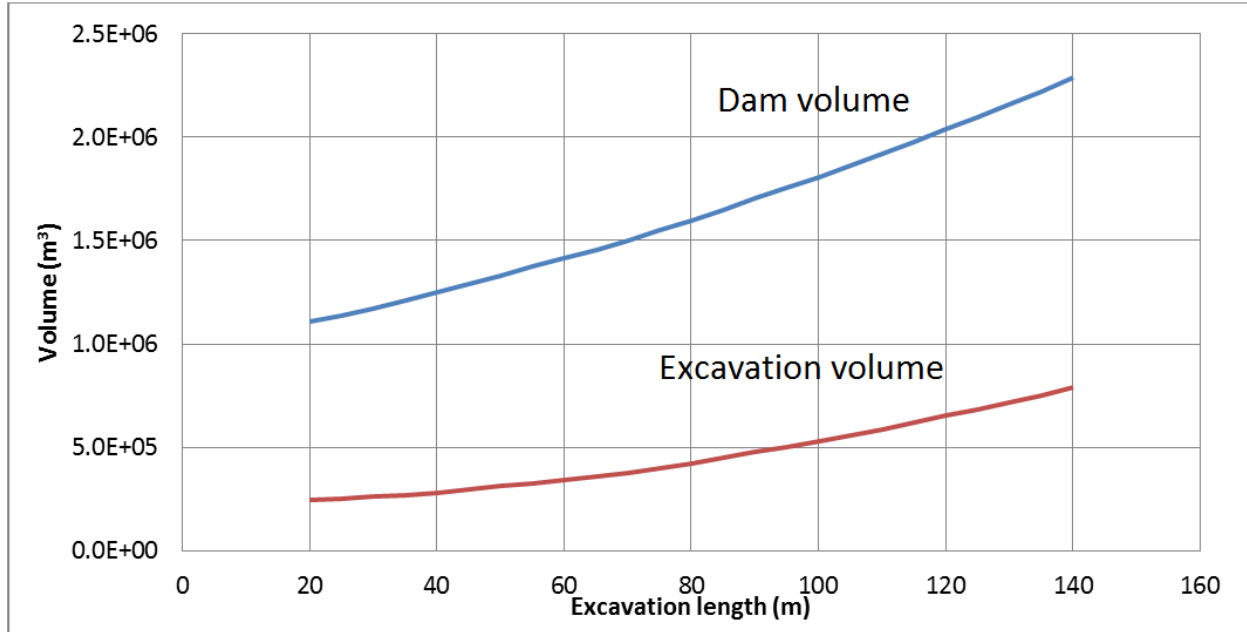


Figure 114: Location B, excavation length vs concrete and excavation volume.

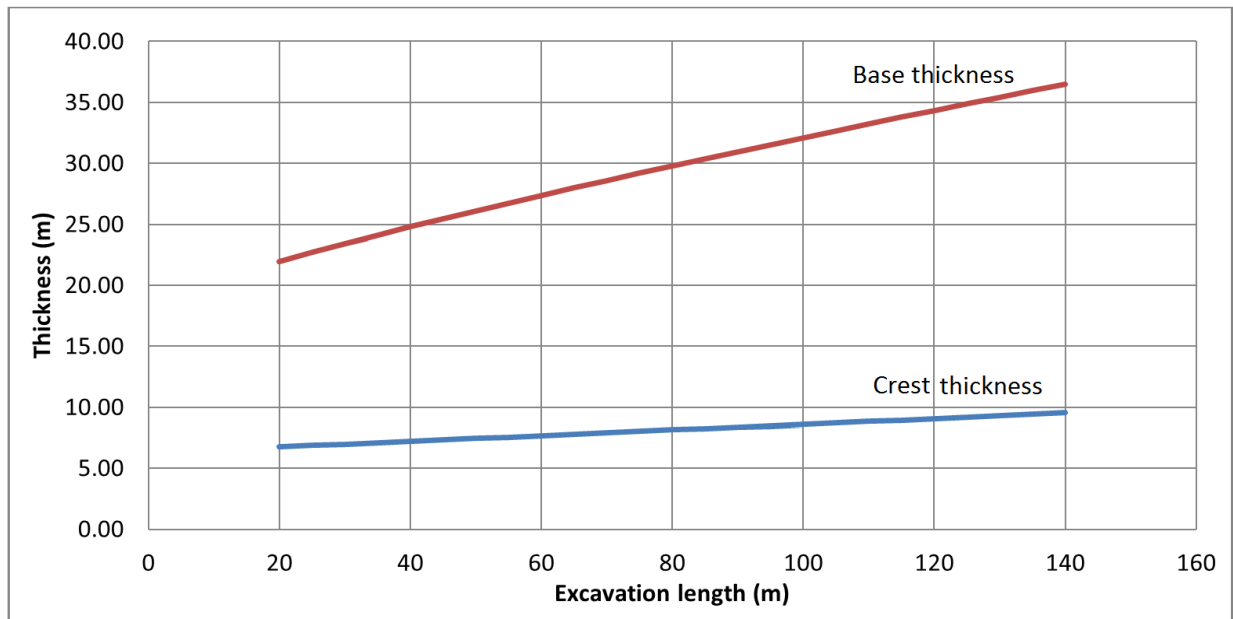


Figure 115: Location B, excavation length vs crest and base thickness.

7.3. The influence of the shape of the foundation area

In this section it is investigated how the shape of the foundation area influences the principal stresses.

As described before the final foundation area consists of the main upstream and side downstream endpoints, which should satisfy the criteria from Section 4.9. Its shape is very complex and it is dependent on many different factors. For this reason it cannot be treated as one-dimensional problem.

The main factors that influence the shape of the foundation area are the following.

- The basic variables, which determine the boundaries of the foundation area [Section 4.4].
- The variables of the side parabolas, which change the location of the downstream endpoints by adding more concrete in the abutment [Section 5.1.1].
- The variables of the redefined crown cantilever section, which affect both the upstream and downstream endpoints by thickening the dam along the height [Section 5.1.2].
- The variables of the redefined line of main centers, which influence the entire geometry of the foundation area as well. It is mentioned that sharper parabolas add volume and vice versa [Section 5.1.3].

It can be concluded that the shape of the foundation area can effectively influence the dam volume in accordance with the principal stresses but the proper combination of more than fifteen different variables should be found. This is not an easy process at all, especially when it is performed using a “manual” optimization [Section 5.4]. Changing only one variable or some of them the foundation area is indeed changed but the respective principal stresses may not be changed accordingly.

Hence, the following process is recommended based on the influence level of the variables and the proposed design stages. First the basic variables should be defined to obtain the best alternative from the preliminary design stage.

Afterwards, the tensile stresses from the downstream stress key points should be eliminated [Figure 58, red circle] as this area contains the most critical tensile stresses. For this reason the crown cantilever section and the line of main centers should be simultaneously redefined till the allowable stress level is reached (1 MPa).

Finally, the tensile stresses from the upstream stress key points should be eliminated [Figure 58, green circles] by adding the side parabolas until the allowable stress level is reached (1 MPa). In this way, the shape of the foundation area is changed progressively till all the constraints are satisfied. Note that, many combinations should be checked to obtain the most efficient dam and consequently the best shape for the foundation area.

8. Conclusions

The main goal of this master project was achieved by creating a process based on Python scripting and Finite Element Software DIANA. Through this process the model of a double-curvature arch dam is automatically generated, taking into account the essential geometric and stress constraints.

Through the developed process any location around the world can be used to design a double-curvature arch dam as long as the canyon profile and the foundation characteristics are appropriate. The topographic data must be given in a text file which contains the essential coordinates.

Using the developed script the modelling effort is drastically reduced, because only topographic data and a small number of basic parameters, like dam height, base elevation etc., are required.

A large variety of double-curvature arch dams can be generated by only changing the values of the basic parameters in the developed script. The designer should choose these values appropriately, or else an unrealistic dam can be generated.

Even with a fine mesh, some thousands of elements, the preliminary (linear static) and the final (nonlinear static) analysis require around five and ten minutes respectively. In this way, more dam models can be analyzed and evaluated in less time.

Using interface elements the designer can easily detect the critical dam areas. This does not only result in a faster optimization process but to a more economical dam as concrete is added locally.

The developed process and the empirical method, described in the Engineer Manual [1], follow the same guidelines, but they are not identical. The main difference is that different equations are used to describe the dam geometry.

9. Recommendations

Parabolic equations were used to describe the main parts of the dam geometry assuming that this is the most widely accepted solution. Further research should be done by using even higher order equations aiming to minimize the concrete volume by applying different dam geometries.

Bezier Surfaces were used in Diana Interactive Environment (DianaIE) to generate the dam model. As described before, it is a powerful but very sensitive tool. If the grid of the used points is irregular then an abnormal surface is generated and this is not allowed. For this reason, the relation between Bezier Surfaces and the used points should be investigated in depth, aiming to eliminate possible distance errors.

The load combination that was used for this master project should be improved, as only the self-weight and the hydrostatic pressure on the dam are taken into account. The script should be modified taking into account the temperature load on the dam and the hydrostatic pressure on the upstream rock at the same time. In this way a more realistic dam design can be obtained.

Non-linear static analyses were performed to demonstrate how the script code works. However, this is not efficient in practice. The script should be modified to take into account phased analyses in combination with non-linear dynamic analyses. In this way, the essential construction stages can be taken into account and seismic excitation is applied for the final analyses, which is the most critical load.

In the final design stage a “manual” optimization technique was suggested where the final variables are modified progressively till the geometric and stress constraints are satisfied. In this way, a valid dam model is obtained but it is not certain if this model is the optimal one at the same time. For this reason, it is recommended the use of automated optimization techniques, like Probabilistic Analysis or neural networks, to find the optimal solution.

The script can be used for topographies where real dams are constructed. In this way, the generated dams can be directly compared to real dams and the efficiency of the method can be validated. Afterwards, the script should be modified by changing the used assumptions to approximate an even more realistic dam design.

To minimize the volume of the final dam more variables can be used for the side parabolas, the redefined crown cantilever section and the redefined line of main centers. In this way, the locations that have to be reshaped can be changed more efficiently adding volume only on the affected areas. Note that, increasing the number of the final variables the computational cost of the design process will increase accordingly.

References

- [1] U.S. Army Corps of Engineers. 1994. Engineer Manual 1110-2-2201, Arch Dam Design. USA, Washington.
- [2] Gunn, Russel. 2006. Report-Dam Modelling, Design and Analysis-Diana Software Development for STUCKY LTD. Switzerland, Renens.
- [3] Gunn, Russel. 2008. Concrete Dam Design and Analysis Methods, Chapter C2.1.6, EPFL-ENAC-LCH, GC A3. Switzerland. Lausanne.
- [4] Salamon, Jerzy. 2012. Technical Memorandum No. EM36-86-68110 (In Progress), Draft Double Curvature Arch Dams-Planning, Appraisal, and Feasibility Level. Colorado. Denver.
- [5] Duivendijk, J van. 2007. Water Power Engineering, Principles and Characteristics, Course Book CIE-5304. Netherlands. Delft
- [6] Goulas, Evangelos. 2015. Shape Optimization of Double-Curvature Arch Dams Using Python Scripting and DIANA Finite Element Software. Netherlands. Delft.
- [7] Diana User's Manual. 2015. *Diana User's Manual*. [ONLINE] Available at: <https://support.tnodiana.com/manuals/d96/Diana.html>. [Accessed 24 December 2015].
- [8] Siemens Product Lifecycle Management Software Inc. 2014. Parasolid On-Line Documentation Web, Parasolid V27.1.141.
- [9] Wikipedia, the free encyclopedia. 2016. *Wikipedia, the free encyclopedia*. [ONLINE] Available at: https://en.wikipedia.org/wiki/Main_Page. [Accessed 07 March 2016].
- [10] SketchUp | 3D for Everyone. 2016. *SketchUp | 3D for Everyone*. [ONLINE] Available at: <http://www.sketchup.com/>. [Accessed 08 February 2016].
- [11] Dxf2xyz Free DXF to XYZ file convertor - guthrie CAD::GIS. 2016. *Dxf2xyz Free DXF to XYZ file convertor - guthrie CAD::GIS*. [ONLINE] Available at: <http://www.guthcad.com.au/freestuff.htm>. [Accessed 08 February 2016].

List of symbols

y_{start}	Left Hand Side y-coordinate of upstream crest elevation parabola [m]
H	Height of arch dam [m]
z_{base}	Base elevation of arch dam [m]
θ_{axis}	Orientation of dam axis [°]
$L_{excavation}$	Initial uniform excavation length [m]
$L_{excavation}^{\min}$	Initial minimum excavation length [m]
L_1	Straight line distance between abutments at crest elevation [m]
L_2	Straight line distance between abutments at $0.15H$ above base elevation [m]
V_{theor}	Theoretical concrete volume [m]
β	Angle of incidence [m]
R_{AXIS}	Radius of upstream crest elevation parabola [m]
T_C	Thickness at crest elevation [m]
T_B	Thickness at base elevation [m]
$T_{0.45H}$	Thickness at $0.45H$ above base elevation [m]
USP_{CREST}	Upstream projection point at crest elevation [m]
$USP_{0.45H}$	Upstream projection point at $0.45H$ above base elevation [m]
USP_{BASE}	Upstream projection point at base elevation [m]
DSP_{CREST}	Downstream projection point at crest elevation [m]

$DSP_{0.45H}$	Downstream projection point at $0.45H$ above base elevation [m]
DSP_{BASE}	Downstream projection point at base elevation [m]
y_{up}^{CC}	Equation for upstream line of crown cantilever section [m]
y_{down}^{CC}	Equation for downstream line of crown cantilever section [m]
θ_{LHS}^{crest}	Left Hand Side angle between the end point and the reference plane at crest elevation [°]
θ_{LHS}^{base}	Left Hand Side angle between the end point and the reference plane at base elevation [°]
θ_{LHS}^{diff}	Angle difference between θ_{LHS}^{crest} and θ_{LHS}^{base} [°]
θ_{LHS}^{inc}	Left Hand Side increment [°]
θ_{RHS}^{crest}	Right Hand Side angle between end point and the reference plane at crest elevation [°]
θ_{RHS}^{base}	Right Hand Side angle between end point and reference plane at base elevation [°]
θ_{RHS}^{diff}	Angle difference between θ_{RHS}^{crest} and θ_{RHS}^{base} [°]
θ_{RHS}^{inc}	Right Hand Side increment [°]
k	Number of the used parabolas
x_c^i	X coordinate of the crown cantilever section at elevation i [m]
L_s^i	Developed length of Left Hand Side end point at elevation i [m]
θ_s^i	Left Hand Side angle between the end point and reference plane [°]
L_{LHS}^i	Developed length of Left Hand Side original topographic point at elevation i [m]

θ_{LHS}^i	Left Hand Side angle between the original topographic point and reference plane [°]
L_E^i	Developed length of Left Hand Side end point at elevation i [m]
θ_E^i	Right Hand Side angle between the end point and the reference plane [°]
L_{RHS}^i	Developed length of Right Hand Side original topographic point at elevation i [m]
θ_{RHS}^i	Right Hand Side angle between the original topographic point and the reference plane [°]
Z_i	Elevation i [m]
L_{segm}	Curved length between two joint centers [m]
E	Young's modulus [N/m ²]
ν	Poisson's ratio
G	Shear modulus [N/m ²]
ρ	Mass density [kg/m ³]
V_s	Wave travelling speed to travel across an element [m/s]
f_{max}	Maximum frequency of the seismic signal [Hz]
λ_{min}	Shortest wave length [m]
<i>control_angle</i>	Proportion which defines the location of the transition points along the dam height
<i>control_crest</i>	Proportion which defines the location of the side center at crest elevation

$control_050H$	Proportion which defined the location of the side center at $0.50H$ above base elevation
$control_base$	Proportion which defined the location of the side center at base elevation
$cc_down_tol_crest$	Tolerance that is added in the y-coordinate of the downstream projection point at crest elevation [m]
$cc_down_tol_045H$	Tolerance that is added in the y-coordinate of the downstream projection point at $0.45H$ above base elevation [m]
$cc_down_tol_base$	Tolerance that is added in the y-coordinate of the downstream projection point at base elevation [m]
$center_tol_z_crest$	Tolerance that is added in the y-coordinate of the initial main center point at crest elevation [m]
$center_tol_z_075H$	Tolerance that is added in the y-coordinate of the initial main center point at $0.75H$ above base elevation [m]
$center_tol_z_050H$	Tolerance that is added in the y-coordinate of the initial main center point at $0.50H$ above base elevation [m]
$center_tol_z_025H$	Tolerance that is added in the y-coordinate of the initial main center point at $0.25H$ above base elevation [m]
$center_tol_z_base$	Tolerance that is added in the y-coordinate of the initial main center point at base elevation [m]
K_n	Normal stiffness modulus-z* [N/m ³]
K_t	Tangential stiffness modulus-y* [N/m ³]
l^{el}	Characteristic length of the smallest element [m]
X_{rate}	Transformation factor from static to dynamic strength
X_{spec}	Transformation factor from apparent to actual stiffness

α	Ratio between the maximum principal stress σ_1 and the minimum principal stress σ_2
R	Distance from the origin to the failure envelope
f_{sc}	Compressive strength safety factor
f_{st}	Tensile strength safety factor
f_{si}	Intermediate safety factor

List of figures

Figure 1: Single- and double-curvature arch dam [1].	10
Figure 2: The equation of the parabola, the focus point and the symmetry point (plan view).	12
Figure 3: Crown cantilever section (side view) [2].	14
Figure 4: Upstream and downstream symmetry lines and the line of centers (side view) [2].	15
Figure 5: Upstream and the downstream main parabolas at elevation i (plan view) [2].	16
Figure 6: Left and right bank side parabolas at elevation i (plan view) [2].	17
Figure 7: Left figure, line of side centers. Right figure, line of tangent points [Side view] [2].	17
Figure 8: Foundation area (plan view) [2].	18
Figure 9: The general workflow.	20
Figure 10: The workflow of the dam design.	21
Figure 11: Recommended size of the topographical map (plan view).	23
Figure 12: SketchUp 2015 – Deriner Dam – From 2D to 3D.	24
Figure 13: The dwg file obtained from SketchUp and the respective topographic points (3D view).	25
Figure 14: Excavation polylines (plan view, river profile in blue based on non-flood or conditions).	26
Figure 15: Definition of the values L_1 and L_2 (plan view) [1].	27
Figure 16: Layout of the dam axis, the reference cylinder and the central angle (plan view) [1].	29
Figure 17: Angle β between thrust and rock contours (plan view) [1].	29
Figure 18: The workflow of the reference cylinder.	30
Figure 19: Reference plane of the arch dam (plan view).	31
Figure 20: Projection points (left) and crown cantilever section (right) (side view) [2].	33
Figure 21: Upstream contact line (plan view) [1].	34
Figure 22: Start, end and upstream projection point of the parabola i (plan view).	35
Figure 23: The workflow of the layout of the arches.	36
Figure 24: Angles of the reference cylinder and the upstream base elevation parabola (plan view).	37
Figure 25: Smooth end points of the upstream parabola i (plan view).	39
Figure 26: Points of the smooth upstream foundation area (plan view).	39
Figure 27: End points of the downstream parabola i (plan view).	40
Figure 28: Upstream and downstream points of the smooth foundation area (plan view).	41
Figure 29: The workflow of the smooth dam shape method.	42
Figure 30: Left Hand Side of the arch i (plan view).	43
Figure 31: The workflow of the review of the arches.	45
Figure 32: Valid developed profile view [1].	46
Figure 33: Invalid developed profile view [1].	46
Figure 34: Cylindrical projection method (developed view).	47
Figure 35: Transformation from global to cylindrical coordinates (plan view).	47
Figure 36: Polylines of the foundation grade and the dam base (developed profile view).	48
Figure 37: The workflow of the profile view using the developed cylinder.	49
Figure 38: LHS joint centers at the reference cylinder (plan view).	50
Figure 39: LHS contraction joints of the reference cylinder (plan view).	52
Figure 40: Minimum distance between a point and a parabola.	52

Figure 41: Upstream contraction joints at elevation i (plan view).....	53
Figure 42: Downstream contraction joints at elevation i (plan view).	53
Figure 43: The workflow of the contraction joints.....	55
Figure 44: Cloud of points of the upstream face (left). Bezier Surface of the upstream face (right).....	56
Figure 45: Cloud of points of downstream face (left). Bezier Surface of downstream face (right).	57
Figure 46: Clouds of points of foundation area (left). Bezier Surfaces of foundation area (right).	58
Figure 47: Solid block of the arch dam.....	59
Figure 48: The dam solid before (left) and after (right) the subtraction with the foundation surfaces. ...	59
Figure 49: The dam solid before (left) and after (right) the subtraction with the upstream and downstream surfaces.....	60
Figure 50: Solid shape of the dam removing the unsuitable solids.....	60
Figure 51: The topography solid before (left) and after (right) the subtraction with the topographic surface.....	61
Figure 52: The topography solid before (left) and after (right) the subtraction with the dam solid.	61
Figure 53: Geometry of the contraction joints.	62
Figure 54: Bezier Surfaces of the contraction joints (left). The dam cantilevers after the subtraction (right).	63
Figure 55: Visualization of the helical surfaces of a cantilever.....	63
Figure 56: Boundary conditions of the model.	64
Figure 57: Hydrostatic load on the upstream face of the dam.....	64
Figure 58: Key stress points of a double-curvature arch dam [3].	67
Figure 59: Transition (tangent) and side center point at elevations i (plan view) [2].	69
Figure 60: Lines of transition (tangent) points along the dam height (front view) [2].....	69
Figure 61: RHS line of side centers (side view) [2].	70
Figure 62: Lines of side centers along the dam height (front view) [2].	70
Figure 63: Redefinition of the crown cantilever section (side view) [2].	72
Figure 64: Redefinition of the line of main centers (side view) [2].	73
Figure 65: Constitutive model for interfaces in normal and tangential direction.	74
Figure 66: Concrete-concrete interfaces (3D view).....	75
Figure 67: Side concrete-rock interfaces (3D view).....	76
Figure 68: Base concrete-rock interfaces (3D view).....	76
Figure 69: Static (inner) and dynamic (outer) concrete biaxial failure envelope [7].	78
Figure 70: Vikos Gorge surface from Sketchup2015 to DianaE.	81
Figure 71: The chosen locations on the topographic surface (plan view).	82
Figure 72: Location A, concrete and excavation volume vs axis angle.....	85
Figure 73: Location B, concrete and excavation volume vs axis angle.	87
Figure 74: Location C, concrete and excavation volume vs axis angle.	88
Figure 75: Location A-Mesh 10-Displacement field DtXYZ (3D view).....	90
Figure 76: Location A-Mesh 10-In plane principal stresses (Upstream view).	90
Figure 77: Location A-Mesh 10-In plane principal stresses (Downstream view).....	90
Figure 78: Location B-Mesh 10-Displacement field DtXYZ (3D view).....	91

Figure 79: Location B-Mesh 10-In plane principal stresses (Upstream view).	91
Figure 80: Location B-Mesh 10-In plane principal stresses (Upstream view).	91
Figure 81: Location C-Mesh 10-Displacement field DtXYZ (3D view).	92
Figure 82: Location C-Mesh 10-In plane principal stresses (Upstream view).	92
Figure 83: Location C-Mesh 10-In plane principal stresses (Upstream view).	92
Figure 84: Concrete and excavation volume for the fitting dams for the chosen locations.	93
Figure 85: Iteration 0-Displacement field DtXYZ (3D view).	97
Figure 86: Iteration 0-In plane principal stresses (Upstream view).	97
Figure 87: Iteration 0-In plane principal stresses (Downstream view).	98
Figure 88: Iteration 0-Interface relative displacements DUNz (3D view).	98
Figure 89: Iteration 0-Interface tractions STNz (3D view).	98
Figure 90: Iteration 0-Biaxial failure envelope-Static usual (FSstus) (Upstream view).	99
Figure 91: Iteration 0-Biaxial failure envelope-Static usual (FSstus) (Downstream view).	99
Figure 92: Iteration 1-Displacement field DtXYZ (3D view).	100
Figure 93: Iteration 1-In plane principal stresses (Upstream view).	100
Figure 94: Iteration 1-In plane principal stresses (Downstream view).	101
Figure 95: Iteration 1-Interface relative displacements DUNz (3D view).	101
Figure 96: Iteration 1-Interface tractions STNz (3D view).	101
Figure 97: Iteration 1-Biaxial failure envelope-Static usual (FSstus) (Upstream view).	102
Figure 98: Iteration 1-Biaxial failure envelope-Static usual (FSstus) (Downstream view).	102
Figure 99: Iteration 2-Displacement field DtXYZ (3D view).	103
Figure 100: Iteration 2-In plane principal stresses (Upstream view).	103
Figure 101: Iteration 2-In plane principal stresses (Downstream view).	104
Figure 102: Iteration 2-Interface relative displacements DUNz (3D view).	104
Figure 103: Iteration 2-Interface tractions STNz (3D view).	104
Figure 104: Iteration 2-Biaxial failure envelope-Static usual (FSstus) (Upstream view).	105
Figure 105: Iteration 2-Biaxial failure envelope-Static usual (FSstus) (Downstream view).	105
Figure 106: Iteration 3-Displacement field DtXYZ (3D view).	106
Figure 107: Iteration 3-In plane principal stresses (Upstream view).	106
Figure 108: Iteration 2-In plane principal stresses (Downstream view).	107
Figure 109: Iteration 3-Interface relative displacements DUNz (3D view).	107
Figure 110: Iteration 3-Interface tractions STNz (3D view).	107
Figure 111: Iteration 3- Biaxial failure envelope-Static usual (FSstus) (Upstream view).	108
Figure 112: Iteration 3- Biaxial failure envelope-Static usual (FSstus) (Downstream view).	108
Figure 113: Location B, theoretical vs numerical concrete volume.	110
Figure 114: Location B, excavation length vs concrete and excavation volume.	113
Figure 115: Location B, excavation length vs crest and base thickness.	113
Figure 116: Location A-Mesh 21-Mode 1-Eigen value 1.7373 (3D view).	133
Figure 117: Location A-Mesh 21-Mode 2-Eigen value 1.9840 (3D view).	133
Figure 118: Location A-Mesh 21-Mode 3-Eigen value 2.8802 (3D view).	133
Figure 119: Location A-Mesh 21-Displacement field DtXYZ (3D view).	134

Figure 120: Location A-Mesh 21-In plane principal stresses (Upstream view).	134
Figure 121: Location A-Mesh 21-In plane principal stresses (Downstream view).	134
Figure 122: Location A-Mesh 5-Mode 1-Eigen value 1.6021 (3D view).....	135
Figure 123: Location A-Mesh 5-Mode 2-Eigen value 1.9168 (3D view).....	135
Figure 124: Location A-Mesh 5-Mode 3-Eigen value 2.5866 (3D view).....	135
Figure 125: Location A-Mesh 5-Displacement field DtXYZ (3D view).....	136
Figure 126: Location A-Mesh 5-In plane principal stresses (Upstream view).	136
Figure 127: Location A-Mesh 5-In plane principal stresses (Downstream view).....	136
Figure 128: Location B-Mesh 21-Mode 1-Eigen value 1.9110 (3D view).....	137
Figure 129: Location B-Mesh 21-Mode 2-Eigen value 2.0261 (3D view).....	137
Figure 130: Location B-Mesh 21-Mode 3-Eigen value 3.0665 (3D view).....	137
Figure 131: Location B-Mesh 21-Displacement field DtXYZ (3D view).....	138
Figure 132: Location B-Mesh 21-In plane principal stresses (Upstream view).....	138
Figure 133: Location B-Mesh 21-In plane principal stresses (Downstream view).....	138
Figure 134: Location B-Mesh 5-Mode 1-Eigen value 1.7567 (3D view).....	139
Figure 135: Location B-Mesh 5-Mode 2-Eigen value 1.9727 (3D view).....	139
Figure 136: Location B-Mesh 5-Mode 3-Eigen value 2.7986 (3D view).....	139
Figure 137: Location B-Mesh 5-Displacement field DtXYZ (3D view).....	140
Figure 138: Location B-Mesh 5-In plane principal stresses (Upstream view).	140
Figure 139: Location B-Mesh 5-In plane principal stresses (Downstream view).....	140
Figure 140: Location C-Mesh 21-Mode 1-Eigen value 1.5742 (3D view).....	141
Figure 141: Location C-Mesh 21-Mode 2-Eigen value 1.7443 (3D view).....	141
Figure 142: Location C-Mesh 21-Mode 3-Eigen value 2.3652 (3D view).....	141
Figure 143: Location C-Mesh 21-Displacement field DtXYZ (3D view).	142
Figure 144: Location C-Mesh 21-In plane principal stresses (Upstream view).....	142
Figure 145: Location C-Mesh 21-In plane principal stresses (Downstream view).	142
Figure 146: Location C-Mesh 5-Mode 1-Eigen value 1.4745 (3D view).....	143
Figure 147: Location C-Mesh 5-Mode 2-Eigen value 1.7045 (3D view).....	143
Figure 148: Location C-Mesh 5-Mode 3-Eigen value 2.2051 (3D view).....	143
Figure 149: Location C-Mesh 5-Displacement field DtXYZ (3D view).	144
Figure 150: Location C-Mesh 5-In plane principal stresses (Upstream view).	144
Figure 151: Location C-Mesh 5-In plane principal stresses (Downstream view).....	144

List of Tables

Table 1: Location A, concrete and excavation volume vs axis angle.....	84
Table 2: Location B, concrete and excavation volume vs axis angle.....	86
Table 3: Location C, concrete and excavation volume vs axis angle.....	88
Table 4: Preliminary material properties.....	89
Table 5: Concrete and excavation volume for the fitting dams for the chosen locations.....	93
Table 6: Final material properties.....	94
Table 7: Final results for the characteristic iterations.....	96
Table 8: Location B, theoretical vs numerical concrete volume.....	109
Table 9: Location B, the influence of the excavation length.....	112

Appendix 1: Preliminary results

- Location A-Mesh 21

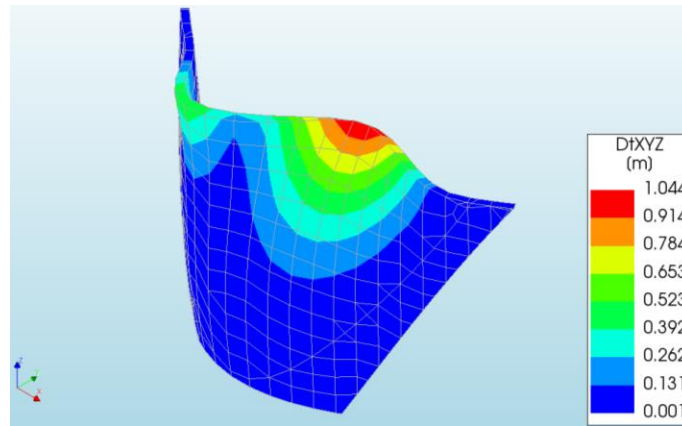


Figure 116: Location A-Mesh 21-Mode 1-Eigen value 1.7373 (3D view).

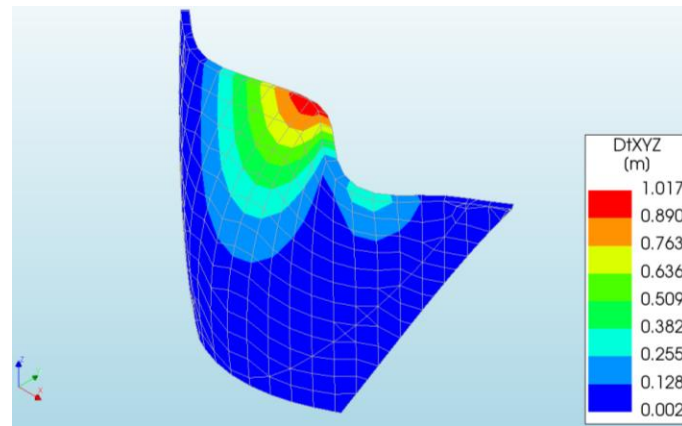


Figure 117: Location A-Mesh 21-Mode 2-Eigen value 1.9840 (3D view).

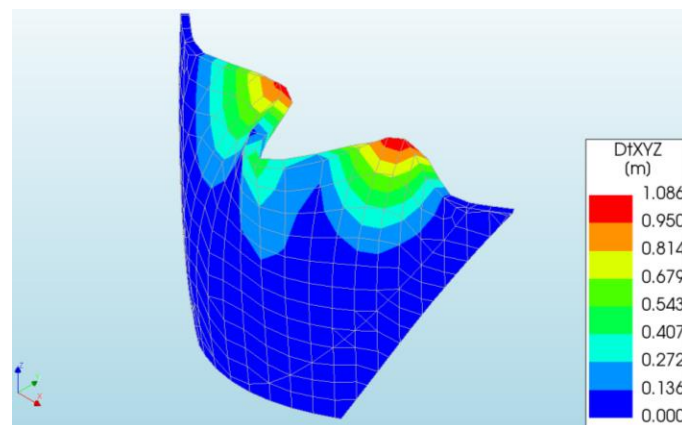


Figure 118: Location A-Mesh 21-Mode 3-Eigen value 2.8802 (3D view).

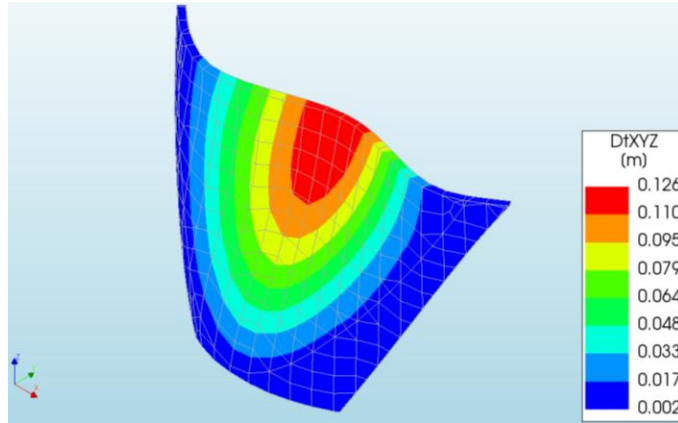


Figure 119: Location A-Mesh 21-Displacement field DtXYZ (3D view).

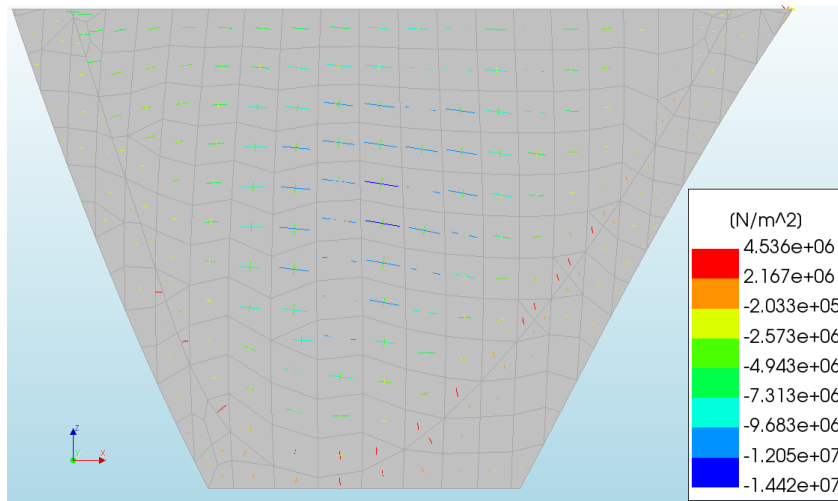


Figure 120: Location A-Mesh 21-In plane principal stresses (Upstream view).

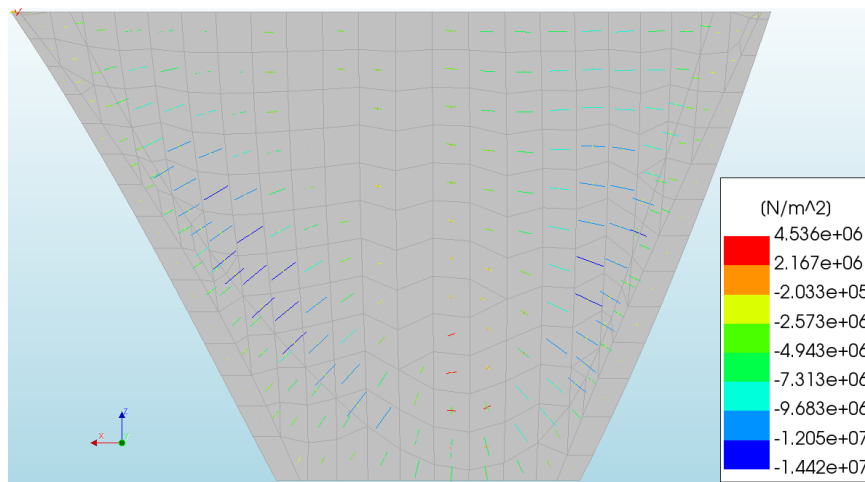


Figure 121: Location A-Mesh 21-In plane principal stresses (Downstream view).

- Location A-Mesh 5

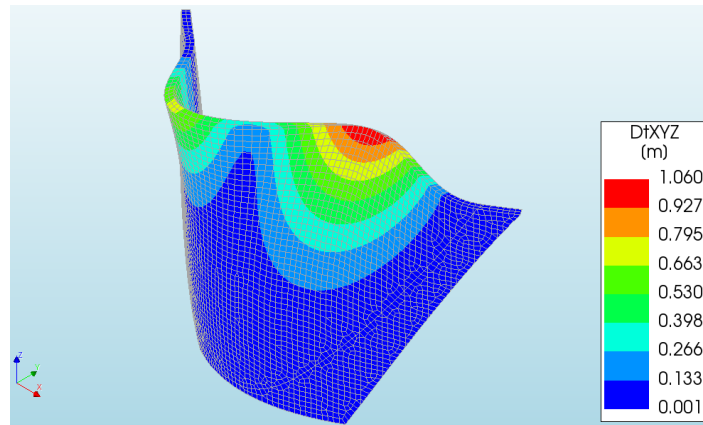


Figure 122: Location A-Mesh 5-Mode 1-Eigen value 1.6021 (3D view).

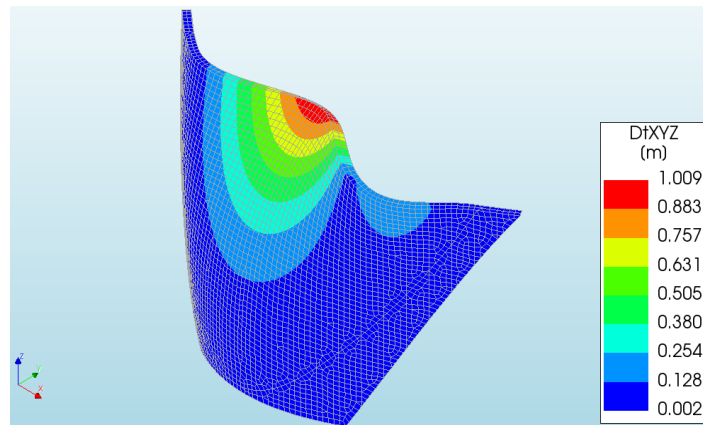


Figure 123: Location A-Mesh 5-Mode 2-Eigen value 1.9168 (3D view).

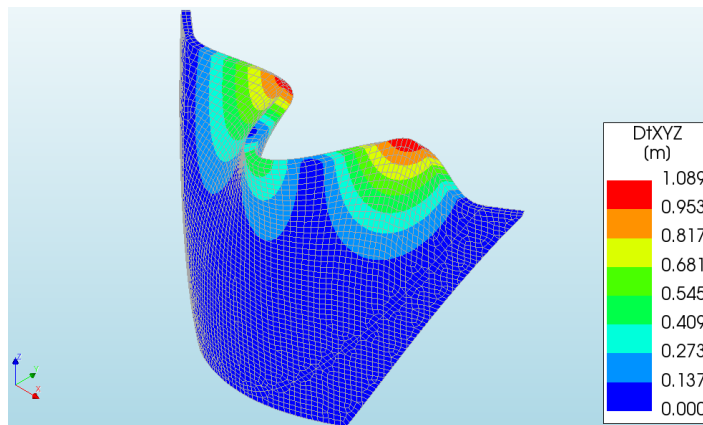


Figure 124: Location A-Mesh 5-Mode 3-Eigen value 2.5866 (3D view).

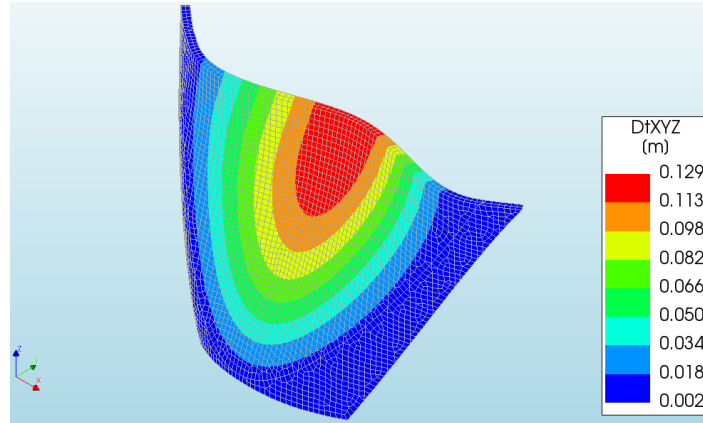


Figure 125: Location A-Mesh 5-Displacement field DtXYZ (3D view).

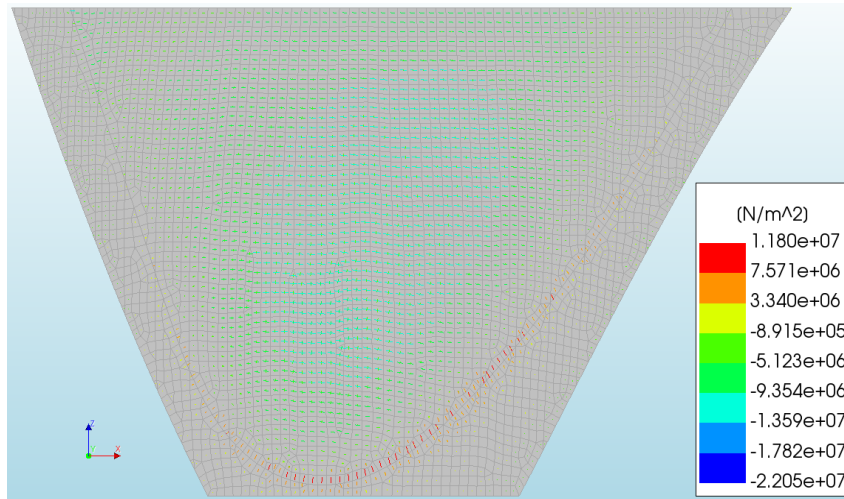


Figure 126: Location A-Mesh 5-In plane principal stresses (Upstream view).

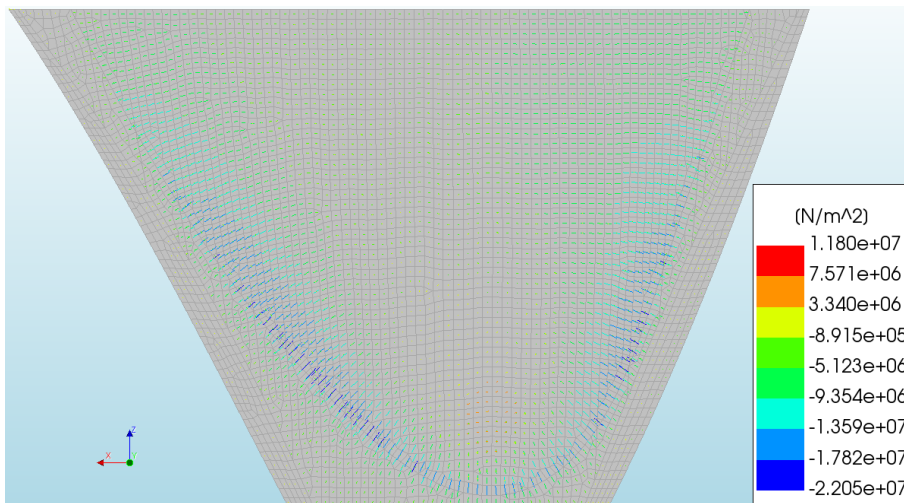


Figure 127: Location A-Mesh 5-In plane principal stresses (Downstream view).

- Location B-Mesh 21

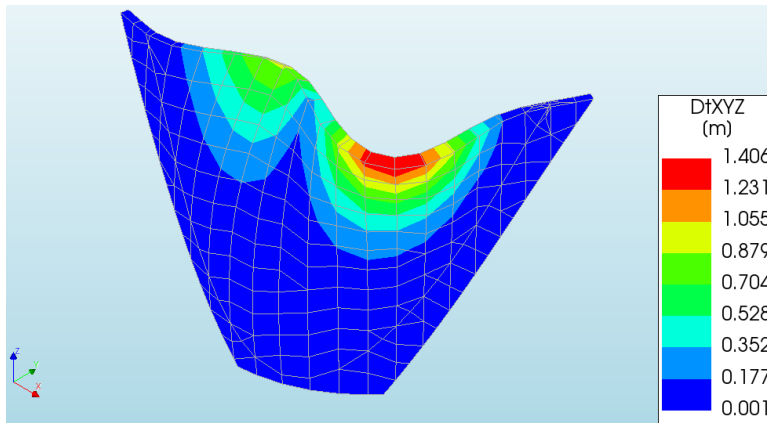


Figure 128: Location B-Mesh 21-Mode 1-Eigen value 1.9110 (3D view).

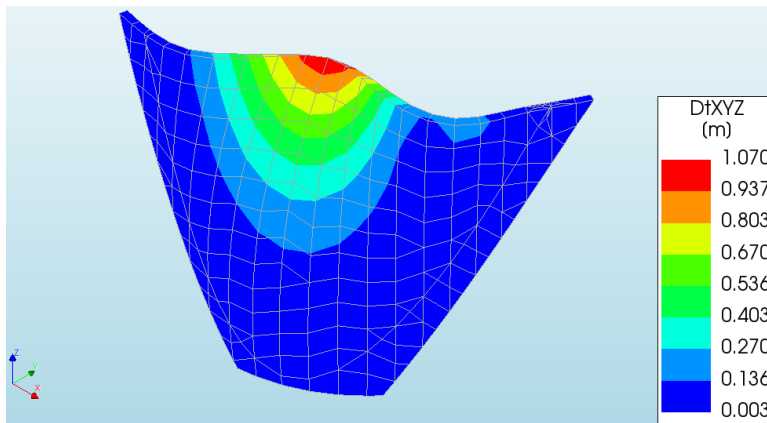


Figure 129: Location B-Mesh 21-Mode 2-Eigen value 2.0261 (3D view).

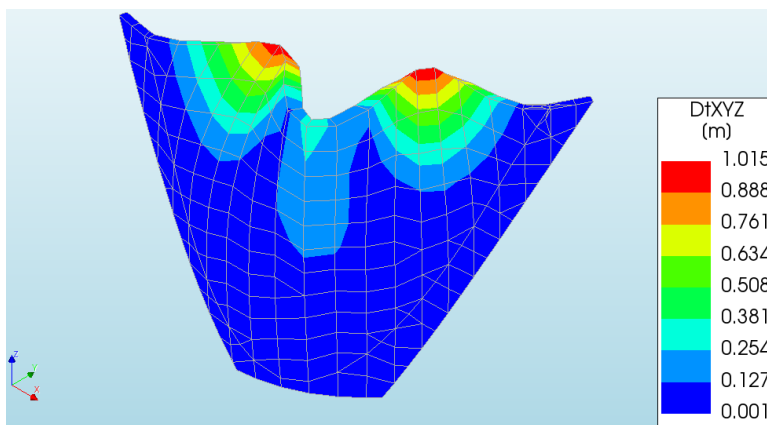


Figure 130: Location B-Mesh 21-Mode 3-Eigen value 3.0665 (3D view).

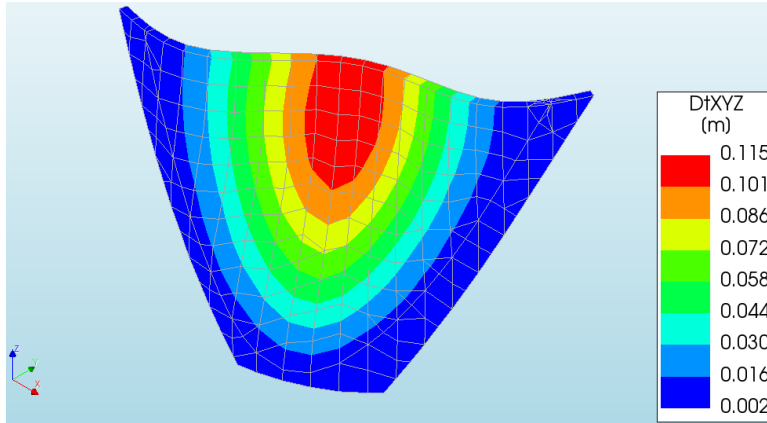


Figure 131: Location B-Mesh 21-Displacement field DtXYZ (3D view).

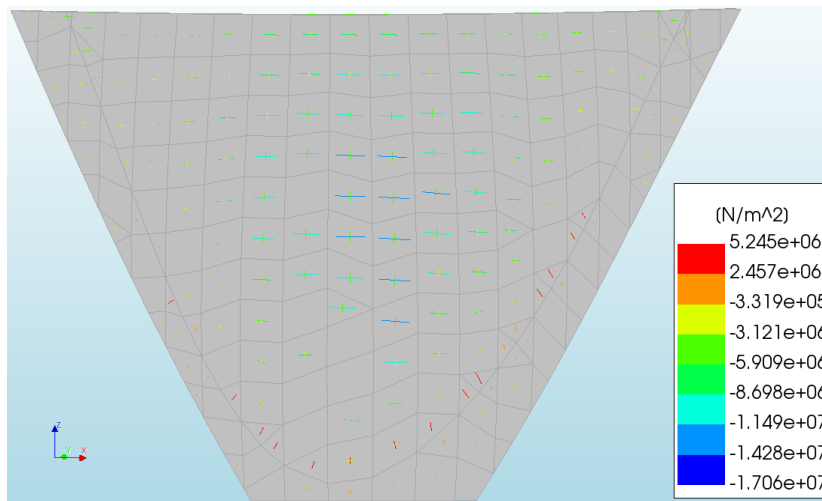


Figure 132: Location B-Mesh 21-In plane principal stresses (Upstream view).

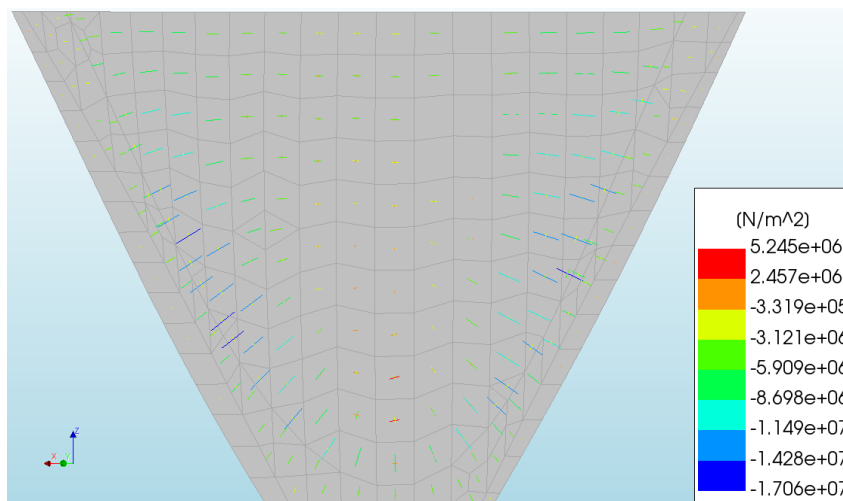


Figure 133: Location B-Mesh 21-In plane principal stresses (Downstream view).

- Location B-Mesh 5

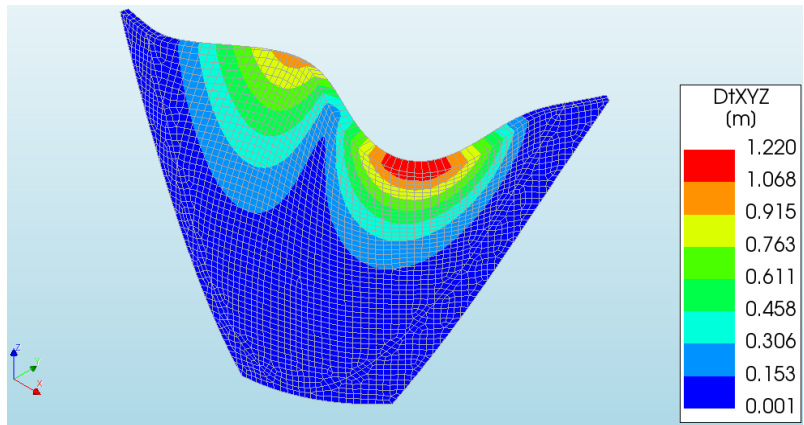


Figure 134: Location B-Mesh 5-Mode 1-Eigen value 1.7567 (3D view).

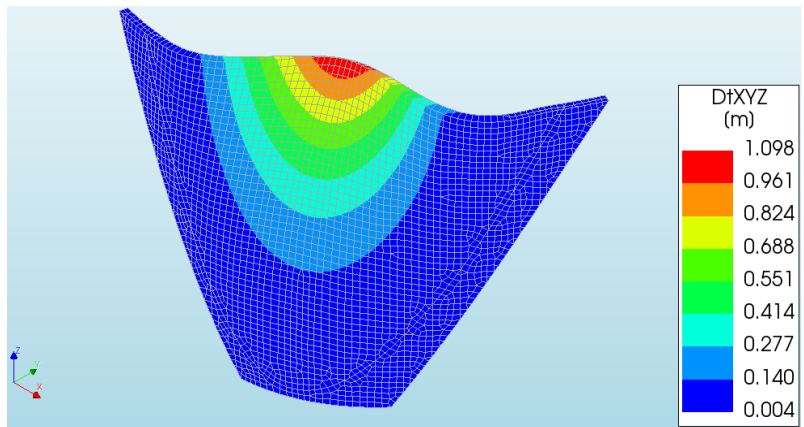


Figure 135: Location B-Mesh 5-Mode 2-Eigen value 1.9727 (3D view).

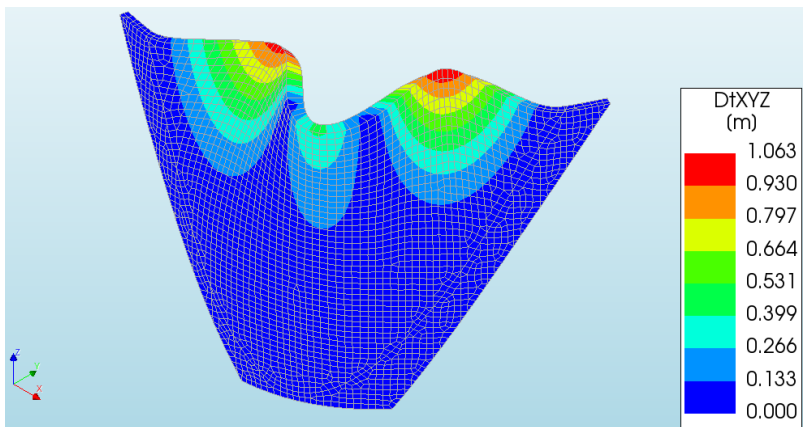


Figure 136: Location B-Mesh 5-Mode 3-Eigen value 2.7986 (3D view).

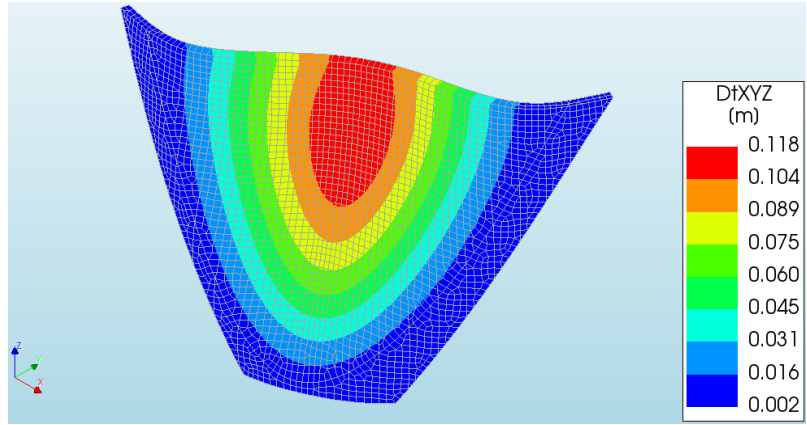


Figure 137: Location B-Mesh 5-Displacement field $DtXYZ$ (3D view).

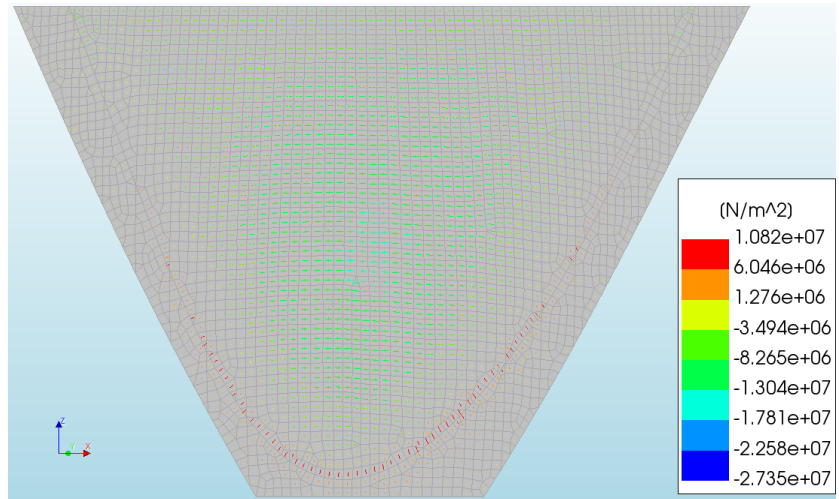


Figure 138: Location B-Mesh 5-In plane principal stresses (Upstream view).

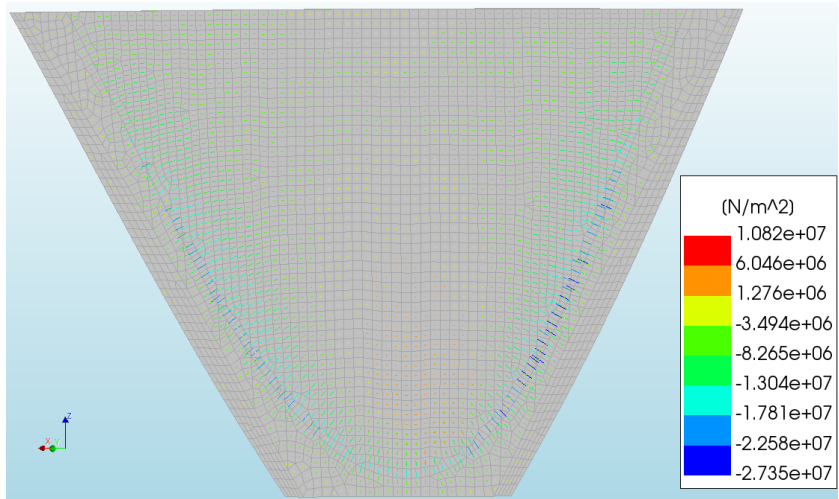


Figure 139: Location B-Mesh 5-In plane principal stresses (Downstream view).

- Location C-Mesh 21

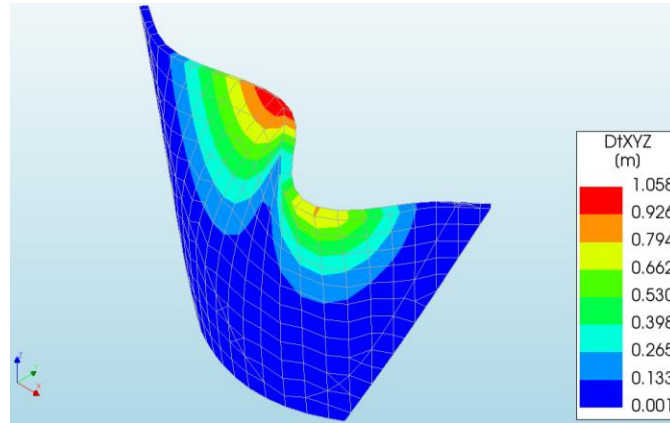


Figure 140: Location C-Mesh 21-Mode 1-Eigen value 1.5742 (3D view).

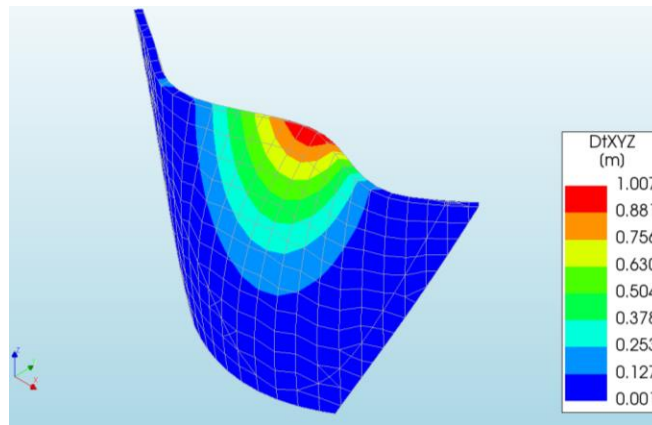


Figure 141: Location C-Mesh 21-Mode 2-Eigen value 1.7443 (3D view).

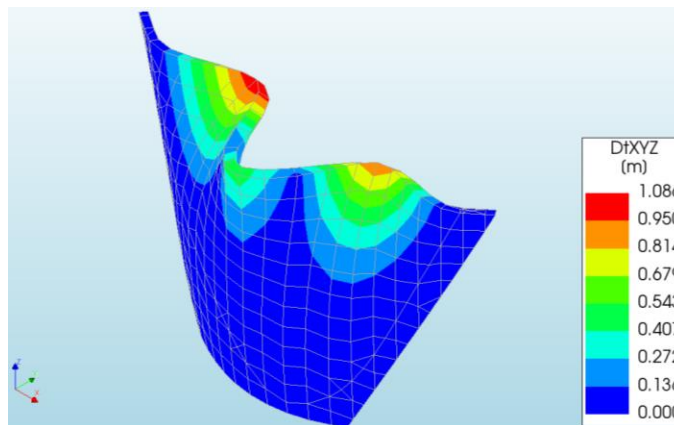


Figure 142: Location C-Mesh 21-Mode 3-Eigen value 2.3652 (3D view).

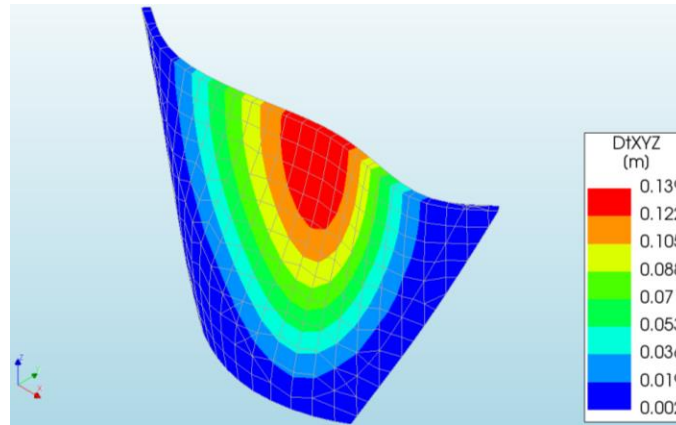


Figure 143: Location C-Mesh 21-Displacement field DtXYZ (3D view).

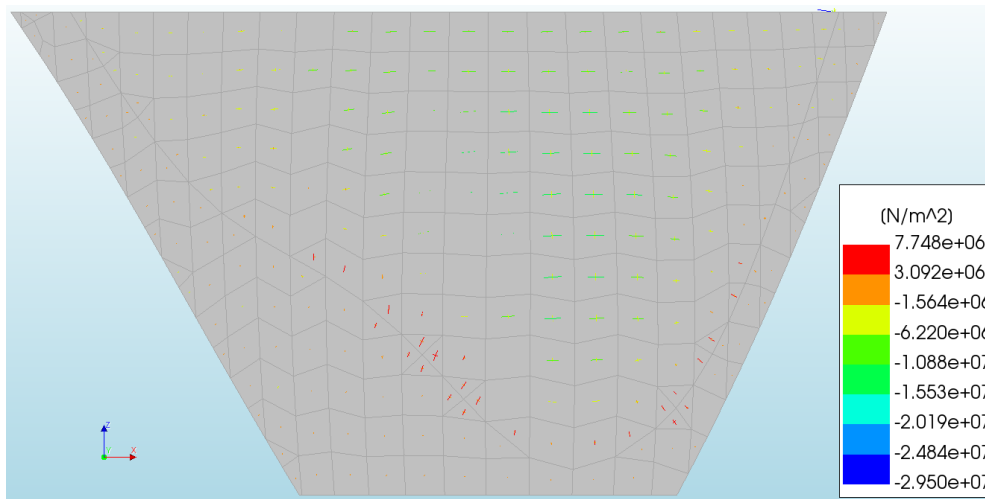


Figure 144: Location C-Mesh 21-In plane principal stresses (Upstream view).

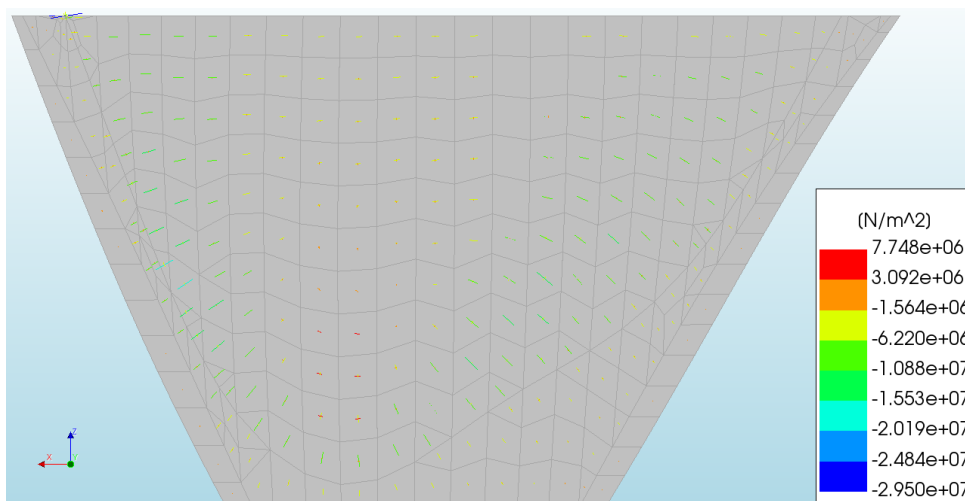


Figure 145: Location C-Mesh 21-In plane principal stresses (Downstream view).

- Location C-Mesh 5

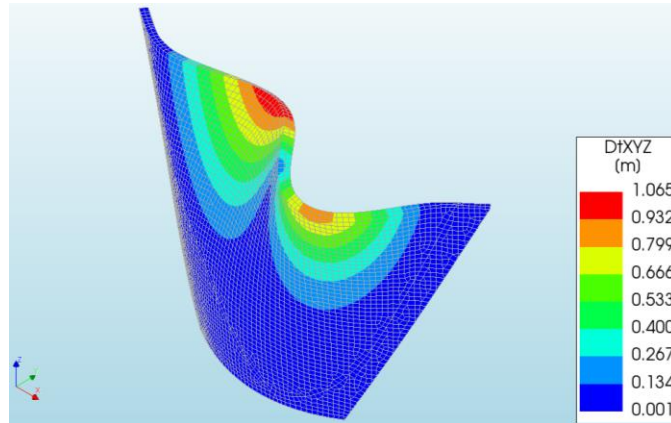


Figure 146: Location C-Mesh 5-Mode 1-Eigen value 1.4745 (3D view).

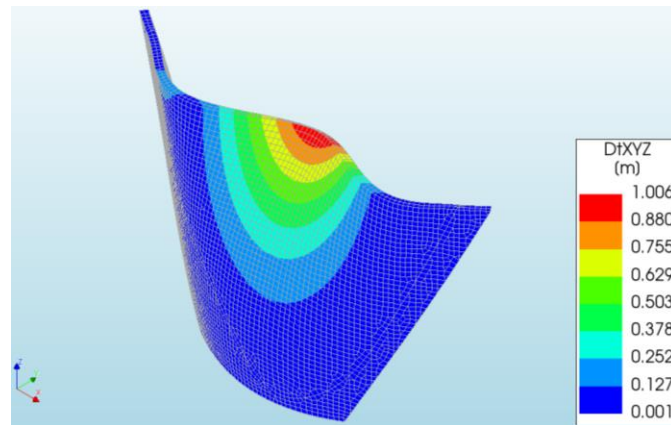


Figure 147: Location C-Mesh 5-Mode 2-Eigen value 1.7045 (3D view).

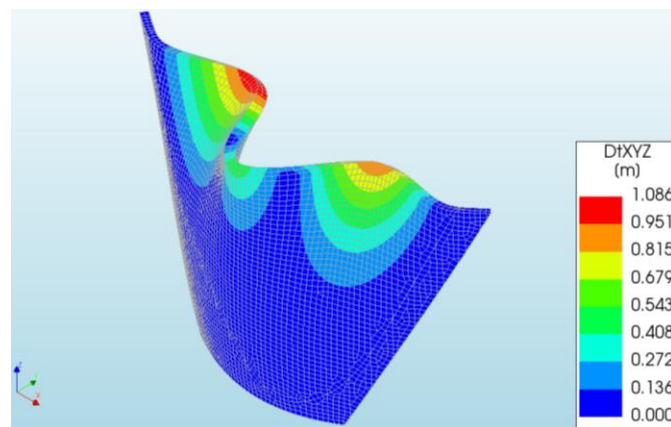


Figure 148: Location C-Mesh 5-Mode 3-Eigen value 2.2051 (3D view).

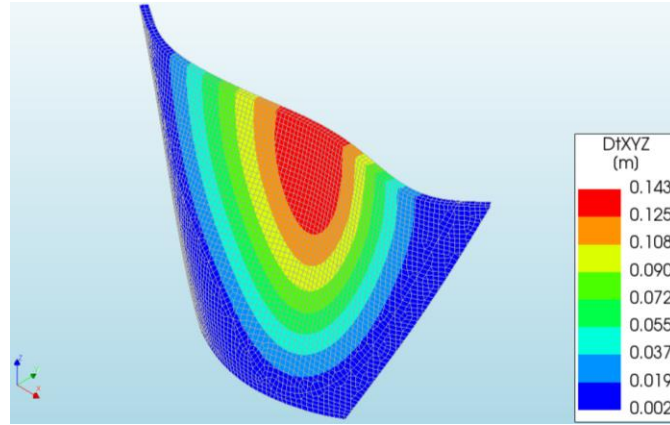


Figure 149: Location C-Mesh 5-Displacement field DtXYZ (3D view).

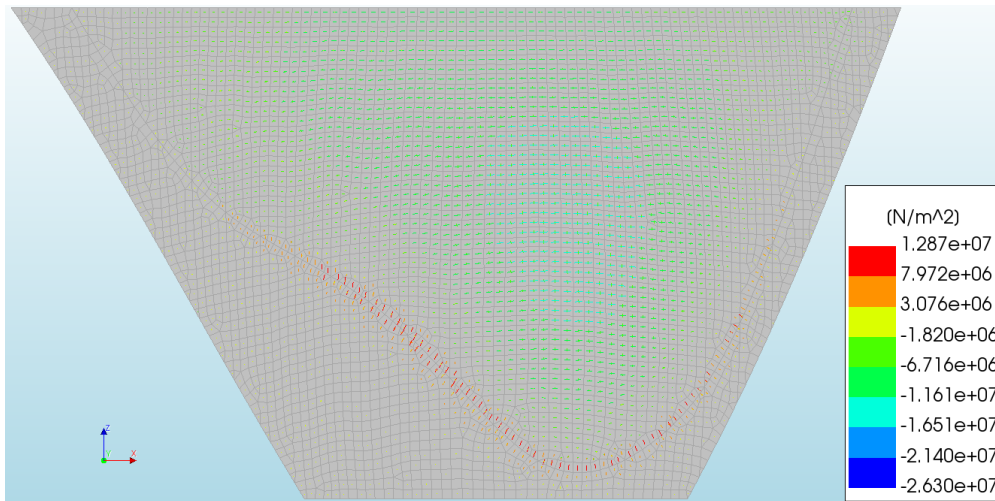


Figure 150: Location C-Mesh 5-In plane principal stresses (Upstream view).

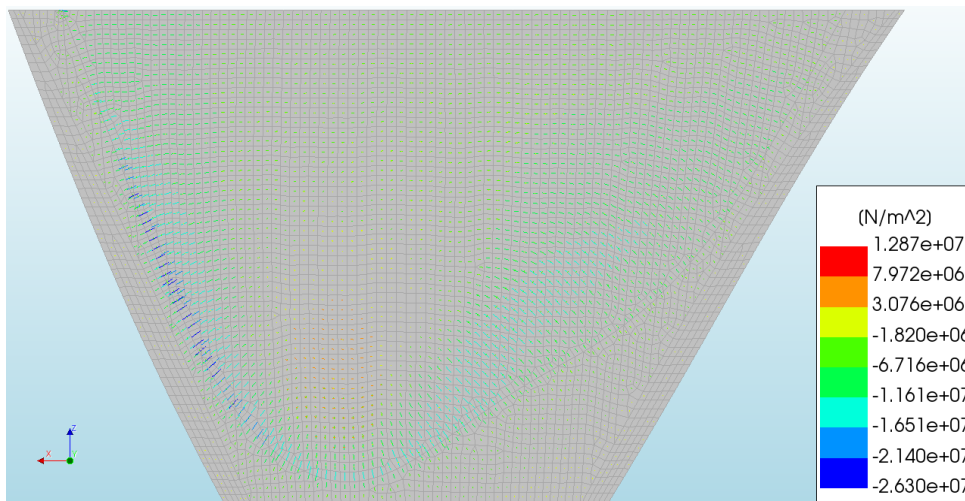


Figure 151: Location C-Mesh 5-In plane principal stresses (Downstream view).